United States
Environmental Protection
Agency

Office of Air Quality
Planning and Standards
Research Triangle Park NC 27711

EPA-450/2-78-042b
October 1978

Air

EPA

Stack Sampling Technical Information

GRIMLEY

A Collection of Monographs and Papers Volume II

EPA-450/2-78-042b

Stack Sampling Technical Information
A Collection of Monographs and Papers
Volume II

Emission Standards and Engineering Division

U.S. ENVIRONMENTAL PROTECTION AGENCY
Office of Air, Noise, and Radiation
Office of Air Quality Planning and Standards
Research Triangle Park, North Carolina 27711

October 1978

This report has been reviewed by the Emission Standards and Engineering Division, Office of Air Quality Planning and Standards, Office of Air, Noise and Radiation, Environmental Protection Agency, and approved for publication. Mention of company or product names does not constitute endorsement by EPA. Copies are available free of charge to Federal employees, current contractors and grantees, and non-profit organizations - as supplies permit - from the Library Services Office, MD-35, Environmental Protection Agency, Research Triangle Park, NC 27711; or may be obtained, for a fee, from the National Technical Information Service, 5285 Port Royal Road, Springfield, VA 22161.

Publication No. EPA-450/2-78-042b

PREFACE

The Clean Air Act of 1970 requires the Administrator of the Environmental Protection Agency to establish national emission standards for new stationary sources (Section 111) and hazardous air pollutants (Section 112). The development of these emission standards required the concurrent development of reference test methods and procedures. The reference test methods and procedures are published in the Federal Register along with the appropriate regulations.

From time to time, questions would surface concerning the methods and procedures. In many cases, specific studies would be needed to provide informed, objective answers. The papers and monographs resulting from these studies were usually distributed to people involved in emission measurement; a major method of distribution has been the Source Evaluation Society Newsletter.

To provide a readily available resource for new and experienced personnel, and to further promote standardized reference methods and procedures, it has been decided to publish the papers and monographs in a single compendium. The compendium consists of four volumes. The Table of Contents for all four volumes is reproduced in each volume for ease of reference.

Congratulations and sincere appreciation to the people who did the work and took the time to prepare the papers and monographs. For the most part the work was done because of personal commitments to the development of objective, standardized methodology, and a firm belief that attention to the details of stack sampling makes for good data. The foresight of Mr. Robert L. Ajax, the former Chief of the Emission Measurement Branch and now the Assistant Director, Emission Standards and Engineering Division, in providing the atmosphere and encouragement to perform the studies is gratefully acknowledged. The skill and dedication of Mr. Roger Shigehara, in providing personal supervision for most of the work, is commended.

Don R. Goodwin
Director
Emission Standards and
Engineering Division

VOLUME I

TABLE OF CONTENTS

Method for Calculating Power Plant Emission Rate 1

by R. T. Shigehara, R. M. Neulicht, and W. S. Smith

Emission Correction Factor for Fossil Fuel-Fired Steam Generators (CO_2 Concentration Approach) 10

by R. M. Neulicht

Derivation of Equations for Calculating Power Plant Emission Rates (O_2 Based Method - Wet and Dry Measurements) 20

by R. T. Shigehara and R. M. Neulicht

Summary of F Factor Methods for Determining Emissions from Combustion Sources 29

by R. T. Shigehara, R. M. Neulicht, W. S. Smith, and J. W. Peeler

Validating Orsat Analysis Data from Fossil-Fuel-Fired Units 44

by R. T. Shigehara, R. M. Neulicht, and W. S. Smith

A Guideline for Evaluating Compliance Test Results (Isokinetic Sampling Rate Criterion) 56

by R. T. Shigehara

VOLUME II

TABLE OF CONTENTS

A Type-S Pitot Tube Calibration Study 1

by Robert F. Vollaro

The Effect of Aerodynamic Interference Between a Type-S Pitot Tube and Sampling Nozzle on the Value of the Pitot Tube Coefficient 24

by Robert F. Vollaro

The Effects of the Presence of a Probe Sheath on Type-S Pitot Tube Accuracy 30

by Robert F. Vollaro

An Evaluation of Single-Velocity Calibration Technique as a Means of Determining Type-S Pitot Tube Coefficients 48

by Robert F. Vollaro

Guidelines for Type-S Pitot Tube Calibration 63

by Robert F. Vollaro

The Effects of Impact Opening Misalignment on the Value of the Type-S Pitot Tube Coefficient 89

by Robert F. Vollaro

Establishment of a Baseline Coefficient Value for Properly Constructed Type-S Pitot Tubes 95

by Robert F. Vollaro

A Survey of Commercially Available Instrumentation for the Measurement of Low-Range Gas Velocities 104

by Robert F. Vollaro

The Use of Type-S Pitot Tubes for the Measurement of Low Velocities 122

by Robert F. Vollaro

VOLUME III

TABLE OF CONTENTS

Thermocouple Calibration Procedure Evaluation 1
by Kenneth Alexander

Procedure for Calibrating and Using Dry Gas Volume Meters As Calibration Standards 10
by P. R. Westlin and R. T. Shigehara

Dry-Gas Volume Meter Calibrations 24
by Martin Wortman, Robert Vollaro, and Peter Westlin

Calibration of Dry Gas Meter at Low Flow Rates 33
by R. T. Shigehara and W. F. Roberts

Calibration of Probe Nozzle Diameter 41
by P. R. Westlin and R. T. Shigehara

Leak Tests for Flexible Bags 45
by F. C. Biddy and R. T. Shigehara

Adjustments in the EPA Nomograph for Different Pitot Tube Coefficients and Dry Gas Molecular Weights 48
by R. T. Shigehara

Expansion of EPA Nomograph (Memo) 60
by R. T. Shigehara

EPA Nomograph Adjustments (Memo) 63
by R. T. Shigehara

Graphical Technique for Setting Proportional Sampling Flow Rates 65
by R. T. Shigehara

VOLUME IV

TABLE OF CONTENTS

Recommended Procedure for Sample Traverses in Ducts Smaller Than 12 Inches in Diameter 1

by Robert F. Vollaro

Guidelines for Sampling in Tapered Stacks 24

by T. J. Logan and R. T. Shigehara

Considerations for Evaluating Equivalent Stack Sampling Train Metering Systems 28

by R. T. Shigehara

Evaluation of Metering Systems for Gas-Sampling Trains 40

by M. A. Wortman and R. T. Shigehara

An Evaluation of the Current EPA Method 5 Filtration Temperature-Control Procedure 49

by Robert F. Vollaro

Laboratory Evaluation of Silica Gel Collection Efficiency Under Varying Temperature and Pressure Conditions 67

by Peter R. Westlin and Fred C. Biddy

Spurious Acid Mist Results Caused by Peroxides in Isopropyl Alcohol Solutions Used in EPA Test Method 8 (Memo) 79

by Dr. Joseph E. Knoll

Determination of Isopropanol Loss During Method 8 Simulation Tests (Memo) 80

by Peter R. Westlin

Comparison of Emission Results from In-Stack Filter Sampling and EPA Method 5 Sampling 82

by Peter R. Westlin and Robert L. Ajax

EPA Method 5 Sample Train Clean-Up Procedures 98

by Clyde E. Riley

October 15, 1975

A TYPE-S PITOT TUBE CALIBRATION STUDY

Robert F. Vollaro

INTRODUCTION

A study in which 51 Type-S pitot tubes were calibrated against a standard (Type-P) pitot tube was recently undertaken in response to growing concern over reports of pitot calibration work in which certain observers had obtained Type-S pitot coefficient values consistently below the range 0.83 to 0.87.[1] The 51 Type-S tubes selected for calibration varied a great deal in physical condition and geometry. Some of the tubes were commercial models, representing various manufacturers; the rest had been made within the U. S. Environmental Protection Agency. This paper discusses the calibration study, its results, and its significance.

PRELIMINARY CONSIDERATIONS

The following things were done prior to calibration:

1. Each Type-S pitot tube was assigned a permanent identification number.
2. Each pitot tube was assigned an "A" side and a "B" side. Both the A and B sides were calibrated (see Figure 1).
3. The physical condition of each Type-S pitot tube was evaluated. The appearance of each tube was described in detail and, when necessary, sketches were made to supplement the verbal description.

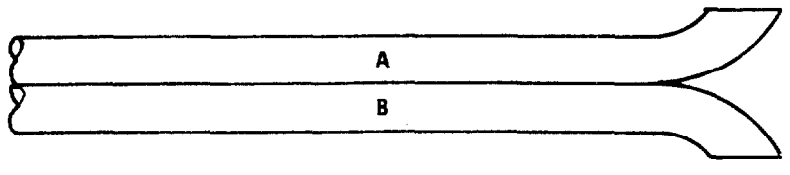

Figure 1. Type-S pitot tube, top view, with A and B sides marked.

4. The following dimensions of each tube were measured and recorded:

   a. Tube length, in inches, measured from the center of the impact openings to the quick-disconnect fittings (Figure 2, dimension a);

   b. Distance between the A-side and B-side impact openings*, expressed in inches (Figure 2, dimension b);

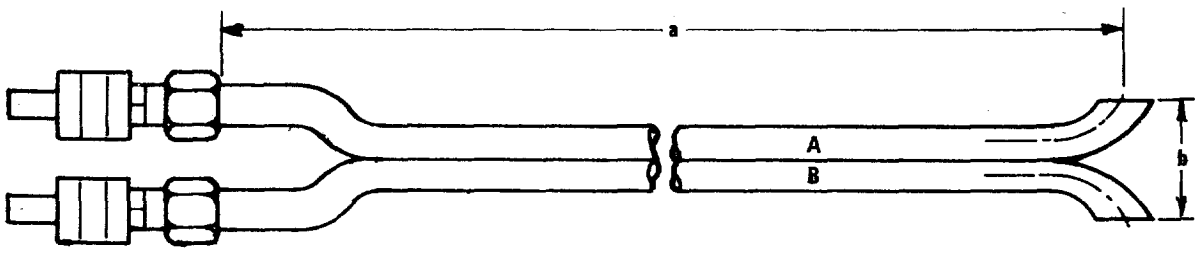

Figure 2. Measurement of Type-S pitot tube length (dimension "a") and impact-plane separation distance (dimension "b").

   c. Length and width, in inches, of A-side and B-side elliptical impact openings. Since some of the tubes were made of thin-walled stainless steel and others of heavy-walled material, impact opening dimensions were measured as shown in Figures 3a (thin-walled) and 3b (heavy-walled).

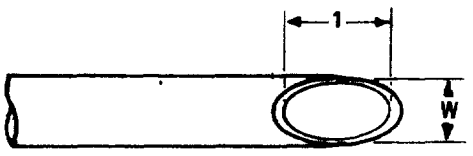

Figure 3a. Measurement of Type-S pitot tube impact-opening dimensions (thin-walled tube).

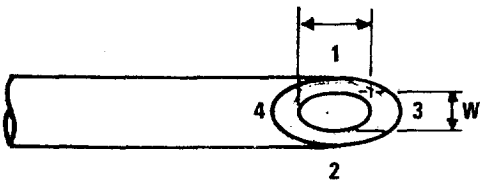

Figure 3b. Measurement of Type-S pitot tube impact-opening dimensions (heavy-walled tube).

* Measured with a digital micrometer.

5. The alignment of the A-side and B-side impact openings of each tube was checked, as follows:

   a. First, the tube was examined in end view to determine whether its impact planes were perpendicular to the transverse tube axis (see Figure 4a). Micrometer readings (M_1 and M_2 in Figure 4b, below) were taken to confirm the visual observations.*

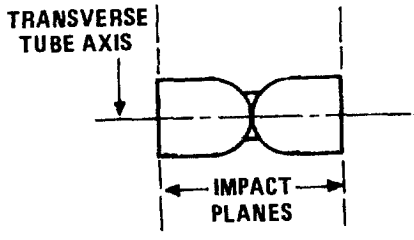

Figure 4a. Type-S pitot tube, end view; impact-opening planes perpendicular to transverse tube axis.

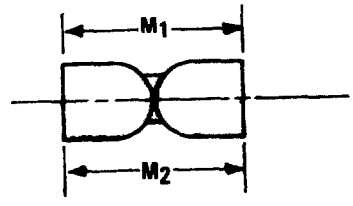

Figure 4b. Micrometer readings M_1 and M_2, taken to check impact-plane alignment with respect to transverse axis.

   b. Second, the tube was examined in top view to determine whether its impact planes were parallel to the longitudinal tube axis (see Figure 5a). Micrometer readings (M_3 and M_4 in Figure 5b) were taken to confirm the visual observations.**

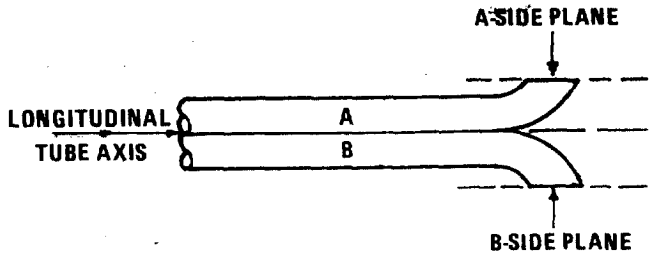

Figure 5a. Type-S tube, top view; impact-opening planes parallel to longitudinal tube axis.

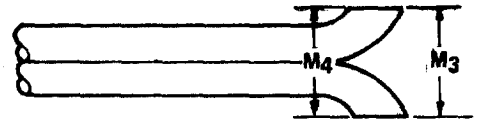

Figure 5b. Micrometer readings M_3 and M_4, taken to check impact-plane alignment with respect to longitudinal axis.

---

* Note that M_1 and M_2 readings were taken approximately halfway across the elliptical impact openings (points 1 and 2, Figure 3b).

** M_3 and M_4 readings were taken halfway down the elliptical openings (points 3 and 4, Figure 3b). Note that M_3 and dimension b in Figure 2 are identical.

c. Third, the tube was examined in side view (from both sides), for two specific types of misalignment: (1) length misalignment (A and B tubes of unequal length) and (2) planar misalignment (impact opening center-lines noncoincident). Figures 6a, 6b, and 6c illustrate properly aligned openings, length misalignment, and planar misalignment, respectively.

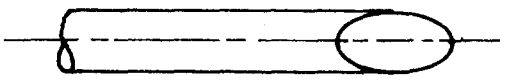

Figure 6a. Type-S pitot tube, side view; impact-openings properly aligned.

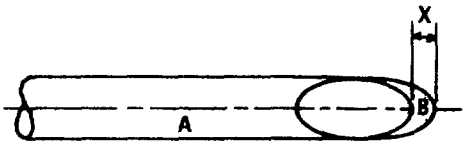

Figure 6b. Type-S pitot tube, side view, showing length misalignment (dimension "X").

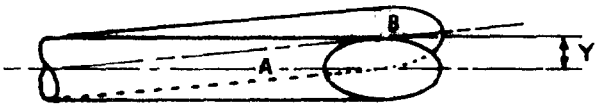

Figure 6c. Type-S pitot tube, side view; showing planar misalignment (dimension "Y").

EXPERIMENTAL SET-UP

The calibrations were done in a wind tunnel (see Figure 7) consisting of a centrifugal blower with adjustable speed drive unit, a surge tank, and a long, straight duct section made of 12 in. i.d. smooth-walled polyvinyl chloride (PVC). The purpose of the surge tank was to dampen pulsations in the blower discharge; the long straight run of pipe was necessary to ensure the presence of stable, well-developed flow profiles in the test section. Test section velocities during calibration ranged from approximately 1500 ft/min to 3500 ft/min; the A and B sides of each Type-S pitot tube were calibrated at six different velocities within this range, spaced at approximately equal intervals.

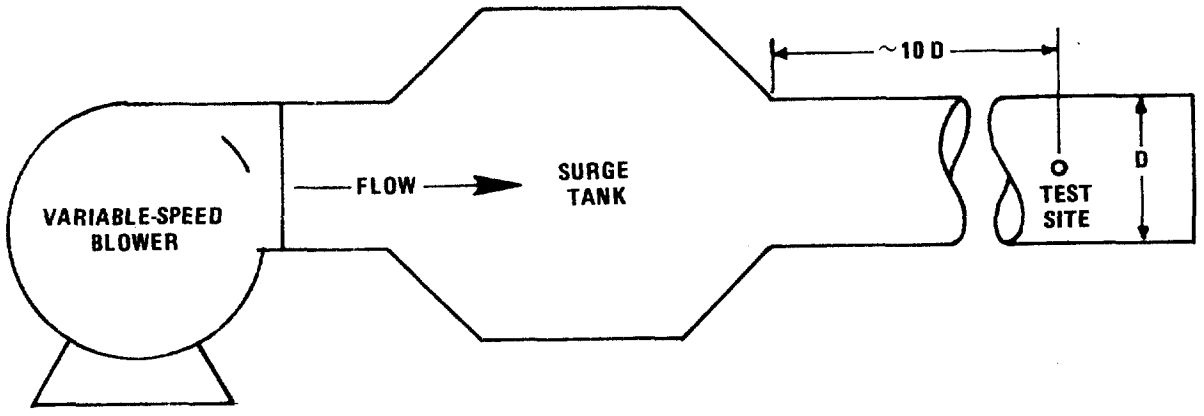

Figure 7. Pitot tube calibration system.

Two test ports were cut in the test section of the PVC duct, 90° apart.* One port was cut slightly upstream of the other, to ensure that the impact openings of both the standard pitot tube and the Type-S tube would be in the same plane during calibration (see Figure 8). To minimize misalignment of the pitot tubes with respect to the flow (yaw and pitch angles), the tubes were not hand-held; instead, special holders, properly aligned with the ductwork, were used.

* Figure 7, for illustrative purposes only, shows the ports 180° apart.

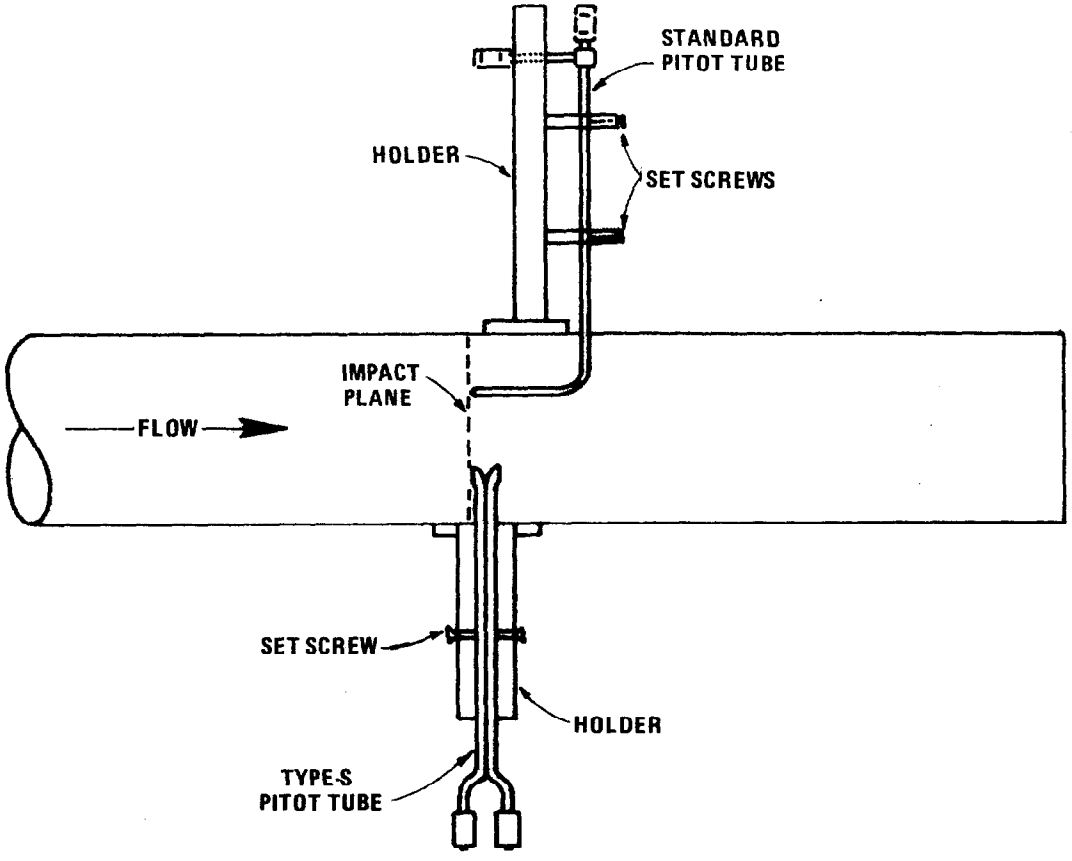

Figure 8. Experimental set-up.

An inclined-vertical gage-oil manometer (Dwyer Model 421-10) was used to read all ΔP values. The inclined part of the manometer scale had a range of 0 to 1.0 in. of water, graduated in divisions of 0.01 in. H_2O. All of the calibration data were within this 0 to 1 in. range; ΔP readings falling in between two divisions were read to the nearest 0.005 in. H_2O, as shown in Figure 9. The "Experimental Error Considerations" section of the Appendix discusses the

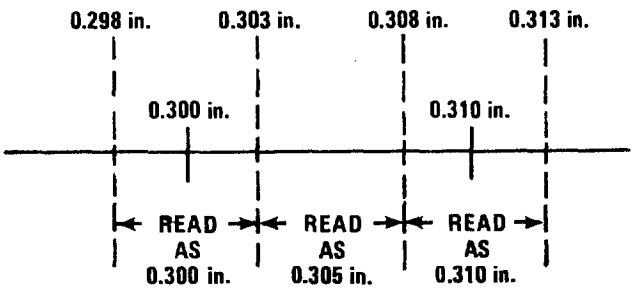

Figure 9. Reading of ΔP to the nearest 0.005 in. H_2O.

implications of reading ΔP this way.

For convenience, the Tygon lines from both the Type-S and standard pitot tubes were connected to a pair of panel-mounted 2-way valves, which, in turn, were connected to the manometer. By opening these valves to the correct position, either ΔP_s or ΔP_{std} could be read without disconnecting any pitot lines.

The calibration standard used in these tests was a Prandtl-type pitot tube, meeting certain design criteria that ensure its coefficient to be 0.99 $\pm$ 0.01 (for velocities above 600 ft/min).[2,4]

CALIBRATION PROCEDURES

The following procedures were used to perform the A and B side calibrations of each Type-S pitot tube:

a. The manometer was cleaned, filled, leveled, and zeroed. All pitot lines and fittings were leak-checked.

b. The standard pitot tube was inserted into the duct, with its impact opening at the duct center.

c. The valves were opened to the ΔP_{std} position.

d. The fan was turned on to setting #1; the flow was allowed to stablilize.

e. The value of ΔP_{std} was read and recorded.

f. The standard pitot tube was withdrawn from the duct.

g. The Type-S pitot tube was inserted into the duct, with its impact opening at the duct center.

h. The valves were positioned to read ΔP_s.

i. The value of ΔP_s was read and recorded.

j. The Type-S pitot tube was withdrawn from the duct.

k. The standard pitot tube was reinserted into the duct; the valves were re-positioned to read ΔP_{std}.

Steps d through k above were repeated at fan settings #2 through #6.

CALCULATIONS

The following formula was used to determine the coefficients of the Type-S pitot tubes:

$$C_p = C_p \text{ (Standard)} \sqrt{\frac{\Delta P_{std}}{\Delta P_s}} \qquad \text{(Equation 1)}$$

where:

C_p = Type-S pitot tube coefficient

C_p(Standard) = coefficient of standard pitot tube = 0.99

ΔP_{std} = standard pitot tube reading (in. H_2O)

ΔP_s = Type-S pitot tube reading (in. H_2O)

For each calibration (A or B side), six values of C_p were computed using the above formula, i.e., one at each fan setting. From these six C_p values, an average coefficient was determined, as follows:

$$\overline{C}_p \text{ (A or B side)} = \frac{\sum_{1}^{6} C_p}{6} \qquad \text{(Equation 2)}$$

SUMMARY OF RESULTS

A. Preliminary Considerations - The results of the preliminary examinations and measurements of the 51 Type-S pitot tubes are presented in Table I (see Appendix). From Table I, it is evident that there was considerable dimensional variation among the tubes; for example, their lengths varied from 29 in. to 113 in., their impact plane separation distances (Figure 2, dimension b) ranged from 0.679 in. to 1.079 in., and their impact opening sizes ranged from 0.43 in. to 0.59 in. in length and from 0.26 in. to 0.39 in. in width. Table I also shows that 39 of the 51 tubes had seen at least some field use; 22 of 51 had been used extensively. Finally, Table I shows that nearly all of the tubes were imperfect geometrically. The four most frequently observed types of geometric misalignment were as follows:

1. Minor impact-plane misalignemnt (one or both planes) with respect to the transverse tube axis (88 percent of the tubes).
2. Minor impact-plane misalignment (one or both planes) with respect to the longitudinal tube axis (61 percent of the tubes).
3. Length misalignment (16 percent of the tubes).
4. Planar misalignment (16 percent of the tubes).

Sixty-seven percent of the tubes exhibited two or more of the above types of misalignment.

B. Calibrations - The results of the calibrations are also presented in Table I. One hundred-two values of $\overline{C}_p$ were obtained (i.e., 51 A-side and 51 B-side coefficients), ranging from 0.805 to 0.880, with a mean value of 0.848 and an average deviation of 0.008 (see "Statistical Considerations" section in the Appendix). Ninety-four of the 102 coefficients (92 percent) fell within the range 0.83 to 0.87, which is cited in the literature as "normal" for the Type-S instrument.[3] The average A-to-B-side coefficient difference was 0.005, and 46 of 51 tubes (90 percent) had an A-to-B-side difference of 0.010 or less.

CONCLUSIONS

A recent study in which 51 isolated (i.e., not attached to sample probes) Type-S pitot tubes were calibrated against a standard pitot tube has demonstrated the following:

1. It is highly probable that a given Type-S pitot tube will have A-side and B-side coefficients within the range 0.83 to 0.87 and an A-to-B-side coefficient difference of 0.010 or less. Therefore, in reference to the previously mentioned studies in which C_p values consistently below the range 0.83 to 0.87 were obtained (see Introduction), it appears unlikely that the pitot tubes themselves were responsible for the low coefficient values; other factors were probably involved. It has recently been learned that when a Type-S pitot tube is used in the presence of a sampling nozzle, there must be adequate separation distance between the tube and nozzle, or they will interfere aerodynamically, causing a reduction in the value of C_p. In the studies reporting low coefficients, calibration was done in the presence of a nozzle; hence, aerodynamic interference is a possible explanation for the consistent departure of the C_p values from the 0.83 to 0.87 range.

For each calibration (A or B side), six values of C_p were computed using the above formula, i.e., one at each fan setting. From these six C_p values, an average coefficient was determined, as follows:

$$\overline{C}_p \text{ (A or B side)} = \frac{\sum_{1}^{6} C_p}{6} \qquad \text{(Equation 2)}$$

SUMMARY OF RESULTS

A. Preliminary Considerations - The results of the preliminary examinations and measurements of the 51 Type-S pitot tubes are presented in Table I (see Appendix). From Table I, it is evident that there was considerable dimensional variation among the tubes; for example, their lengths varied from 29 in. to 113 in., their impact plane separation distances (Figure 2, dimension b) ranged from 0.679 in. to 1.079 in., and their impact opening sizes ranged from 0.43 in. to 0.59 in. in length and from 0.26 in. to 0.39 in. in width. Table I also shows that 39 of the 51 tubes had seen at least some field use; 22 of 51 had been used extensively. Finally, Table I shows that nearly all of the tubes were imperfect geometrically. The four most frequently observed types of geometric misalignment were as follows:

1. Minor impact-plane misalignemnt (one or both planes) with respect to the transverse tube axis (88 percent of the tubes).
2. Minor impact-plane misalignment (one or both planes) with respect to the longitudinal tube axis (61 percent of the tubes).
3. Length misalignment (16 percent of the tubes).
4. Planar misalignment (16 percent of the tubes).

Sixty-seven percent of the tubes exhibited two or more of the above types of misalignment.

B. Calibrations - The results of the calibrations are also presented in Table I. One hundred-two values of $\overline{C}_p$ were obtained (i.e., 51 A-side and 51 B-side coefficients), ranging from 0.805 to 0.880, with a mean value of 0.848 and an average deviation of 0.008 (see "Statistical Considerations" section in the Appendix). Ninety-four of the 102 coefficients (92 percent) fell within the range 0.83 to 0.87, which is cited in the literature as "normal" for the Type-S instrument.[3] The average A-to-B-side coefficient difference was 0.005, and 46 of 51 tubes (90 percent) had an A-to-B-side difference of 0.010 or less.

CONCLUSIONS

A recent study in which 51 isolated (i.e., not attached to sample probes) Type-S pitot tubes were calibrated against a standard pitot tube has demonstrated the following:

1. It is highly probable that a given Type-S pitot tube will have A-side and B-side coefficients within the range 0.83 to 0.87 and an A-to-B-side coefficient difference of 0.010 or less. Therefore, in reference to the previously mentioned studies in which C_p values consistently below the range 0.83 to 0.87 were obtained (see Introduction), it appears unlikely that the pitot tubes themselves were responsible for the low coefficient values; other factors were probably involved. It has recently been learned that when a Type-S pitot tube is used in the presence of a sampling nozzle, there must be adequate separation distance between the tube and nozzle, or they will interfere aerodynamically, causing a reduction in the value of C_p. In the studies reporting low coefficients, calibration was done in the presence of a nozzle; hence, aerodynamic interference is a possible explanation for the consistent departure of the C_p values from the 0.83 to 0.87 range.

2. Generally speaking, the value of the Type-S pitot tube coefficient (C_p) seems to be relatively unaffected by the following: (a) variations in tube dimensions (length, impact opening size, etc.), (b) various types of minor imperfections in tube geometry, and (c) deterioration in the physical condition of the tube, resulting from field use. It is not readily apparent, however, why 8 percent of the tubes calibrated in this study had coefficients outside the range 0.83 to 0.87, or why 10 percent of them had A-to-B-side coefficient differences greater than 0.010. Impact-opening misalignment may have been a factor, but this cannot be ascertained without further study. Therefore, although it is likely that the coefficient of a given Type-S pitot tube will be between 0.83 and 0.87 and that its A-to-B-side coefficient difference will be 0.010 or less, these points are by no means certain and should not be assumed without calibration.

REFERENCES

1. Herrick, R..General Environments Corporation. Springfield, Virginia. (Unpublished data). 1973.
2. Fluid Meters, Their Theory and Application. Published by the American Socity of Mechanical Engineers. 5th Edition. New York, 1959.
3. Smith, W. S., W. F. Todd, and R. T. Shigehara. Significance of Errors in Stack Sampling Measurements. Presented at the Annual Meeting of APCA. St. Louis, Missouri. June 14-19, 1970.
4. Perry, Robert H., Cecil H. Chilton, and Sidney D. Kirkpatrick. (editors). Chemical Engineers' Handbook. Fourth Edition. McGraw-Hill Book Company. New York, 1963.

APPENDIX

TABLE I: Summary of Results

Pitot Tube Number	Pitot Tube Dimensions				Geometric Misalignment*				Amount of Field Use**	Coefficients		A-to-B Side Difference
	Tube Length (in.)	Impact Plane Separation (in.)	Impact Opening Size (in. x 10^{-2}) A(l x w)	B(l x w)	Transverse Axis	Longitudinal Axis	Length	Planar		$\overline{C}_p$ A-side	$\overline{C}_p$ B-side	
2-02	30	0.828	53 x 33	56 x 33	5° A	1° B	1/16"	1/16"	E	0.805	0.805	-
2-03	31	0.847	47 x 28	47 x 28	4° A	3° B	-	-	E	0.849	0.855	0.006
2-05	30	0.798	56 x 31	56 x 31	3° B	4° B	1/16"	-	E	0.855	0.861	0.006
2-07	29	0.825	56 x 33	56 x 33	2° A	-	-	-	E	0.835	0.854	0.019
2-08	29	0.795	56 x 33	58 x 33	3° A	4° B	1/16"	1/32"	E	0.821	0.815	0.006
2-09	31	0.857	47 x 28	47 x 28	2° A	2° B	-	-	N	0.848	0.850	0.002
3-03	40	0.794	56 x 31	59 x 33	5° B	4° B	-	1/32"	E	0.855	0.855	-
3-04	41	0.752	59 x 38	52 x 31	-	6° B	-	-	E	0.858	0.864	0.006
3-05	41	0.775	56 x 31	56 x 31	2° A	5° B	1/16"	-	E	0.852	0.852	-
3-06	43	0.850	47 x 28	47 x 28	4° A	2° B	-	-	N	0.853	0.850	0.003
3-07	36	0.797	56 x 33	53 x 31	4° B	5° B	-	-	E	0.862	0.859	0.003
4-02	52	0.820	53 x 34	56 x 33	2° A	2° B	-	-	E	0.830	0.827	0.003
4-03	51	0.891	45 x 27	45 x 27	5° A	-	-	-	L	0.847	0.850	0.003

* Note: The angular values listed in the "Transverse Axis" and "Longitudinal Axis" columns above refer to the total number of degrees by which the impact plane(s) were misaligned with respect to those axes; the letter "A" indicates that only one plane was misaligned, while "B" signifies that both were misaligned. The angular values are estimates, based on micrometer readings taken prior to calibration; the "Mathematical Models" section of the Appendix shows how these estimates were made. The numerical values listed in the "Length" and "Planar" misalignment columns above refer, respectively, to dimensions x and y of Figures 6b and 6c.

**Note: The letters E, L, and N stand for "Extensive," "Limited," and "None," respectively.

TABLE I: Summary of Results

(Continued)

Pitot Tube Number	Pitot Tube Dimensions				Geometric Misalignment				Amount of Field Use	Coefficients		A-to-B Side Difference
	Tube Length (in.)	Impact Plane Separation (in.)	Impact Opening Size (in. x 10-2)		Transverse Axis	Longitudinal Axis	Length	Planar		$\overline{C}_p$ A-side	$\overline{C}_p$ B-side	
			A(l x w)	B(l x w)								
4-04	51	0.812	58 x 31	55 x 34	-	-	-	1/32"	E	0.815	0.815	-
4-05	50	0.819	47 x 28	47 x 28	2° A	3° A	-	-	N	0.853	0.856	0.003
4-06	50	0.871	47 x 28	47 x 28	1° A	-	-	-	N	0.857	0.853	0.004
4-07	50	0.850	47 x 28	47 x 28	2° A	2° B	-	-	N	0.857	0.853	0.004
4-08	51	0.895	45 x 27	45 x 27	9° A	-	-	-	L	0.846	0.851	0.005
4-09	52	0.776	56 x 31	53 x 31	4° A	6° B	-	-	E	0.855	0.864	0.009
4-10	50	0.849	47 x 28	47 x 28	4° A	1° B	-	-	L	0.854	0.853	0.001
4-11	50	0.886	48 x 28	50 x 28	-	-	1/16"	-	L	0.859	0.839	0.020
4-14	48	0.812	47 x 28	47 x 28	9° B	2° B	-	-	L	0.853	0.857	0.004
4-15	56	1.079	55 x 28	55 x 28	-	-	-	-	L	0.845	0.841	0.004
4-16	55	1.070	56 x 28	55 x 28	-	-	-	-	E	0.843	0.850	0.007
4-17	48	0.821	48 x 28	48 x 28	6° B	1° A	-	-	N	0.851	0.856	0.005
4-18	50	0.868	47 x 28	48 x 28	8° B	1° B	-	-	L	0.850	0.851	0.001

TABLE I: Summary of Results
(Continued)

Pitot Tube Number	Pitot Tube Dimensions				Geometric Misalignment				Amount of Field Use	Coefficients		A-to-B Side Difference
	Tube Length (in.)	Impact Plane Separation (in.)	Impact Opening Size (in. x 10^{-2})		Transverse Axis	Longitudinal Axis	Length	Planar		$\overline{C}_p$ A-side	$\overline{C}_p$ B-side	
			A(l x w)	B(l x w)								
4-19	52	0.941	44 x 27	47 x 28	3° A	1° B	1/16"	1/32"	E	0.834	0.855	0.021
4-20	54	0.844	48 x 28	48 x 28	-	-	-	-	N	0.846	0.853	0.007
4-21	50	0.815	55 x 33	56 x 33	-	2° A	-	-	E	0.845	0.855	0.010
4-22	48	0.818	47 x 28	47 x 28	3° B	-	-	-	N	0.848	0.848	-
5-01	66	0.865	47 x 28	47 x 28	3° A	1° B	-	-	L	0.852	0.851	0.001
5-02	66	0.864	47 x 28	47 x 28	2° A	1° B	-	-	L	0.854	0.842	0.012
5-03	66	0.858	47 x 28	47 x 28	5° B	1° B	-	-	L	0.853	0.850	0.003
5-05	63	0.962	45 x 28	45 x 28	9° B	3° B	-	-	L	0.848	0.847	0.001
5-06	66	0.865	47 x 28	47 x 28	2° A	1° B	-	-	N	0.843	0.849	0.006
5-07	66	0.875	47 x 28	47 x 28	3° A	-	-	-	N	0.852	0.855	0.003
5-08	65	0.800	53 x 32	56 x 32	2° A	4° B	1/16"	-	E	0.845	0.843	0.002
5-09	66	0.864	47 x 28	47 x 28	3° A	1° B	-	-	L	0.855	0.850	0.005
6-01	76	0.679	55 x 33	53 x 30	8° B	16° B	-	1/32"	E	0.864	0.880	0.016

(Continued)

Pitot Tube Number	Pitot Tube Dimensions				Geometric Misalignment				Amount of Field Use	Coefficients		A-to-B Side Difference
	Tube Length (in.)	Impact Plane Separation (in.)	Impact Opening Size (in. x 10^{-2})		Transverse Axis	Longitudinal Axis	Length	Planar		$\bar{C}_p$ A-side	$\bar{C}_p$ B-side	
			A(l x w)	B(l x w)								
6-02	76	0.845	47 x 28	47 x 28	6° B	-	-	-	L	0.844	0.847	0.003
6-03	76	0.818	56 x 31	53 x 31	4° B	3° B	1/16"	-	E	0.861	0.848	0.013
6-05	72	0.795	50 x 28	48 x 27	6° A	5° B	-	1/16"	N	0.853	0.852	0.001
6-06	72	0.845	47 x 28	47 x 28	11° B	-	-	-	L	0.846	0.855	0.009
6-07	72	0.831	47 x 28	47 x 28	6° A	-	-	-	L	0.851	0.845	0.006
7-01	88	0.875	47 x 28	47 x 28	8° B	-	-	-	N	0.842	0.848	0.006
7-02	89	0.778	59 x 30	59 x 31	6° A	5° B	-	-	E	0.840	0.849	0.009
7-03	93	0.884	47 x 28	47 x 28	5° B	-	-	-	E	0.840	0.843	0.003
8-01	96	0.841	50 x 28	50 x 28	5° B	-	-	-	N	0.839	0.844	0.005
8-02	96	0.875	47 x 28	47 x 28	4° B	1° B	-	-	L	0.847	0.841	0.006
9-01	113	0.906	56 x 31	58 x 31	11° B	2° B	-	1/32"	E	0.840	0.843	0.003
9-02	112	0.884	47 x 28	47 x 28	11° B	1° B	-	-	E	0.850	0.847	0.003

STATISTICAL CONSIDERATIONS

The 102 values of $\overline{C}_p$ (the average A or B side pitot tube coefficient) obtained by calibration had a mean value of 0.848 and an average deviation of 0.008. The following formula was used to compute the average deviation:

$$\sigma = \frac{\sum_{1}^{n} \left| x_i - \overline{x} \right|}{n}$$

where:

σ = average deviation

n = number of coefficients = 102

$\overline{x}$ = mean coefficient value = 0.848

x_i = individual coefficient value.

About 75 percent of the coefficients were within one average deviation (σ) of the mean; 91 percent were within 2σ, and 98 percent were within 4σ. Figure A-1 represents this graphically.

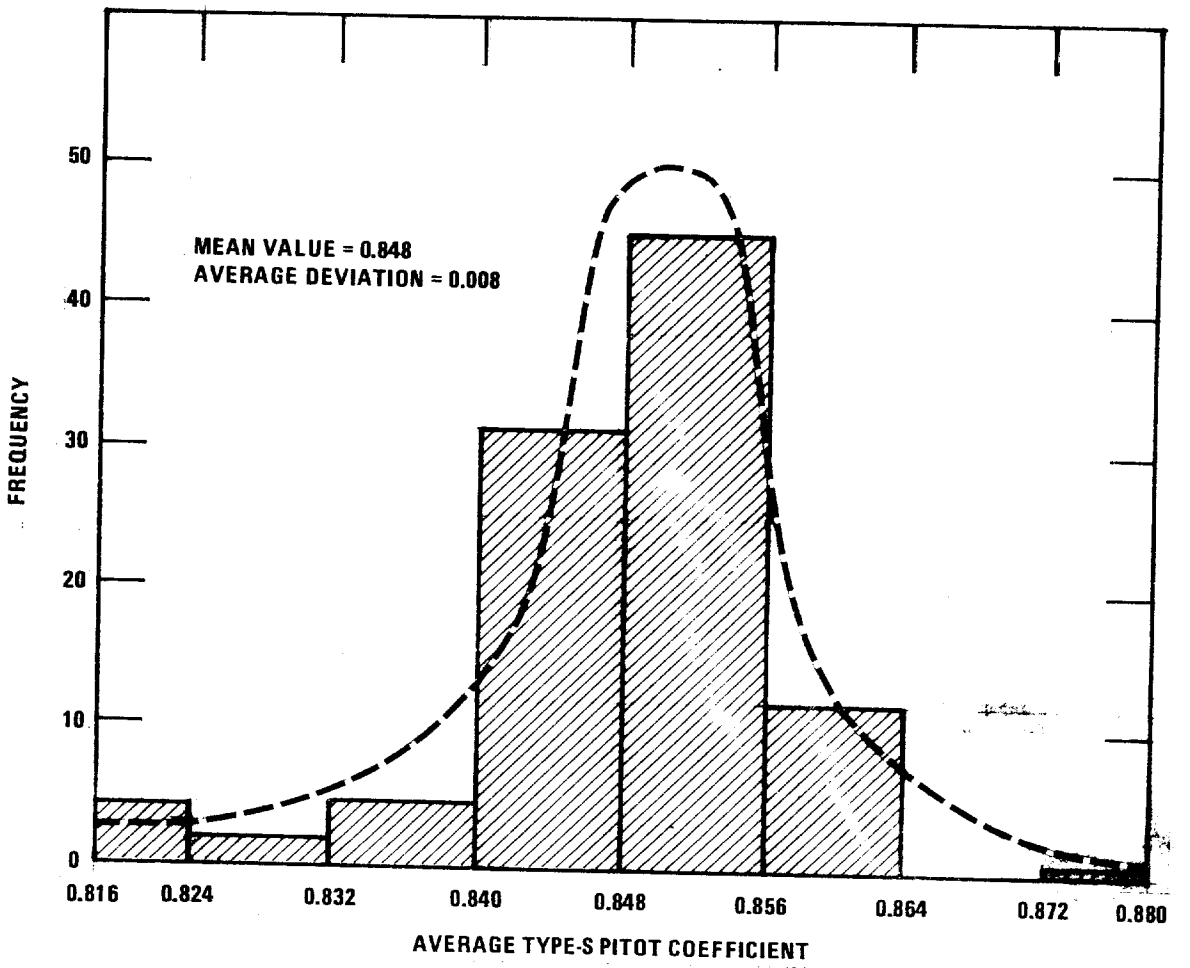

Figure A-1. Frequency distribution of $\overline{Cp}$ values.

EXPERIMENTAL ERROR CONSIDERATIONS

It has been shown (Figure 9) that because of the sensitivity limitations of the gage-oil manometer used in this study, each ΔP could be read only to the nearest 0.005 in. H_2O, thus making the uncertainty of each recorded value of ΔP about 0.002 to 0.003 in. H_2O. The uncertainty of each C_p value (calculated from two such ΔP readings) is, consequently, greater than this. Consider the following example:

Suppose that during calibration, values of ΔP_{std} and ΔP_s equal to 0.300 in. H_2O and 0.400 in. H_2O, respectively, are read and recorded. The recorded value of C_p, based on these readings, would then be (by Equation 1):

$$C_p = 0.99 \sqrt{0.300/0.400} = 0.857$$

Note that although ΔP_{std} was read and recorded as 0.300 in H_2O its true value could have been as high as 0.303 in. H_2O or as low as 0.298 in. H_2O; similarily, ΔP_s could have been as high as 0.403 in. H_2O or as low as 0.398 in. H_2O. Therefore, the value of C_p, recorded as 0.857, could have been (considering only the extreme cases) as high as $0.99 \sqrt{0.303/0.398} = 0.864$, or as low as $0.99 \sqrt{0.298/0.403} = 0.851$. Thus, because of the sensitivity limitations of the manometer, each value of C_p is uncertain by about $\pm$ 0.006. Note, however, that additional uncertainty allowances in C_p are still needed, first to cover possible errors by the observer, in reading the manometer (e.g., because of parallax or incorrect "sight-weighted" averaging of minor flow pulsations) and in handling and aligning the pitot tubes, and second, to account for the uncertainty of the value of the standard pitot tube coefficient. Therefore, an experimental error tolerance of $\pm$ 0.005 (arbitrary) will be assigned to each C_p value to cover observer error, and an additional allowance of $\pm$ 0.01 will be made to account for uncertainty in the value of C_p (standard). Thus, the total uncertainty of each recorded value of C_p is approximately $\pm$ 0.02.

MATHEMATICAL MODELS

In this study four types of impact-plane misalignment with respect to the transverse and longitudinal tube axes were observed. A mathematical model of each type, showing how estimates of misalignment angle were made, is presented below:

1. Transverse Axis Misalignment (one plane only)

In end view, the shape of the pitot tube can be approximated by a trapezoid, with bases b and b', and height h (see Figure A-2). The bases b and b' correspond to micrometer readings M_2 and M_1, respectively (in inches).

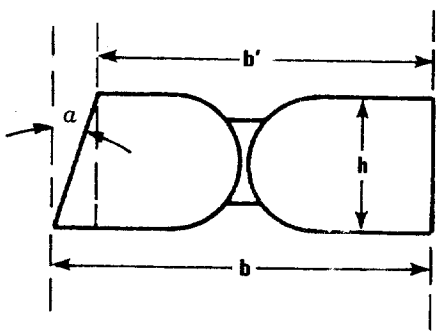

Figure A-2. Transverse axis misalignment, one plane only.

The height h is approximately 0.375 in., since the pitot tube is made of 3/8 in. o.d. stainless steel. The "transverse skew angle," α, can be estimated, making use of the fact that alternate interior angles are equal, as follows:

$$\tan \alpha = \frac{b - b'}{h} = \frac{M_2 - M_1}{0.375}$$

$$\alpha = \arctan \frac{M_2 - M_1}{0.375}$$

2. Transverse Axis Misalignment (both planes)

The approximations are similar to those made for case 1 above, except that the "total" transverse skew angle, $(\alpha_1 + \alpha_2)$, is measured (see Figure A-3). The tangent of the sum of two angles is

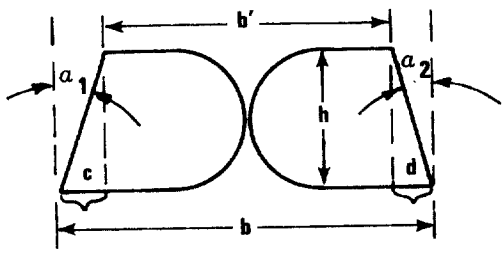

Figure A-3. Transverse axis misalignment, both planes.

determined as follows:

$$\tan(\alpha_1 + \alpha_2) = \frac{\tan\alpha_1 + \tan\alpha_2}{1 + \tan\alpha_1 \tan\alpha_2}$$

Referring to Figure 3A, $\tan\alpha_1 = c/h$, $\tan\alpha_2 = d/h$, and $b - b' = c + d$. Substituting these into the formula for $\tan(\alpha_1 + \alpha_2)$ gives:

$$\tan(\alpha_1 + \alpha_2) = \frac{c/h + d/h}{1 + (c/h)(d/h)} = \frac{c + d}{h + cd} = \frac{b - b'}{h + cd}$$

The height, h, will again be 0.375 in., and b - b' will be the micrometer difference, $M_2 - M_1$. The product, cd, will be negligibly small unless α_1 and α_2 are very large; therefore, the expression can be reduced to:

$$\tan(\alpha_1 + \alpha_2) = \frac{b - b'}{h} = \frac{M_2 - M_1}{0.375},$$

which is the same formula used in case 1 above. Solving for $(\alpha_1 + \alpha_2)$ gives:

$$(\alpha_1 + \alpha_2) = \text{arc tan } \frac{M_2 - M_1}{0.375}$$

3. Longitudinal Axis Misalignment (one plane only)

The mathematical model for this type of misalignment is a trapezoid (see Figure A-4).

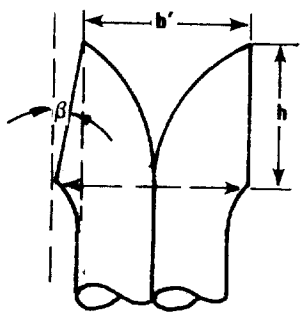

Figure A-4. Longitudinal axis misalignment, one plane only.

The "longtitudinal skew angle," β, is determined by the following formula:

$$\beta = \text{arc tan } \frac{b - b'}{h}$$

In the above formula, b and b' are, respectively, micrometer readings M_4 and M_3; h, the height of the trapezoid, is equal to the projected length of the properly aligned impact opening.

4. Longitudinal Axis Misalignment (both planes)

Using approximations (for the sum of the tangents of two angles) similar to those in case 1 above, the formula for this type of misalignment (see Figure 5A) is:

$$(\beta_1 + \beta_2) = \text{arc tan } \frac{M_4 - M_3}{h}\ ^*$$

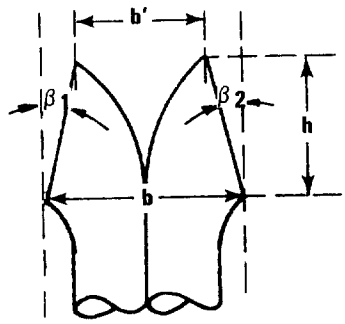

Figure A-5. Longitudinal axis misalignment, both planes.

---

* Note: For small values of β, the height of the trapezoid, h, can be taken to be equal to the projected length of either impact opening, without appreciable error.

THE EFFECT OF AERODYNAMIC INTERFERENCE BETWEEN A TYPE-S PITOT TUBE AND SAMPLING NOZZLE ON THE VALUE OF THE PITOT TUBE COEFFICIENT

Robert F. Vollaro[a]

Introduction

In source sampling, the Type-S pitot tube is the instrument most commonly used to measure stack gas velocity. Before a Type-S pitot tube is used in the field, however, its coefficient (C_p) should be known. The value of C_p is usually determined by calibration against a standard pitot tube, although in many past instances, a "theoretical" C_p value of 0.85 has been assigned to the pitot tube, without calibration.*

Within the past year, however, certain observers have questioned the validity of using, in actual field test situations, either an assumed value of C_p or one obtained by laboratory calibration. It has come to light that when a Type-S pitot tube is used in its customary source-sampling configuration (i.e., attached to a probe sheath, with its impact openings adjacent to a sampling nozzle) the value of C_p can be significantly reduced.[1,2] The reduction in C_p is caused by aerodynamic interference between the pitot tube and nozzle; this interference phenomenon has been shown to be a downstream effect; i.e., it causes a decrease in pressure on the static side of the pitot tube.[1,2] It is believed that the closely spaced pitot tube and nozzle " ... act somewhat as a venturi. The velocity in the space between the tubes ... will be higher than free stream velocity, thereby reducing the static pressure."[1]

---

* This has been thought to be acceptable because Type-S pitot tube coefficients generally range from about 0.83 to 0.87 (Reference 4).

[a] Emission Measurement Branch, ESED, OAQPS, EPA, RTP, NC, June 1975

Consequently, when aerodynamic interference is present, taking C_p to be equal to either 0.85 or a laboratory calibration value* can result in significant velocity measurement error. Accordingly, in February 1975, investigators conducted a study to determine (1) the minimum distance needed between a Type-S pitot tube and sampling nozzle to prevent aerodynamic interference, and (2) whether or not this distance requirement is met when sampling nozzles of various sizes are attached to a probe constructed in compliance with the current guidelines (APTD-0581)[3]. This paper discusses the study, its results, and the significance of these results.

Experimental Set-Up

The effects of aerodynamic interference between a Type-S pitot tube and sampling nozzle on the value of C_p were studied in a wind tunnel with a test section diameter of 12 inches. The experiments consisted of three sets of pitot tube calibrations; in each set, the effects of one particular nozzle size were investigated. Three nozzle sizes - 1/2-inch, 3/8-inch, and 1/2-inch (i.d.) - were studied; to ensure representativeness, each nozzle size was examined at test section velocities approximately equal to those at which the nozzle is ordinarily used in the field.**

At the outset of each set of calibrations, a "background" or reference coefficient for the Type-S pitot tube was obtained by calibrating it, with the sampling nozzle removed, against a standard pitot tube. Calibration was then repeated several times with the nozzle in place, varying only the separation

---

* Unless, of course, calibration was done in the presence of a nozzle.

** For example, a 1/2-inch nozzle is generally used for isokinetic sampling when velocities are about 15 ft/sec or less; therefore, 1/2-inch nozzle interference was studied at test section velocites around 12 ft/sec.

distance (dimension "X", Figure 1) between the pitot tube and nozzle. Initially, the gap was set small enough so that the C_p value obtained was markedly lower than the background value. The gap was then gradually

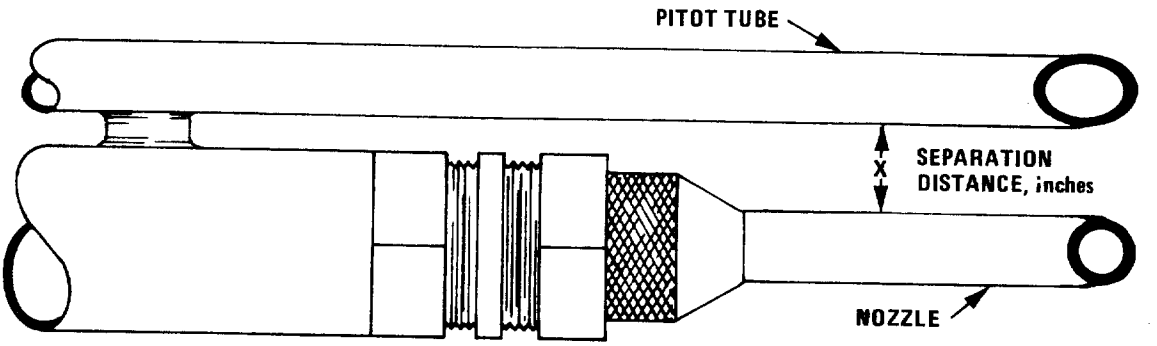

Figure 1. Type-S pitot tube with sampling nozzle in place.

widened until C_p became equal (within experimental error) to the reference value; the value of "X" at which this occurred was assumed to be the minimum pitot-nozzle separation distance needed to prevent aerodynamic interference.

Summary of Results

As shown in Table I, for all three nozzle sizes studied, interference effects become negligible when the gap between the nozzle and pitot tube is about 3/4-inch. It thus becomes clear that the separation distances of 1/2-inch, 7/16-inch, and 3/8-inch which result, respectively, from attachment of 1/4-inch, 3/8-inch, and 1/2-inch (i.d.) nozzles to a pitobe assembly constructed according to the APTD-0581 guidelines, are too small to prevent interference; velocity measurement errors of 6 percent or more are likely to occur at these spacings.

Conclusions

A study of the effect of aerodynamic interference between a Type-S pitot tube and sampling nozzle on the value of the pitot tube coefficient (C_p) has demonstrated the following:

1. When a Type-S pitot tube is used in the presence of a sampling nozzle, there should be at least 3/4-inch free-space between the tube and nozzle, in order to prevent reduction in the effective value of C_p as a result of aerodynamic interference.

2. When sampling nozzles (1/4-inch i.d. and larger) are attached to pitobe assemblies constructed according to the guidelines in APTD-0581, the resulting pitot tube-nozzle separation distances will be much less than 3/4-inch, and hence insufficient to prevent interference.

3. When pitot tube-nozzle interference is present, the use of either an assumed value of 0.85 for C_p or a laboratory calibration value (i.e., one which was not obtained in the presence of a nozzle) can result in velocity measurement errors of 6 percent or more.

Recommendations

To improve the accuracy of velocity measurements made with a Type-S pitot tube when it is used in the presence of a sampling nozzle, either of the following can be done:

1. Construct pitobes so as to provide a separation distance of at least 3/4-inch between the nozzle and pitot tube, with the largest size sampling nozzle (1/2-inch i.d.) in place. This necessitates that the

Table I. SUMMARY OF RESULTS[a]

Case	Reference value of Type-S pitot coefficient (C_p*)	Actual value of Type-S pitot coefficient (C_p)	True velocity measured by standard pitot tube, ft/min	Apparent velocity based on C_p* value, ft/min	Velocity error from interference, %
1/4-in. nozzle gap=1/2-in.	0.815	0.768	2,290	2,430	6.1
1/4-in. nozzle gap=19/32-in.	0.815	0.793	2,315	2,375	2.6
1/4-in. nozzle gap=3/4-in.	0.815	0.808	2,320	2,340	0.9
3/8-in. nozzle gap=7/16-in.	0.814	0.749	1,455	1,585	8.9
3/8-in. nozzle gap=19/32-in.	0.814	0.769	1,470	1,560	6.1
3/8-in. nozzle gap=11/16-in.	0.814	0.811	1,510	1,515	0.3
1/2-in. nozzle gap=7/16-in.	0.822	0.789	680	705	3.7
1/2-in. nozzle gap=5/8-in.	0.822	0.772	645	690	7.0
1/2-in. nozzle gap=11/16-in.	0.822	0.788	660	690	4.4
1/2-in. nozzle gap=25/32-in.	0.822	0.812	690	690	0.0

[a] Each listed value of C_p* and C_p is the average of three independent determinations. All velocity values were calculated using the pitot tube equation (Equation 2-2 of Reference #5).

pitot tube be welded to the probe sheath with short pieces of 5/8-inch (o.d.) stainless steel tubing, instead of the 1/4-inch pieces currently specified in APTD-0581.

2. Calibrate Type-S pitot tubes after installation in the pitobe assembly and in the presence of various size sampling nozzles. The calibration should be performed in the velocity range associated with the respective nozzle sizes.

References

1. Davini, R. J. and D. G. DeCoursin. Progress Report No. 7; Particulate Sampling Strategies for Mechanically Disturbed and Cyclonic Flow; Period January 1 - January 31, 1974. Prepared for EPA by FluiDyne Engineering Corporation; Minneapolis, Minnesota. February 19, 1974.
2. Vollaro, R. F. and P. R. Westlin. Environmental Protection Agency; Durham, N. C.. January 1974. (Unpublished data)
3. Martin, R. M.. Construction Details of Isokinetic Source-Sampling Equipment. Environmental Protection Agency Publication Number APTD-0581. April 1971.
4. Smith, W. S., W. F. Todd, and R. T. Shigehara. Significance of Errors in Stack Sampling Measurements. (Presented at the Annual Meeting of APCA. St. Louis, Missouri. June 14 - 19, 1970)
5. Standards of Performance for New Stationary Sources. Federal Register. 36 (247) December 23, 1971.

THE EFFECTS OF THE PRESENCE OF A PROBE SHEATH ON TYPE-S PITOT TUBE ACCURACY

Robert F. Vollaro*

INTRODUCTION

A number of recent studies have demonstrated that the coefficient (C_p) of a Type-S pitot tube can be substantially lowered when the tube is used as a component of a pitobe assembly (i.e., when the tube is attached to a sample probe equipped with a nozzle and thermocouple).[1,2,3] Complex aerodynamic interactions between the pitot tube and the other components of the assembly are believed to be responsible for the reduction in the value of C_p. The effects of the presence of a sampling nozzle and thermocouple on C_p have been extensively studied.[1,2] Considerably less is known, however, about the way in which a probe sheath affects C_p. Certain observers have reported reductions of up to 5 percent in the value of C_p, believed to be directly attributable to the presence of a probe sheath.[1,4] However, none of the studies cited has discovered the exact nature (mechanism) of this reduction; therefore, it has not been possible, to date, to adjust for it properly during calibration and field use of pitobe assemblies.

When it is attached to a sample probe, a Type-S pitot tube is ordinarily attached in such a way that the center of the sampling nozzle (when in place) will be in line with the center of the pitot tube impact openings (Figure 1). This will, in most cases, leave a distance of 2 to 4 inches between the center of the pitot tube openings and the leading edge of the sample probe (dimension "y", Figure 1). Some observers are of the opinion that a 2-to-4-inch separation distance is insufficient to prevent aerodynamic interactions between the probe and pitot tube; hence, they believe aerodynamic interference to be the cause of the

* Emission Measurement Branch, ESED, OAQPS, EPA, RTP, NC, November 1975

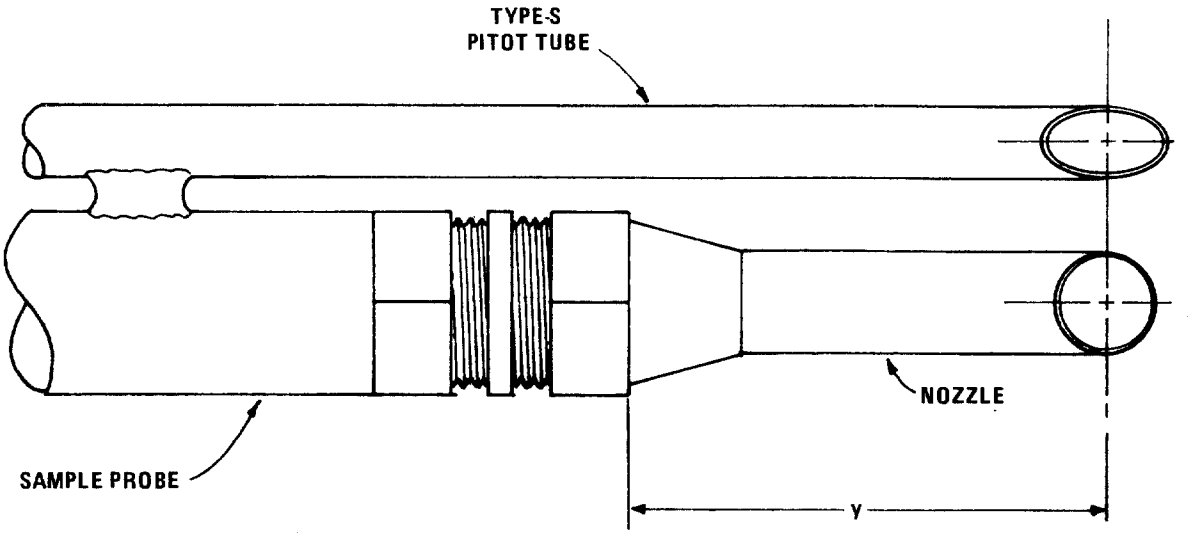

Figure 1. Type-S pitot tube, attached to sample probe.

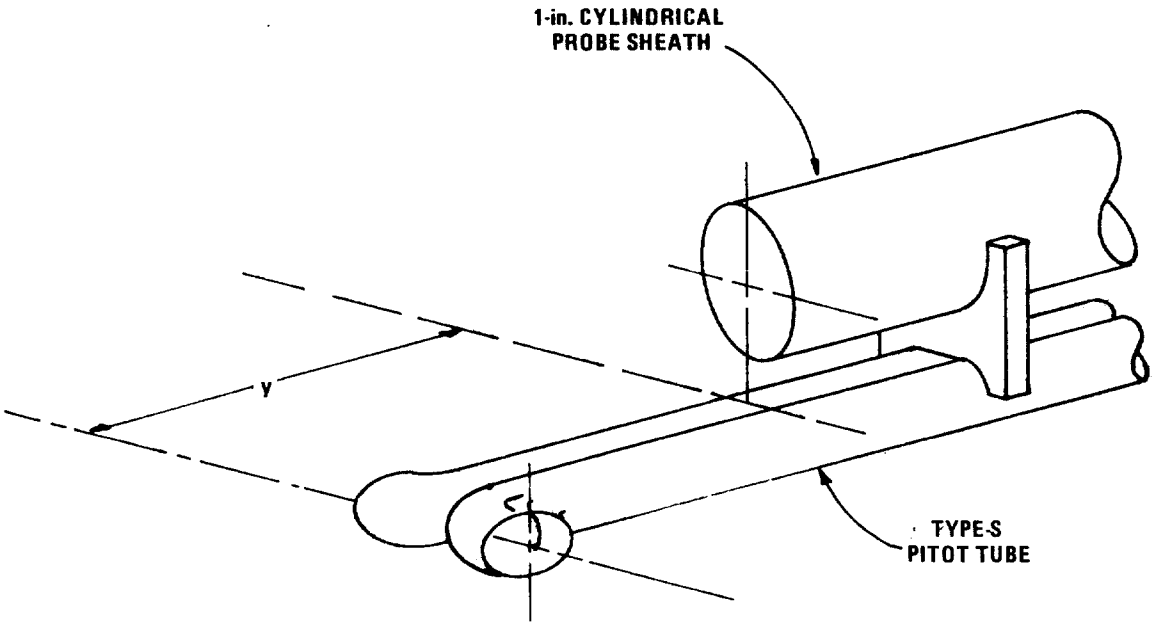

Figure 2. Type-S pitot tube and 1-in. cylindrical probe sheath (Experiment # 1).

probe sheath effect. Others believe, however, that a distance of 2 to 4 inches between the probe and pitot tube openings is more than adequate to eliminate pitot tube-probe sheath interference; and that the pseudo-high velocity head (ΔP) readings and consequent decrease in the value of C_p are the result of a reduction in the effective cross-sectional area of the duct caused by the probe sheath. The question of the nature of the probe sheath effect has not been resolved chiefly because all of the studies reporting a sheath effect were done in small calibration ducts, in which cross-section blockage could have been significant.[1,4] In view of this, experiments were recently undertaken to determine the nature and magnitude of the probe sheath effect. This paper presents the results of the experiments and discusses their significance.

EXPERIMENT #1

SET-UP AND PROCEDURE

The first experiment was done in a wind tunnel having a test-section diameter of 12 inches. At the outset of the experiment, the fan was turned on, generating a test-section velocity of about 2500 ft/min. A Type-S pitot tube was inserted 7 inches into the duct, and aligned so that the pitot impact openings were perpendicular to the direction of flow. The pitot tube was connected to an inclined manometer, and a velocity head (ΔP_s) reading was taken and recorded. Next, the effects of the presence of a probe sheath on the value of ΔP_s were observed. A 1-inch (diameter) cylindrical probe sheath was inserted into the duct, alongside the Type-S pitot tube (see Figure 2). The only variable for the remainder of the experiment was the distance between the center of the pitot tube impact openings and the leading edge of the probe sheath (dimension "y", Figure 2). Velocity head readings were taken at six different values of "y", i.e., y = 6, 5, 4, 3, 2, and 1 inches. Three experimental runs were performed.

RESULTS

The results of the experiment are presented in Table I. Table I shows that as the distance "y" decreased, the manometer reading steadily increased. In the range y = 2 inches to y = 4 inches (which is the range of pitot-probe sheath separation in most pitobe assemblies), the probe sheath caused velocity measurement errors of 1.4 to 4.4 percent.

An attempt was made, based on the results of Experiment #1, to deduce the nature of the probe sheath effect. The hypothesis that the effect is caused by a reduction in the cross-sectional area of the duct by the probe sheath (see Introduction) was tested. A projected-area model of the probe sheath was made as shown in Figure 3. For each value of "y", the percentage theoretical blockage of the duct cross-section was calculated, based on the model, as follows:

$$\text{Percentage theoretical blockage} = \left[\frac{l \times w}{A}\right] \times 100 \qquad \text{(Equation 1)}$$

Where:

l = length of sheath segment inside the duct, in.

w = projected width of sheath segment, in.

A = cross-sectional area of the calibration duct, in.^{2}

According to this model, a 1:1 correspondence would be expected to exist between percentage theoretical blockage (i.e., the percentage decrease in the duct area) and the percentage increase in gas velocity, based on the equation of continuity for steady flow:

$$Q = A_e V \qquad \text{(Equation 2)}$$

Where:

Q = total gas volumetric flow rate, ft^3/sec

Table I. DATA FROM EXPERIMENT #1

Distance (y), in.	Velocity * head (ΔP_s), in. H_2O	$\sqrt{\Delta P_s}$ **	Increase in velocity, %
-	0.536	0.732	-
6	0.536	0.732	0.0
5	0.540	0.735	0.4
4	0.550	0.742	1.4
3	0.562	0.750	2.5
2	0.583	0.764	4.4
1	0.625	0.791	8.1

* Average of three experimental runs.

** Proportional to velocity.

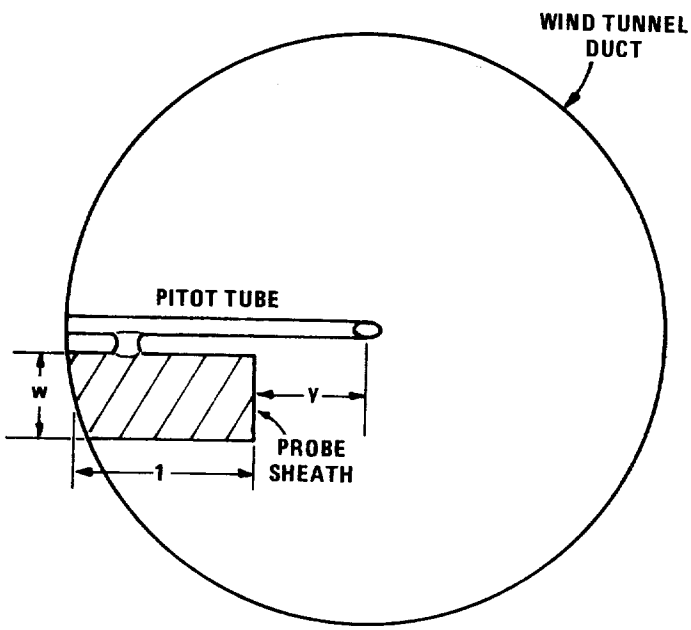

$$\text{PERCENTAGE THEORETICAL BLOCKAGE} = \left[\frac{l \times w}{\text{DUCT AREA}}\right] \times 100$$

Figure 3. Projected-area model of probe sheath.

A_e = effective duct cross-sectional area, ft^2

V = velocity of flowing gas stream, ft/sec

In actuality, however, the experimental results do not show this correspondence (see Table II and Figure 4). For values of "y" greater than or equal to 3 inches, the increase in velocity was consistently less than the increase predicted by Equation 2; at y = 2 inches, the theoretical and actual values were approximately equal; at y = 1 inch, the actual increase in velocity surpassed the theoretical. The following suggestions were put forth as possible explanations of these results:

1. The sheath effect is not a blockage effect at all, but is caused instead by aerodynamic interference between the pitot tube and probe sheath; hence, it is independent of sheath segment size, and is a function only of of the separation distance, "y".

2. The effect is a combination of blockage and aerodynamic interference in varying relative proportions, with the former effect dominating at the larger values of "y" ($\geq$ 3 inches), and the latter beginning to become important at smaller values of "y". A possible reason that, for $y \geq 3$ inches, the actual increase in velocity was less than the theoretical, is that the probe sheath is a cylinder, not a rectangular solid, and therefore does not actually effectively block that percentage of the duct cross-section predicted by the rectangular projected-area model.

Therefore, based on the results of Experiment #1, it was not possible to come to a definite conclusion about the nature of the probe sheath effect.

EXPERIMENT #2

SET-UP AND PROCEDURE

Experiment #2 was essentially the same as experiment #1, except that the

Table II. PROJECTED-AREA, EQUATION OF CONTINUITY MODEL OF DATA FROM EXPERIMENT #1

Distance (y), in.	Theoretical Blockage, %*	Theoretical increase in velocity, %**	Actual increase in velocity, %
6	0.9	0.9	0.0
5	1.7	1.7	0.4
4	2.6	2.6	1.4
3	3.4	3.4	2.5
2	4.3	4.3	4.4
1	5.2	5.2	8.1

* From projected-area model of sheath segment.

** Predicted by equation of continuity, Q = AeV.

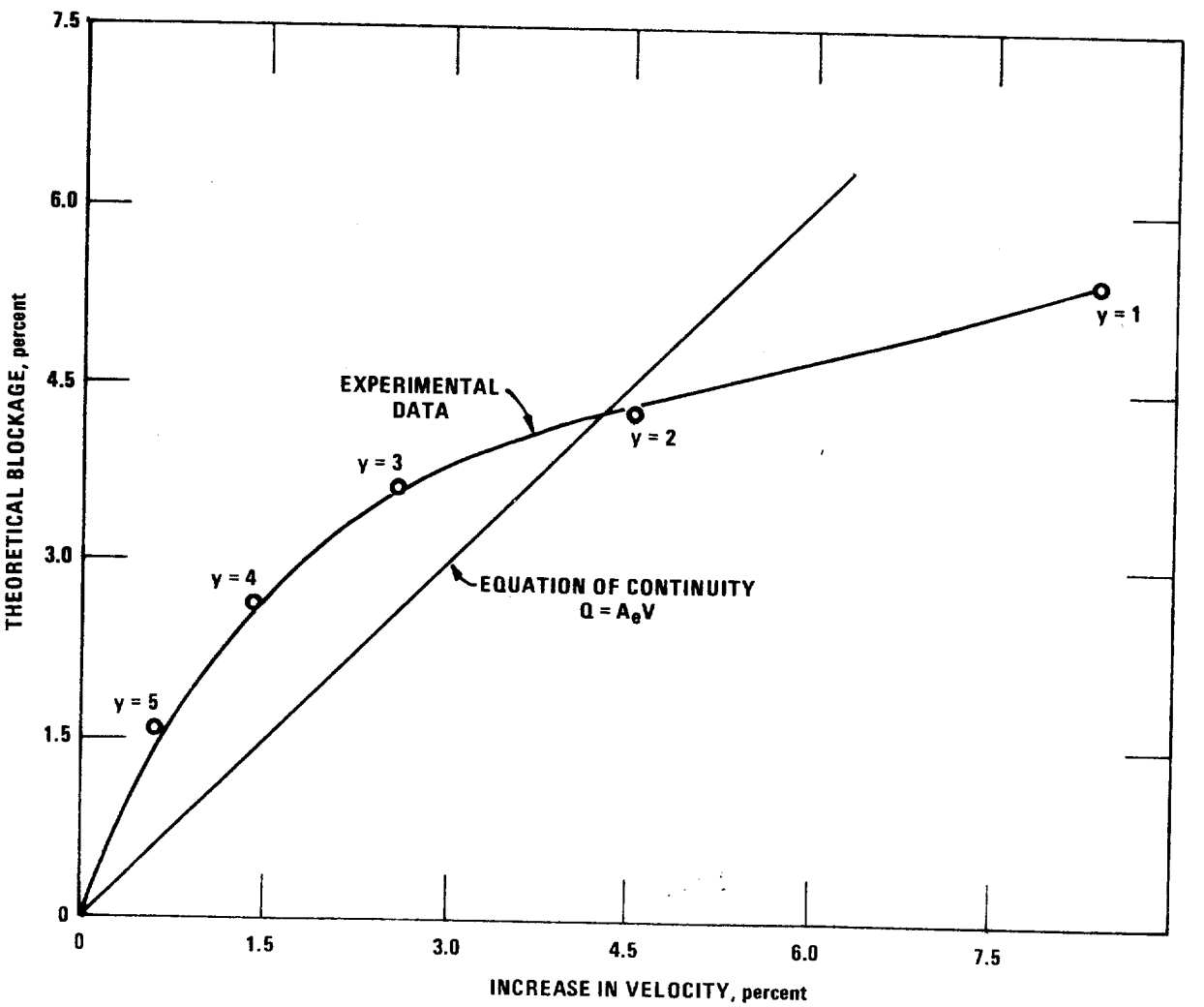

Figure 4. Graphical representation of projected-area, equation of continuity model of data from Experiment # 1.

cylindrical probe sheath was replaced by a 1-inch rectangular solid (see Figure 5). The purpose of this experiment was to test hypothesis "b" of the preceding section, i.e., that the sheath effect is a combination of blockage and aerodynamic interference, in varying relative proportions, depending on the value of "y". As in Experiment #1, velocity head readings were taken at values of "y" equal to 6, 5, 4, 3, 2 and 1 inches; three experimental runs were performed.

RESULTS

The results of experiment #2 are presented in Table III. Once again, a consistent increase in the velocity head readings was observed as the value of "y" decreased. This time, however, the velocity measurement errors ranged from 2.8 to 7.8 percent in the normal pitot - sheath separation range (i.e., y = 2 to 4 inches); these errors are considerably greater than those obtained in experiment #1 with the cylindrical sheath.

As in experiment #1, a projected-area model was made for each value of "y", and a comparison was made between the actual increase in velocity and the theoretical increase predicted by the model and the equation of continuity. The results of this endeavor are presented in Table IV and in Figure 6. It is evident from these results that the correspondence between the percentage theoretical blockage and the actual velocity increase was nearly 1:1 for values of "y" greater than or equal to 3 inches. However, for y = 2 inches and y = 1 inch, the actual velocity increase surpassed the theoretical. From this it can be concluded that hypothesis #2 above, that the probe sheath effect is a combination of blockage and aerodynamic interference in varying relative proportions (depending upon the value of "y"), is valid. At $y \geq 3$ inches, the blockage effect is dominant and aerodynamic interference is minimal; for "y" values less than 3 inches, the total sheath effect becomes a

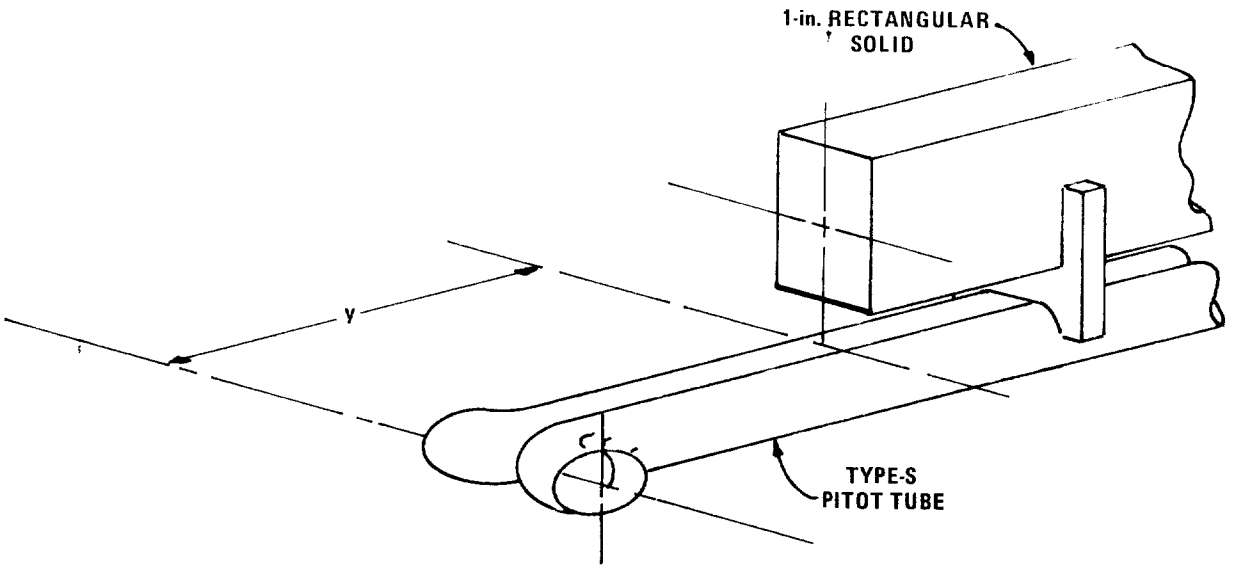

Figure 5. Type-S pitot tube and 1-in. rectangular solid (Experiment # 2).

Table III. DATA FROM EXPERIMENT #2

Distance (y), in.	Velocity* head (ΔP_s), in. H_2O	$\sqrt{\Delta P_s}$ **	Increase in velocity, %
-	0.522	0.722	-
6	0.527	0.726	0.6
5	0.540	0.735	1.8
4	0.550	0.742	2.8
3	0.564	0.751	4.0
2	0.605	0.778	7.8
1	0.663	0.814	12.7

*Average of three experimental runs.

**Proportional to velocity.

Table IV. PROJECTED-AREA, EQUATION OF CONTINUITY MODEL OF DATA FROM EXPERIMENT # 2

Distance (y), in.	Theoretical blockage, %*	Theoretical increase in velocity, %**	Actual increase in velocity, %
6	0.9	0.9	0.6
5	1.7	1.7	1.8
4	2.6	2.6	2.8
3	3.4	3.4	4.0
2	4.3	4.3	7.8
1	5.2	5.2	12.7

*From projected-area model of sheath segment.

**Predicted by equation of continuity, $Q = A_e V$.

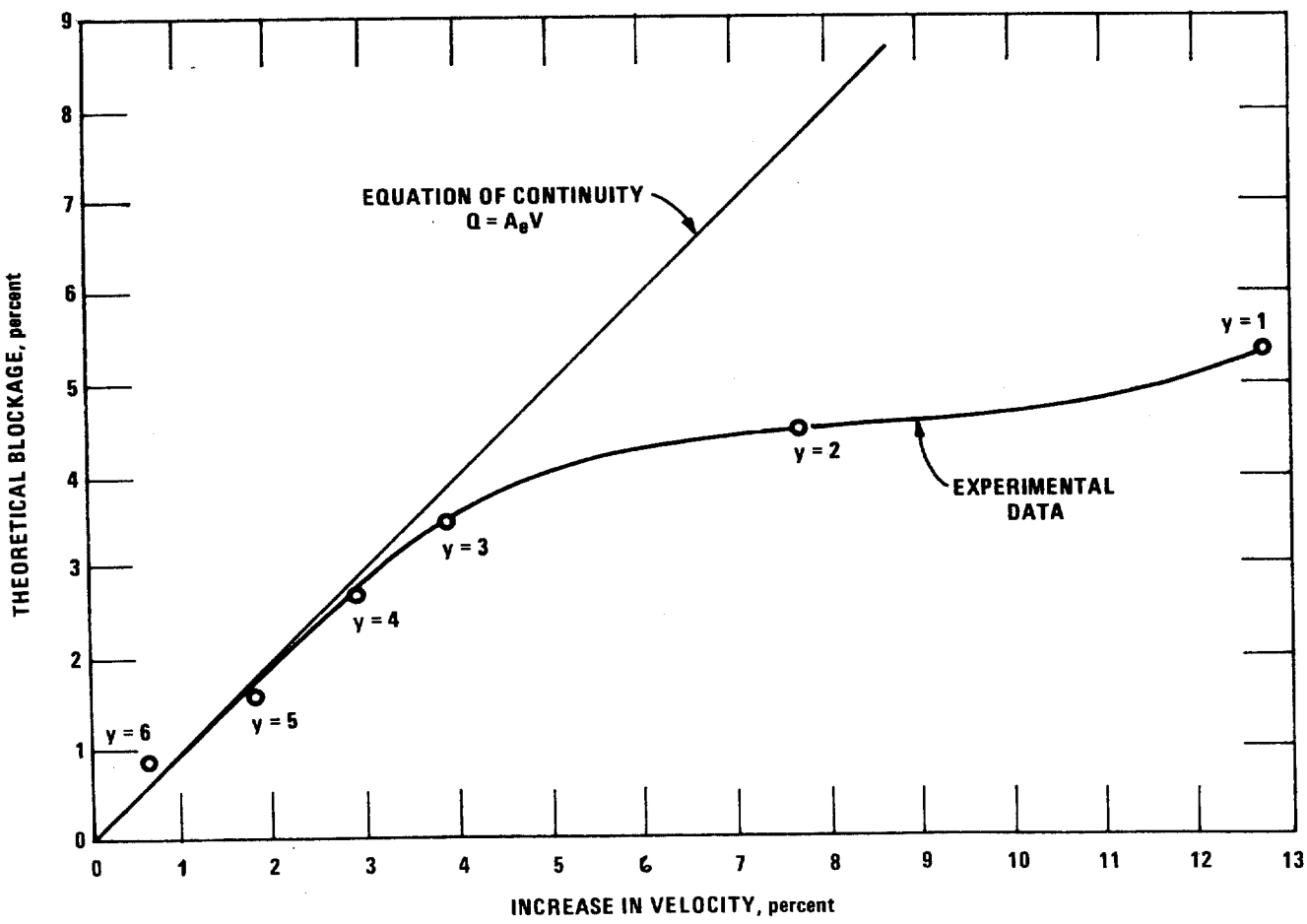

Figure 6. Graphical representation of projected-area, equation of continuity model of data from Experiment # 2.

combination of aerodynamic interference and blockage. Note that [illegible] blockage and aerodynamic interference components of the total sheath effect were, at corresponding "y" values, more pronounced with the rectangular solid of experiment #2 than with the cylindrical sheath of experiment #1. The blockage effect was greater because a rectangular solid more closely follows the projected-area, continuity equation model than does a cylindrical sheath; the likely reason that the aerodynamic effect was greater is that different wakes are formed by sharp-edged, rectangular solids and smooth, cylindrical solids.

EXPERIMENT #3

SET-UP AND PROCEDURE

Experiment #3 was similar to experiment #1, except that it was done in an 18-inch diameter wind tunnel, and a 2.5-inch cylinder was used instead of a 1-inch cylindrical sheath. The purpose of this experiment was to observe the effects of the presence of an external sheath on the value of C_p. Many pitobe assemblies have an external sheath enclosing the sample probe, pitot tube, and thermocouple (see Figure 7); the external sheath will usually have a diameter of about 2 inches. In this experiment, data were taken at values of "y" ranging from 10 inches to 1 inch, at 1-inch intervals. Three experimental runs were made.

RESULTS

The results of experiment #3 are presented in Tables V and VI and in Figure 8. The results are quite consistent with those obtained in experiment #1. Figure 8 shows that for values of "y" $\geq$ 3 inches, the actual velocity increase was consistently less than the increase predicted by the projected-area, continuity equation model. At y = 2 inches, the actual and theoretical velocity increases were nearly coincident, and at y = 1 inch, the actual increase surpassed the theoretical. This

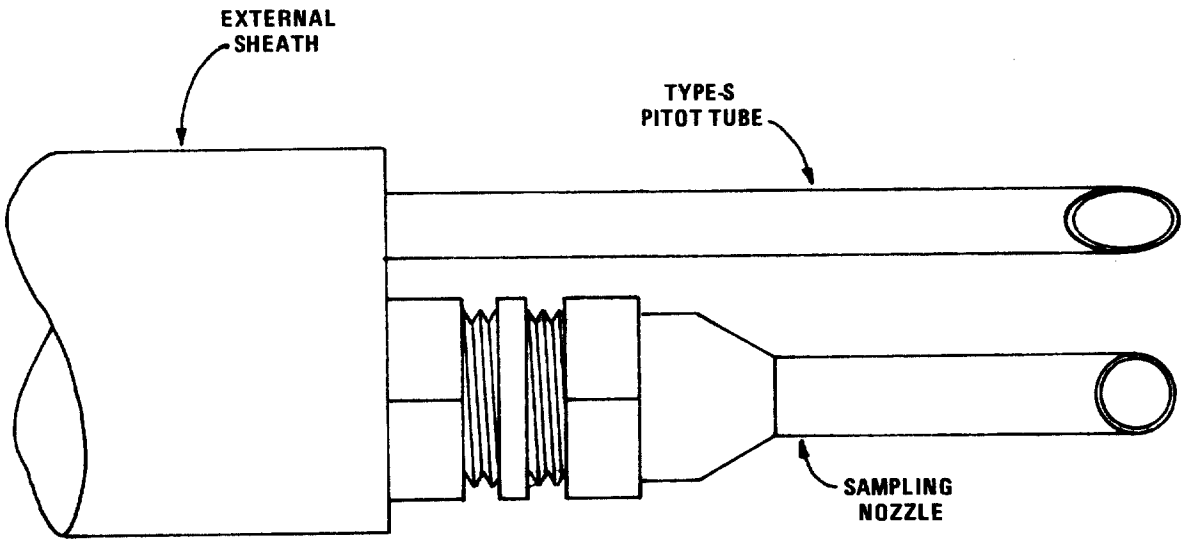

Figure 7. Pitobe assembly with external sheath.

Table V. DATA FROM EXPERIMENT #3

Distance (y), in.	Velocity* head (ΔP_s), in. H_2O	$\sqrt{\Delta P_s}$ **	Increase in velocity, %
-	0.325	0.570	-
10	0.327	0.572	0.4
9	0.331	0.575	0.9
8	0.336	0.580	1.7
7	0.342	0.585	2.6
6	0.349	0.591	3.7
5	0.355	0.596	4.6
4	0.363	0.602	5.6
3	0.376	0.613	7.5
2	0.392	0.626	9.8
1	0.419	0.648	13.4

*Average of three experimental runs.

**Proportional to velocity.

Table VI. PROJECTED-AREA, EQUATION OF CONTINUITY MODEL OF DATA FROM EXPERIMENT # 3

Distance (y), in.	Theoretical blockage, %*	Theoretical increase in velocity, %**	Actual increase in velocity, %
10	1.9	1.9	0.4
9	2.9	2.9	0.9
8	3.9	3.9	1.7
7	4.9	4.9	2.6
6	5.9	5.9	3.7
5	6.9	6.9	4.6
4	7.9	7.9	5.6
3	8.9	8.9	7.5
2	9.8	9.8	9.8
1	10.8	10.8	13.4

*From projected-area model of sheath segment.

**Predicted by equation of continuity, $Q = A_e V$.

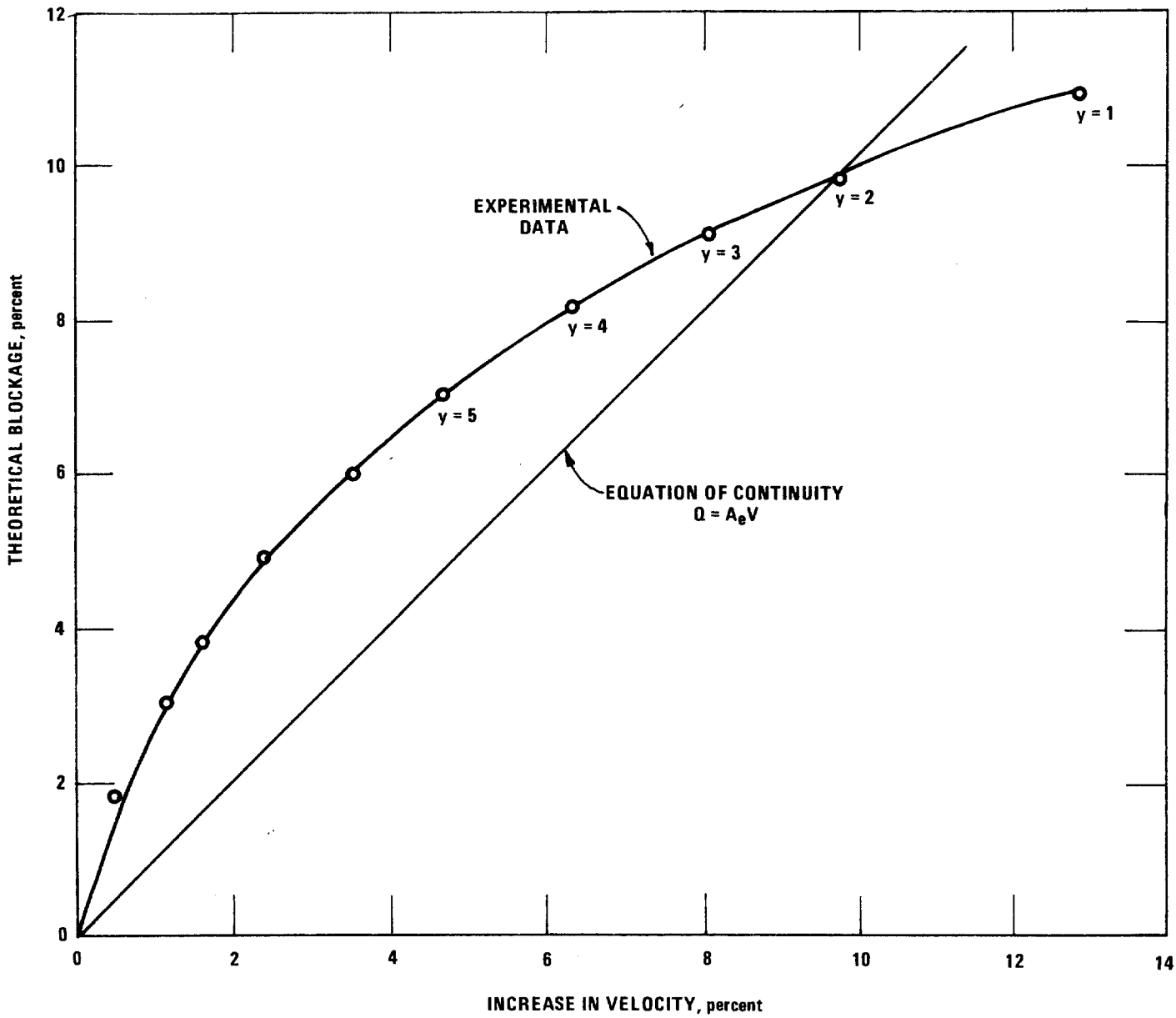

Figure 8. Graphical representation of projected-area, equation of continuity model of data from Experiment # 3.

reaffirms the findings of experiments #1 and #2 that blockage is the primary effect for "y" values of 3 inches or more, and that aerodynamic interference begins to be important when y is less than 3 inches.

CONCLUSIONS

A recent study of the effects of the presence of a probe sheath on Type-S pitot tube accuracy has demonstrated the following:

1. If a Type-S pitot tube is attached to a sample probe (with or without an external sheath), and is used to measure stack gas velocities in a small duct ($\sim$ 12 to 36 inches in diameter), pseudo-high velocity head (ΔP) readings may be obtained, resulting from significant partial blockage of the duct cross-section by the probe sheath. The actual percentage increase in the stack gas velocity caused by blockage (which approximately equals the percentage decrease in C_p, the Type-S pitot tube coefficient) will, for cylindrical sheaths, be less than the theoretical increase predicted by a rectangular projected-area model (e.g., Figure 3) and the equation of continuity for steady flow. It appears safe to conclude that the actual decrease in the value of C_p will be less than 1 percent when: (a) the theoretical blockage is 2 percent or less for pitobe assemblies without external sheaths; and (b) the theoretical blockage is 3 percent or less for pitobe assemblies with external sheaths (see Figure 9).

2. When a Type-S pitot tube is attached to a sample probe, if there is inadequate separation distance between the center of the pitot tube impact openings and the leading edge of the probe, aerodynamic interference will occur, causing a reduction in the effective value of the Type-S pitot tube coefficient (see Figure 10). It has been demonstrated that this interference is minimal for pitot tube - probe sheath separation distances greater than or equal to 3 inches; hence, it will only

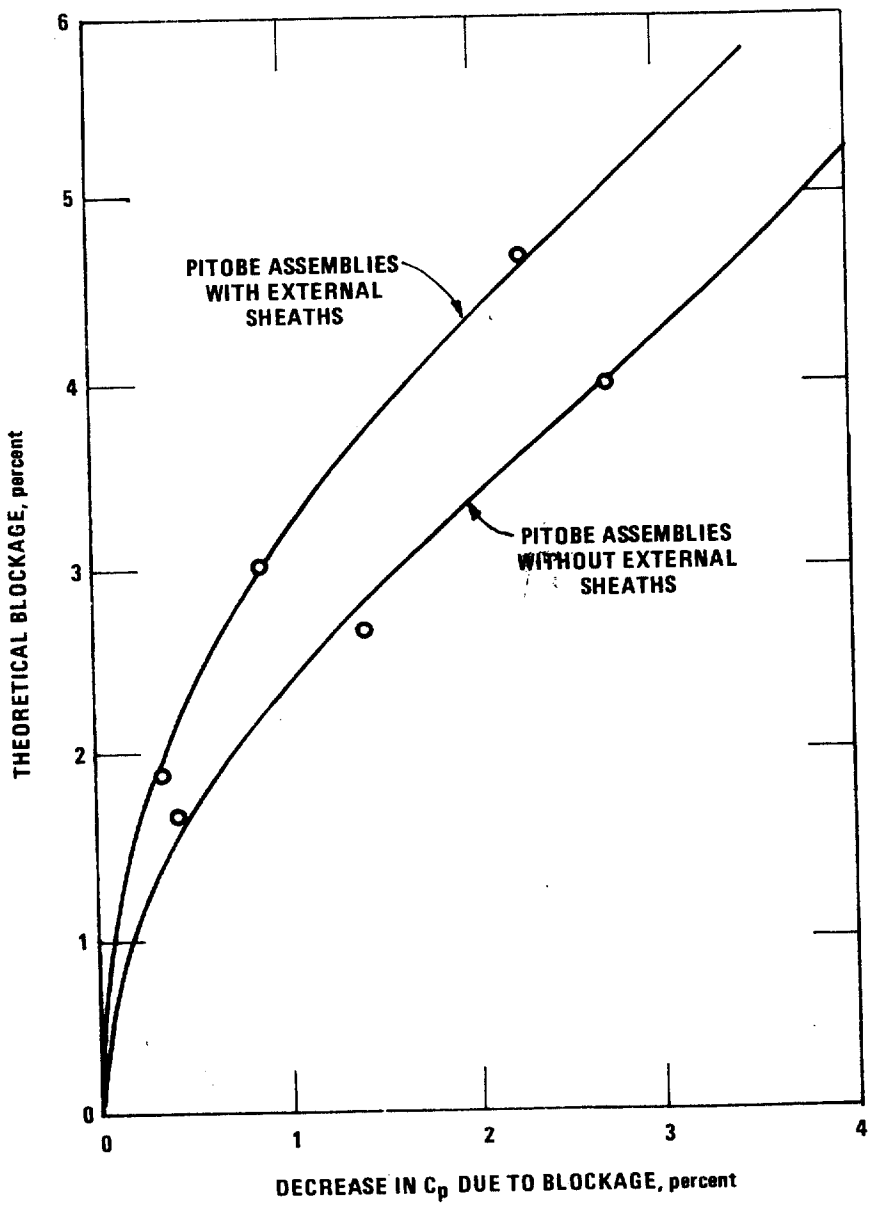

Figure 9. Percentage theoretical blockage versus actual decrease in C_p due to blockage, for pitobe assemblies with and without external sheaths.

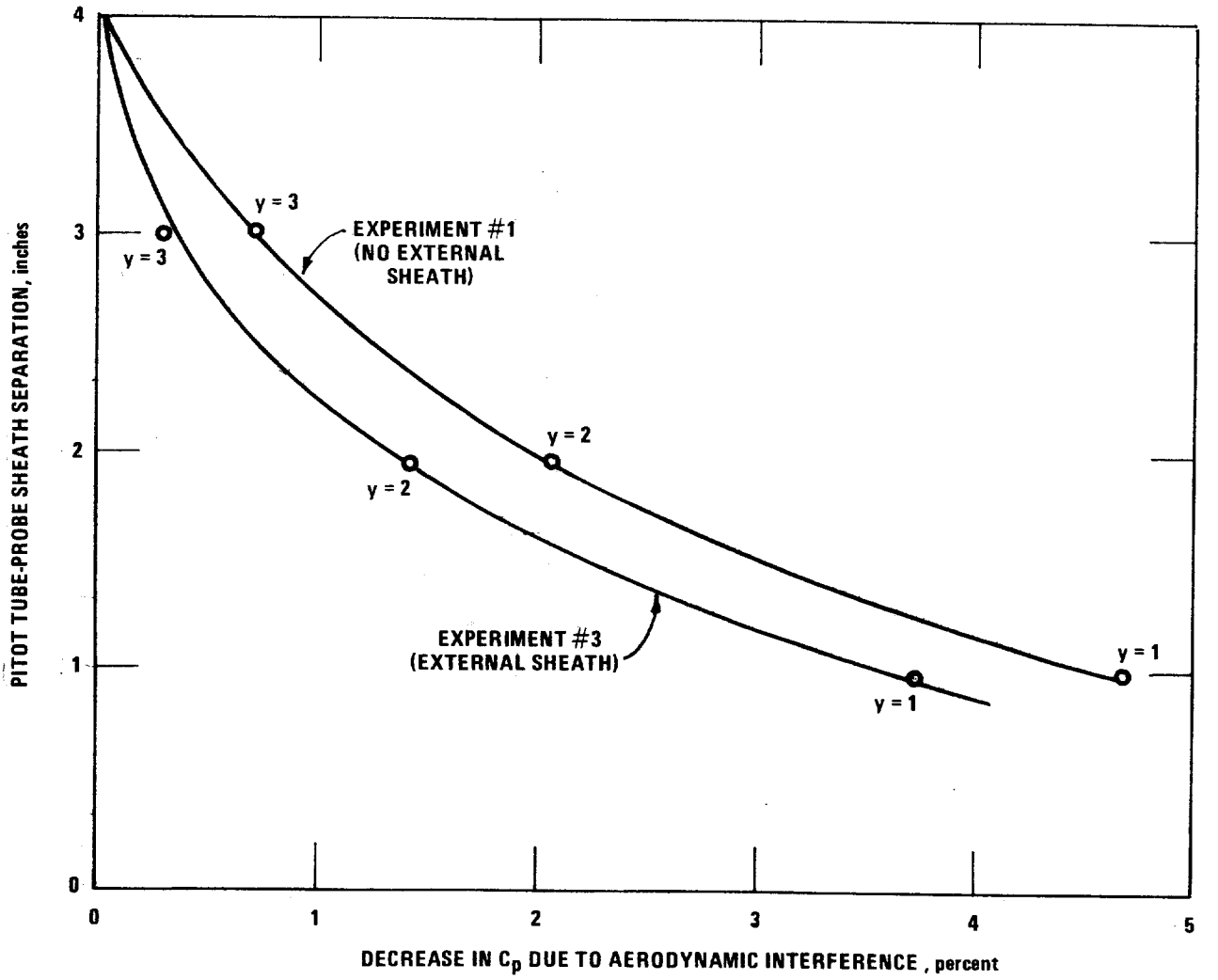

Figure 10. Pitot tube-probe sheath separation (distance "y") versus percentage decrease in C_p due to aerodynamic interference, for pitobe assemblies with and without external sheaths.

be an important consideration for pitobe assemblies that have less than 3 inches between the pitot tube openings and the leading edge of the sheath.

REFERENCES

1. Gnyp, A. W., C. C. St. Pierre, D. S. Smith, D. Mozzon, and J. Steiner. An Experimental Investigation of the Effect of Pitot Tube-Sampling Probe Configurations on the Magnitude of the S-Type Pitot Tube Coefficient for Commercially Available Source Sampling Probes. Prepared by the University of Windsor for the Ministry of the Environment. Toronto, Canada. February, 1975.

2. Vollaro, R. F. The Effect of Aerodynamic Interference Between a Type-S Pitot Tube and Sampling Nozzle on the Value of the Pitot Tube Coefficient. U. S. Environmental Protection Agency, Emission Measurement Branch, Research Triangle Park, N. C. February,1975.

3. Davini, R. J. and D. G. DeCoursin. Progress Report No. 7: Particulate Sampling Strategies for Mechanically Disturbed and Cyclonic Flow; January 1 - 31, 1974. Prepared by FluiDyne Engineering Corporation, Minneapolis, Minn., for U. S. Environmental Protection Agency. Research Triangle Park, N. C. February,1974.

4. Davini, R. J. and H. A. Hanson. Progress Report No. 11: Particulate Sampling Strategies for Mechanically Disturbed and Cyclonic Flow; Period May 1 - 31, 1974. Prepared by FluiDyne Engineering Corporation, Minneapolis, Minn., for U. S. Environmental Protection Agency. Research Triangle Park, N. C. June,1974.

AN EVALUATION OF SINGLE-VELOCITY CALIBRATION TECHNIQUE AS A MEANS OF DETERMINING TYPE-S PITOT TUBE COEFFICIENTS

Robert F. Vollaro*

INTRODUCTION

"Method 2 - Determination of Stack Gas Velocity and Volumetric Flow Rate (Type-S Pitot Tube)," promulgated in the December 23, 1971, Federal Register, specifies that during calibration of Type-S pitot tubes, "... the velocity of the flowing gas stream should be varied over the normal working range."[1] The results of a number of recent pitot calibration studies indicate, however, that acceptable values of C_p (the Type-S pitot tube coefficient) can often be obtained by single-velocity calibration, at the approximate midpoint of the normal working range.[2,3,6] The purpose of this paper is, in light of the results obtained in the studies cited, to evaluate the single-velocity calibration technique as a means of determining Type-S pitot tube coefficients.

STUDY 1

EXPERIMENTAL METHOD

A study was recently conducted in which 51 isolated Type-S pitot tubes (i.e., the tubes alone, not attached to sample probes) were calibrated against a standard pitot tube.[2] The calibrations were done in a wind tunnel having a test-section diameter of 12 inches. Prior to calibration, one leg of each Type-S pitot tube was marked "A", and the other, "B". Each Type-S tube was then calibrated, first with the A-side impact opening facing

* Emission Measurement Branch, ESED, OAQPS, EPA, RTP, NC, March 1976

the flow, and then with the B-side opening facing the flow. During each A- and B-side calibration, data were taken at six different test-section velocities, ranging from about 1500 to 3500 ft/min, and spaced at approximately equal intervals over this range. At each of the six velocity settings, the value of C_p, the Type-S pitot tube coefficient, was calculated, as follows:

$$C_p = C_p(\text{std})\sqrt{\frac{\Delta P_{std}}{\Delta P_s}} \qquad \text{(Eq. 1)}$$

Where:

C_p = Type-S pitot tube coefficient

$C_p(\text{std})$ = coefficient of standard pitot tube

ΔP_{std} = standard pitot tube reading, in. H_2O

ΔP_s = Type-S pitot tube reading, in. H_2O

METHOD OF DATA ANALYSIS

The data from Study 1 were analyzed in the following manner:

1. For each of the 102 (i.e., 51 A-side and 51 B-side) calibrations, σ, the percentage variation in the value of C_p over the velocity range from 1500 to 3500 ft/min, was calculated using the following equation:

$$\text{Percentage Variation in } C_p = \sigma = \left[\frac{C_p(h) - C_p(\ell)}{C_p(\ell)}\right] \times 100 \qquad \text{(Eq. 2)}$$

Where:

$C_p(h)$ = highest value of C_p obtained

$C_p(\ell)$ = lowest value of C_p obtained

A graph (histogram) was then constructed, showing the frequency distribution of the 102 values of σ.

2. For each of the 102 calibrations, the percentage deviation of $C_p(h)$ from C_p^* (the value of C_p obtained at 3000 ft/min, the approximate midpoint of the normal working range) was calculated as follows:

$$\text{Percentage deviation of } C_p(h) \text{ from } C_p^* = \alpha = \left[\frac{C_p(h) - C_p^*}{C_p^*}\right] \times 100 \qquad \text{(Eq. 3)}$$

A histogram was then constructed, showing the frequency distribution of the 102 values of α.

3. For each of the 102 calibrations, the percentage deviation of $C_p(\ell)$ from C_p^* was determined as follows:

$$\text{Percentage deviation of } C_p(\ell) \text{ from } C_p^* = \beta = \left[\frac{C_p^* - C_p(\ell)}{C_p^*}\right] \times 100 \qquad \text{(Eq. 4)}$$

A histogram was then constructed, showing the frequency distribution of the 102 values of β.

RESULTS OF DATA ANALYSIS

The results of the analysis of the data from Study 1 are presented graphically in Figures 1, 2, and 3; in view of the fact that a large number (51) of randomly-selected pitot tubes were calibrated in this study, these results can be considered typical of the Type-S instrument. Figure 1 shows

that the mean value of σ for the velocity range from 1500 to 3500 ft/min was 1.4 percent; about 90 percent of the σ values were 2.2 percent or less, and 99 percent of them were 2.6 percent or less. Figures 2 and 3 show that in general, the percentage deviations of $C_p(h)$ and $C_p(\ell)$ from C_p^* were small; the calculated values of α and β ranged from 0.0 to 1.9 percent, and averaged 0.7 percent. Analysis of the data from Study 1 has therefore demonstrated that the coefficient of a given isolated Type-S pitot tube will vary by 2.6 percent or less over the velocity range from 1500 to 3500 ft/min, and that the value of C_p at any velocity point within this range will be within $\pm$ 2 percent of C_p^*, the coefficient value at 3000 ft/min.

STUDY 2

EXPERIMENTAL METHOD

In June 1974, the University of Windsor conducted a study in which six commercially available Type-S pitot tubes (representing five different manufacturers) were calibrated against a standard pitot tube.[3] The calibrations were done in a wind tunnel having a 30- x 30-inch rectangular test section. A total of 47 calibration runs were performed with the six Type-S pitot tubes. During each run, calibration data were taken at 10 or more different, regularly spaced test-section velocities covering the range from 600 to 4200 ft/min. At each velocity setting, the value of the Type-S pitot tube coefficient was calculated (Equation 1). Note that isolated pitot tubes were calibrated in only 2 of the 47 runs; in the other 45 runs, the tubes were calibrated in various "pitobe assembly" configurations (i.e., while attached to sample probes equipped with nozzles or thermocouples

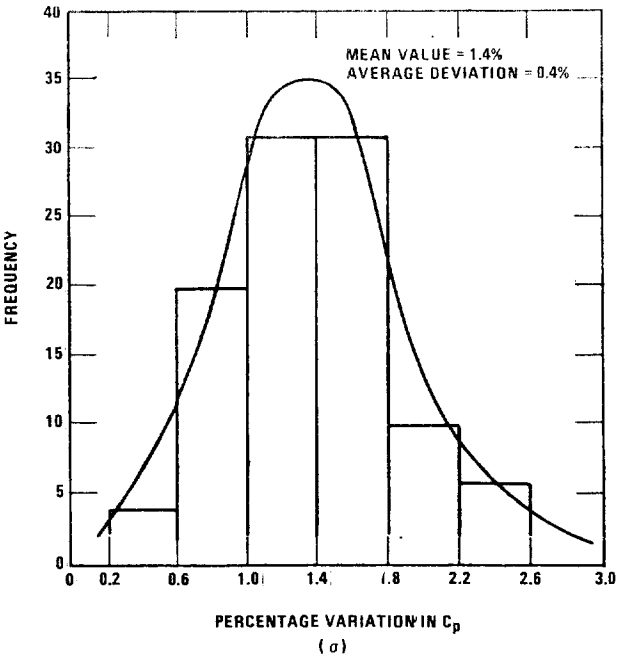

Figure 1. Frequency distribution of σ values; Study 1; velocity range 1500 to 3500 ft/min.

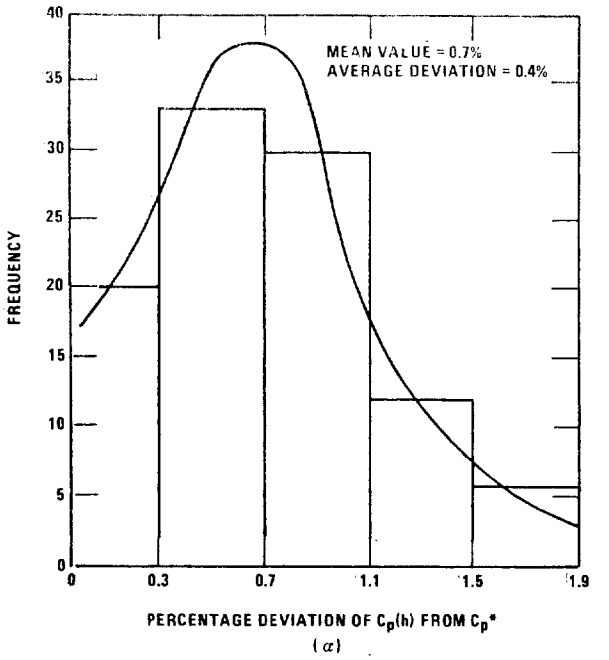

Figure 2. Frequency distribution of α values; Study 1; velocity range 1500 to 3500 ft/min.

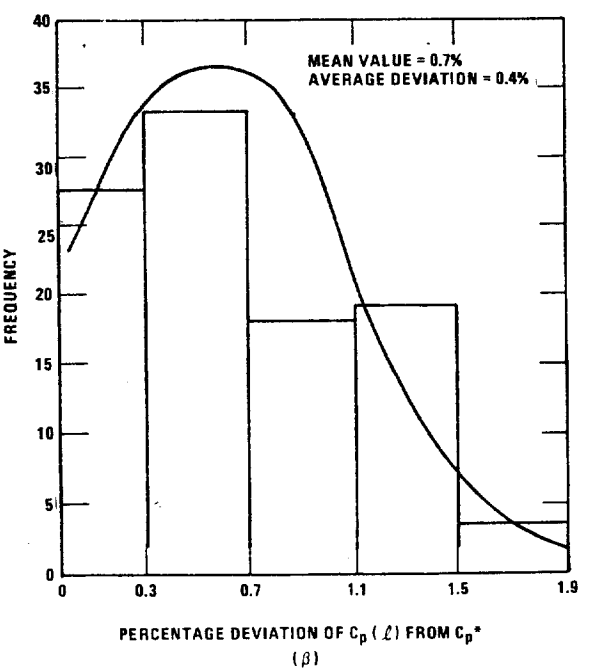

Figure 3. Frequency distribution of β values; Study 1; velocity range 1500 to 3500 ft/min.

or both). Aerodynamic interference effects, caused by the nozzle and/or thermocouple elements being too close to the Type-S pitot tube impact openings, were present in many of the pitobe assemblies; consequently, many of the values of C_p obtained by calibration were considerably below the range (0.83 to 0.87) considered "normal" for the Type-S instrument. In 9 of the 45 pitobe assembly runs, sample gas was drawn through the nozzle (at a number of different flow rates) during calibration.

METHOD OF DATA ANALYSIS

The data from Study 2 were analyzed in the following manner:

1. Considering only those data falling within the velocity range covered in Study 1 ($\sim$ 1500 to 3500 ft/min), values of σ, α, and β were calculated for each of the 45 pitobe assembly runs, using, respectively, equations 2, 3, and 4 above. Histograms, showing the frequency distributions of the σ, α, β values, were then constructed and compared against the σ, α, and β distributions from the first study.
2. Considering only those data falling within the "normal working range" ($\sim$ 1000 to 5000 ft/min), values of σ, α, β were calculated for each of the 47 runs, using Equations 2, 3, and 4, respectively. Histograms were then constructed, showing the σ, α, and β frequency distributions.

RESULTS OF DATA ANALYSIS

The results of the analysis of the data from Study 2 are presented graphically in Figures 4 through 9. Figure 4 shows that the mean value of

for the 45 pitobe assembly runs, in the velocity range from 1500 to 3500 ft/min, was 1.5 percent; more than 90 percent of the σ values were 2.5 percent or less. This is in excellent agreement with the results obtained in Study 1 (see Figure 1), in which the mean value of σ was 1.4 percent, and 99 percent of the σ values were 2.6 percent or less. Figures 5 and 6 show that the mean values of α and β were 0.5 percent and 1.0 percent, respectively. These results also compare favorably with those obtained in the first study (see Figures 2 and 3). It is significant that the data from the pitobe assembly runs of Study 2 agree with the data from Study 1, in which isolated Type-S pitot tubes were calibrated; this indicates that the configuration in which Type-S pitot tubes are calibrated apparently has little or no effect on the values of σ, α, and β.

Figure 7 shows that the mean value of σ (for all runs) in the velocity range from 1000 to 4200 ft/min was 2.4 percent, and that 98 percent of the σ values were 5.4 percent or less. Figure 8 shows that most of the values of α for the 1000 to 4200 ft/min range were small; the average value of α was 0.7 percent; 98 percent of the α values were 2.2 percent or less. Figure 9 shows that the values of β were slightly greater than the α values; the β values ranged from 0.0 to 5.2 percent, and averaged 1.6 percent; approximately 90 percent of the β values were 3 percent or less. Thus, extending the velocity range downward from 1500 to 1000 ft/min, and upward from 3500 to 4200 ft/min, produced only a 1 percent increase in the average value of σ; also, there was essentially no change in the average value of α, and only a slight (0.9%) increase in the average value of β. It therefore appears safe to conclude that had the calibrations been done by single-velocity technique at the midpoint

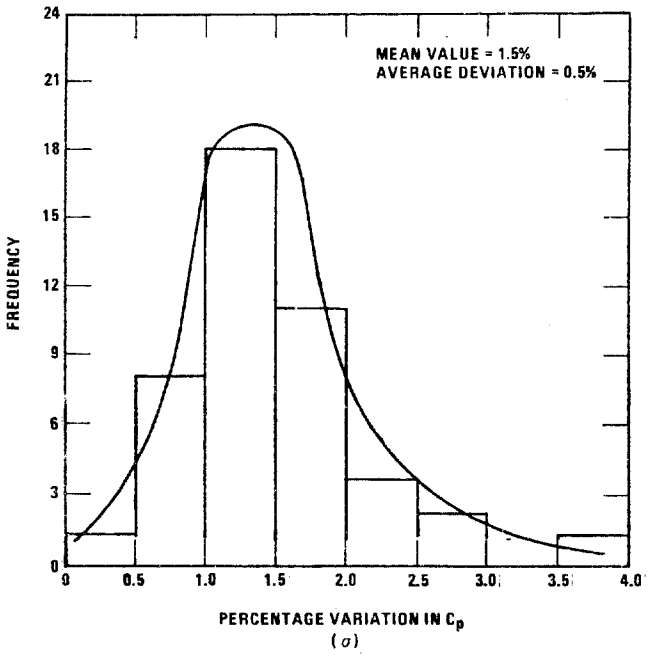

Figure 4. Frequency distribution of σ values; Study 2; velocity range 1500 to 3500 ft/min; pitobe assembly runs only.

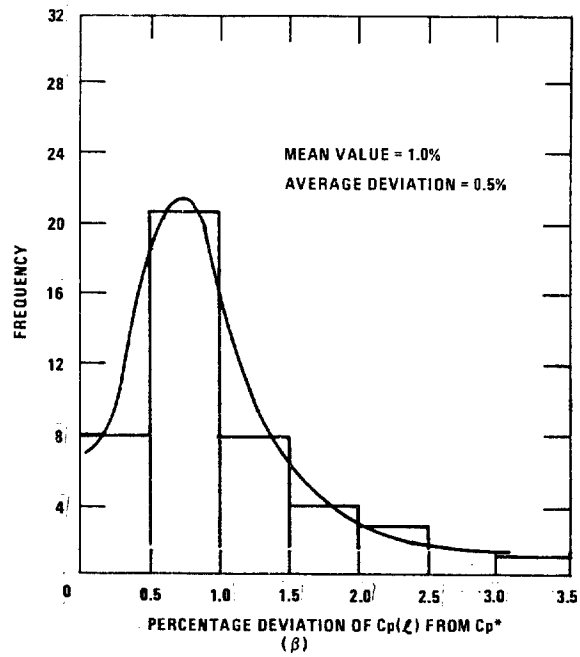

Figure 6. Frequency distribution of β values; Study 2; velocity range 1500 to 3500 ft/min; pitobe assembly runs only.

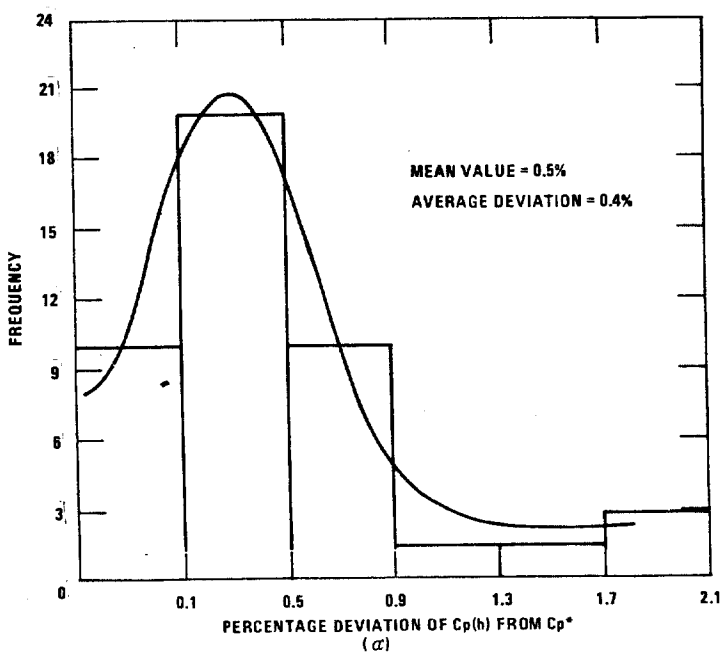

Figure 5. Frequency distribution of α values; Study 2; velocity range 1500 to 3500 ft/min; pitobe assembly runs only.

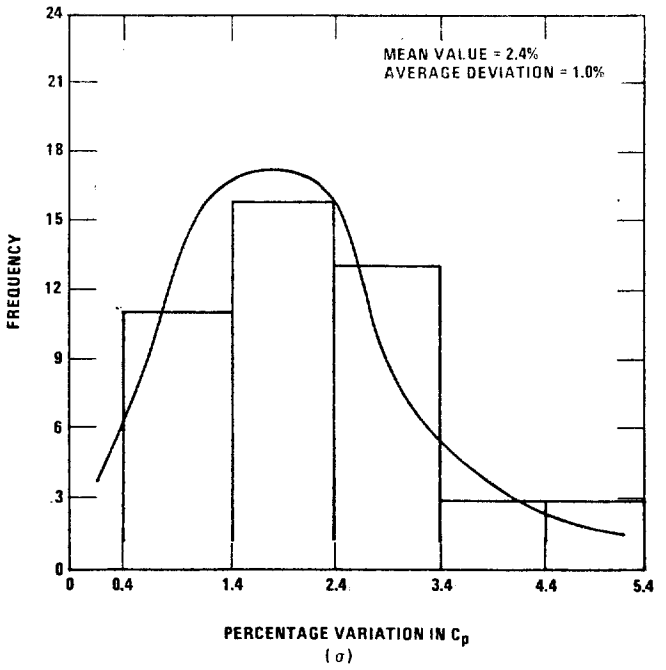

Figure 7. Frequency distribution of σ values; Study 2; velocity range 1000 to 4200 ft/min.

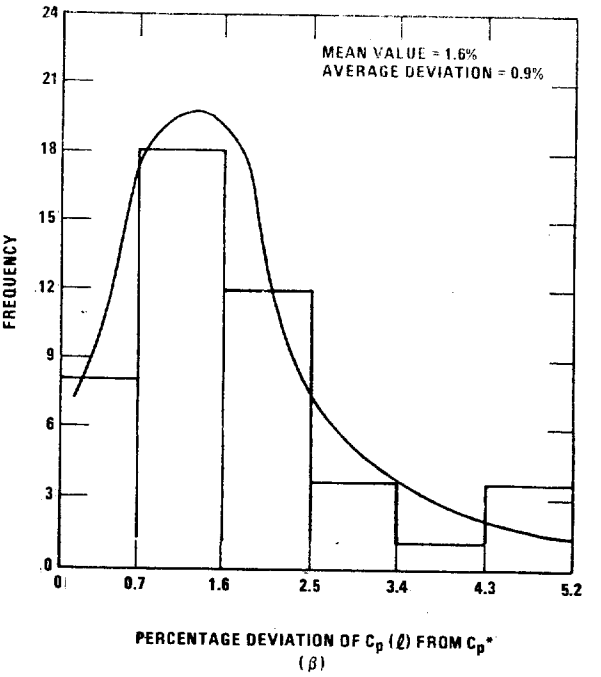

Figure 9. Frequency distribution of β values; Study 2; velocity range 1000 to 4200 ft/min.

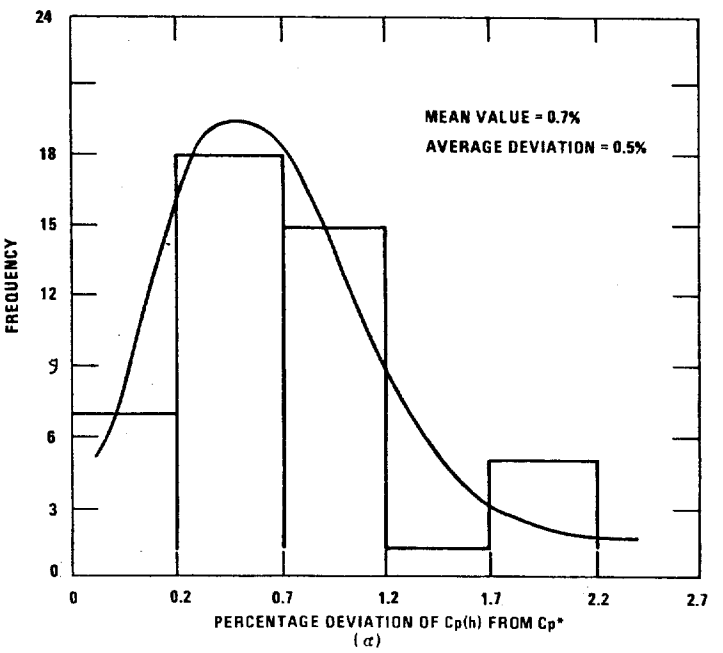

Figure 8. Frequency distribution of α values; Study 2; velocity range 1000 to 4200 ft/min.

of the normal working range ($\sim$ 3000 ft/min), better than 90 percent of the C_p values obtained would have been valid to within $\pm$ 3 percent over the entire 1000 to 4200 ft/min range.

STUDY 3

EXPERIMENTAL METHOD

North Carolina State University (NCSU) recently conducted a study in which six Type-S pitot tubes were calibrated against a standard pitot tube.[4,5,6] The calibrations were done in the NCSU low-speed wind tunnel. More than 60 calibration runs were performed using the six Type-S pitot tubes; data from 59 of the runs (considered sufficient to represent the study) will be analyzed. During each run, calibration data were taken at five or more regularly spaced test-section velocities, covering the range from 600 to 6000 ft/min. At each velocity setting, the value of the Type-S pitot tube coefficient was calculated (Equation 1). In 12 of the 59 runs, isolated pitot tubes were calibrated; in the other 47 runs, pitobe assemblies, some of which had aerodynamic interference problems, were calibrated. In 10 of the 47 pitobe assembly runs, sample gas was drawn through the nozzle during calibration.

METHOD OF DATA ANALYSIS

The data from Study 3 were analyzed in the following manner:

1. Considering only those data falling within the velocity range covered in Study 1 ($\sim$ 1500 to 3500 ft/min), values of σ, α, and β were calculated for each of the 47 pitobe assembly runs, using, respectively,

equations 2, 3, and 4 above. Histograms, showing the frequency distribution of the σ, α, and β values, were then constructed and compared against the σ, α, and β distributions from the first study.

2. Considering only those data falling within the normal working range ($\sim$ 1000 to 5000 ft/min), values of σ, α, and β were calculated for each of the 59 runs, using (respectively) Equations 2, 3, and 4. Histograms were then constructed showing the σ, α, and β frequency distributions.

RESULTS OF DATA ANALYSIS

The results of the analysis of the data from Study 3 are presented graphically in Figures 10 through 15. Figure 10 shows that the mean value of σ for the 47 pitobe assembly runs, in the velocity range from 1500 to 3500 ft/min, was 1.2 percent; approximately 90 percent of the σ values were 3 percent or less. Figures 11 and 12 show that the average values of α and β were, respectively, 0.4 percent and 0.9 percent. These results compare favorably with those obtained in Study 1, once again indicating that the values of σ, α, and β are apparently independent of the configuration in which the pitot tubes are calibrated.

Figure 13 shows that the mean value of σ (for all runs) in the velocity range from 1000 to 5000 ft/min was 2.2 percent; approximately 98 percent of the σ values were 5.2 percent or less. Note that the distribution of σ values obtained in Study 3 is almost identical to the σ distribution obtained for the 1000 to 4200 ft/min range in Study 2 (compare Figures 13 and 7); this

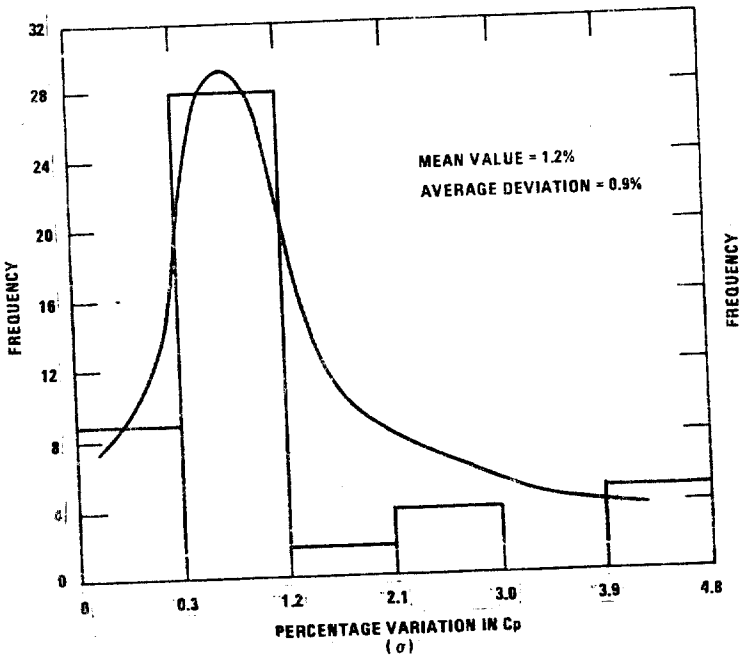

Figure 10. Frequency distribution of σ values; Study 3; velocity range 1500 to 3500 ft/min; pitobe assembly runs only.

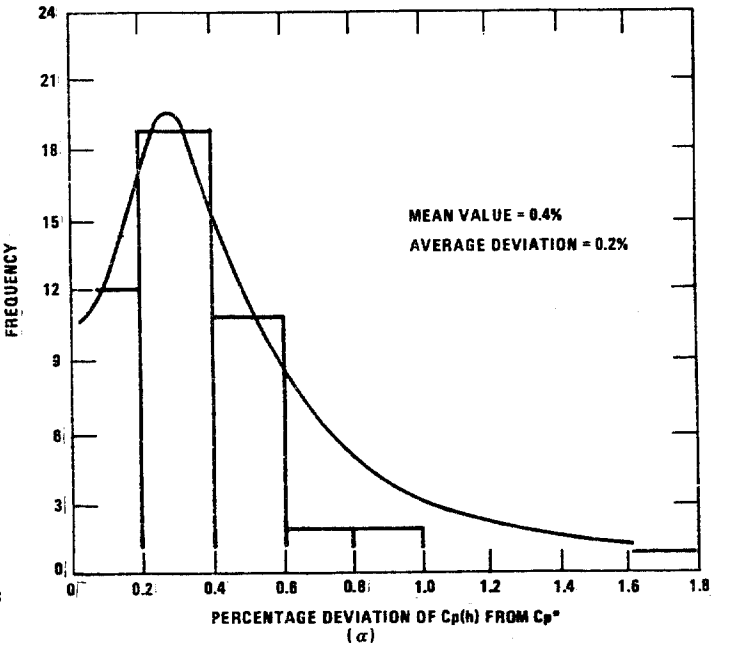

Figure 11. Frequency distribution of α values; Study 3; velocity range 1500 to 3500 ft/min; pitobe assembly runs only.

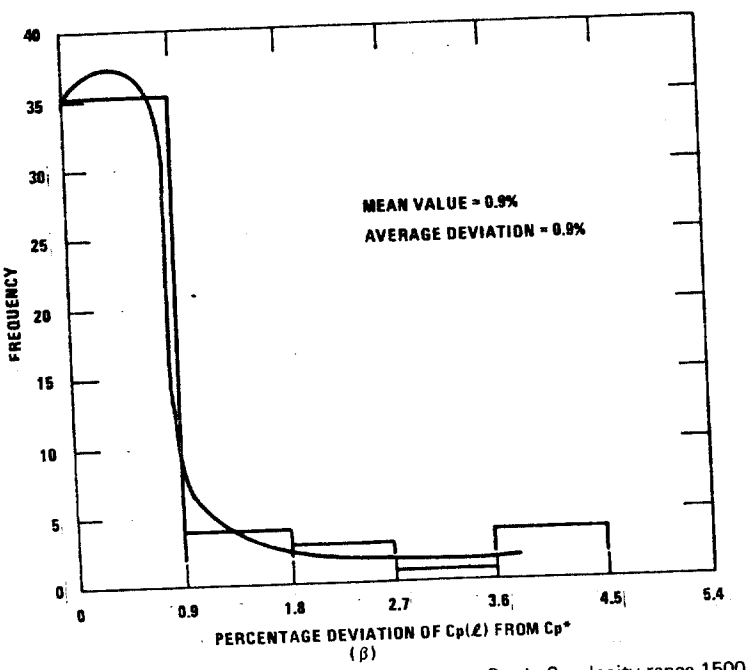

Figure 12. Frequency distribution of β values; Study 3; velocity range 1500 to 3500 ft/min; pitobe assembly runs only.

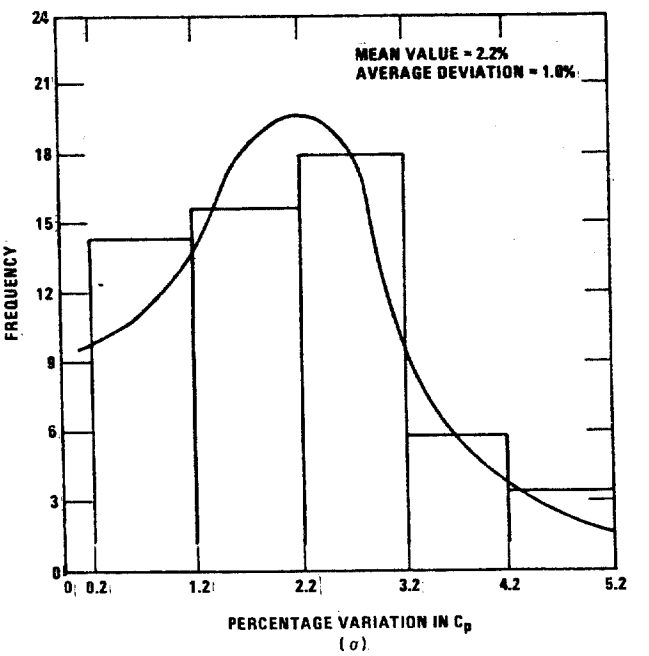

Figure 13. Frequency distribution of σ values; Study 3; velocity range 1000 to 5000 ft/min.

indicates that in the velocity range from 4200 to 5000 ft/min, the amount of variation in the value of C_p is negligibly small. Figure 14 (compare Fig. 8) shows that the average value of α was 1.0 percent; 98 percent of the α values were 3.1 percent or less. Figure 15 (compare Fig. 9) shows that the values of β ranged from 0.0 to 4.4 percent, and averaged 1.2 percent; about 90 percent of the β values were 2.8 percent or less.

Analysis of the data from Study 3 has, therefore, yielded results consistent with those obtained in Studies 1 and 2.

CONCLUSIONS

Careful analysis of data from three recent pitot tube calibration studies has demonstrated the following:

1. The coefficient of a given Type-S pitot tube can be expected to vary by 5 percent or less over the normal working velocity range from 1000 to 5000 ft/min. This should be true whether the Type-S pitot tube is calibrated alone or as a component or a pitobe assembly.
2. For a given Type-S pitot tube, the value of C_p at any point within the normal working range can be expected to be within about $\pm$ 3 percent of C_p^*, the value at 3000 ft/min. This, also, should be true for isolated pitot tubes as well as for pitobe assemblies. Hence, values of C_p obtained by single-velocity calibration at the approximate midpoint of the normal working range will, in general, be valid to within $\pm$ 3 percent over the entire range.

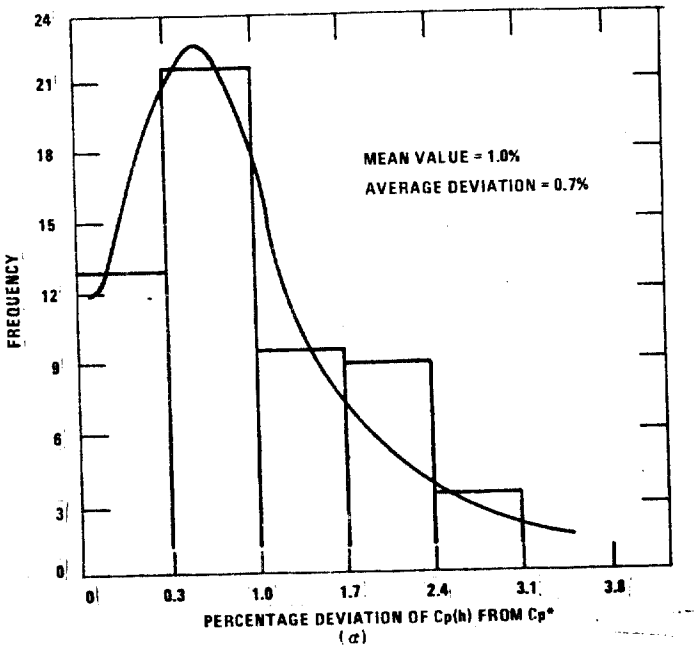

Figure 14. Frequency distribution of α values; Study 3; velocity range 1000 to 5000 ft/min.

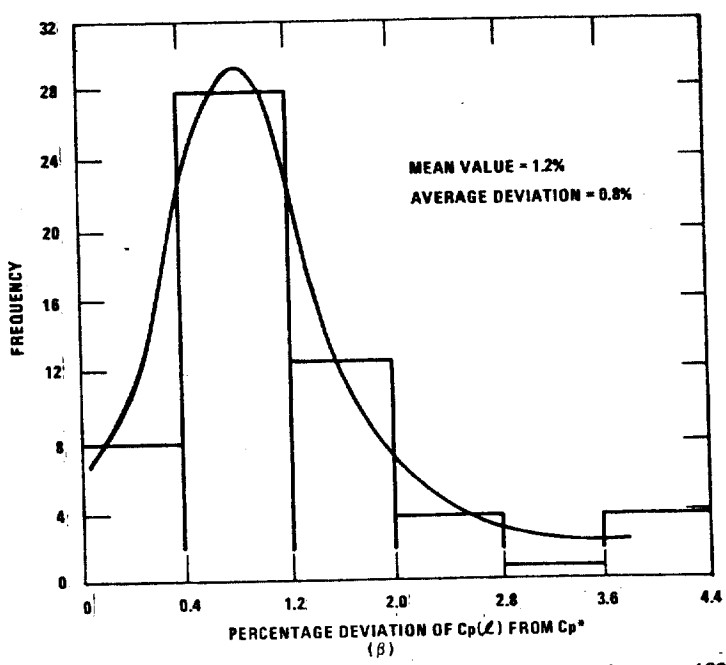

Figure 15. Frequency distribution of β values; Study 3; velocity range 1000 to 5000 ft/min.

REFERENCES

1. Standards of Performance for New Stationary Sources. Federal Register, 36(247). December 23, 1971.

2. Vollaro, R. F. A Type-S Pitot Tube Calibration Study. U. S. Environmental Protection Agency, Emission Measurement Branch. Research Triangle Park, N. C. July 1974.

3. Gnyp, A. W., C. C. St. Pierre, D. S. Smith, D. Mozzon, and J. Steiner. An Experimental Investigation of the Effect of Pitot Tube-Sampling Probe Configurations on the Magnitude of the S-Type Pitot Tube Coefficient for Commercially Available Source Sampling Probes. Prepared by the University of Windsor for the Ministry of the Environment. Toronto, Canada. February 1975.

4. DeJarnette, F. R. and J. C. Williams, III. A Study of the Effects of Probe Design, Construction, and Use on the Accuracy of Type-S Pitot Tubes; Progress Report No. 2. Submitted to U. S. Environmental Protection Agency by the Mechanical and Aerospace Engineering Department of North Carolina State University. Raleigh, N. C. October 10, 1974.

5. Terry, Ellen W. and Herbert E. Moretz. Effects of Geometry and Interference on the Accuracy of S-Type Pitot Tubes. Submitted to U. S. Environmental Protection Agency by the Mechanical and Aerospace Engineering Department of North Carolina State University. Raleigh, N.C. April 1975.

6. Terry, Ellen W. and Herbert E. Moretz. First Annual Report on the Effects of Geometry and Interference on the Accuracy of S-Type Pitot Tubes. Submitted to U. S. Environmental Protection Agency by the Mechanical and Aerospace Engineering Department of North Carolina State University. Raleigh, N. C. August 1975.

GUIDELINES FOR TYPE-S PITOT TUBE CALIBRATION

Robert F. Vollaro*

INTRODUCTION

In source sampling, the Type-S pitot tube is the instrument most commonly used to measure stack gas velocity. Before a Type-S instrument is used in the field, its coefficient (C_p) must be determined by calibration against a standard pitot tube. The current Type-S pitot calibration guidelines (Federal Register, 12/23/71) specify that calibration be done by measuring velocity head ". . . at some point in a flowing gas stream, with both a Type-S pitot tube and standard pitot tube. Calibration should be done in the laboratory, and the velocity of the flowing gas stream should be varied over the normal working range . . ."[1]

A number of recent studies[2,3,4,5] have demonstrated, however, that more detailed and systematic calibration guidelines are needed to ensure uniformity of application by different observers, which is essential for the obtainment of accurate, reproducible results. The purpose of this paper is, based on these recent findings, to present practical, comprehensive guidelines for the calibration of Type-S pitot tubes.

A SUMMARY OF FACTORS WHICH CAN AFFECT THE VALUE OF C_p

A number of recent studies have shown that when a Type-S pitot tube is used as a component of a pitobe assembly (i.e., when the tube is attached to a sample probe equipped with appropriate nozzle and thermocouple), aerodynamic interactions between the pitot tube and the other components of the assembly can cause a substantial lowering in the value of the pitot coefficient (C_p).[2,3,4,5] At present, there are four specific known types of aerodynamic effect associated with pitobe assemblies. These have been spoken of extensively in the references cited; nevertheless, it will be advantageous to briefly review them at this time.

(1) Effect of Sampling Nozzle - If there is insufficient separation distance between a Type-S pitot tube and sampling nozzle, the tube and nozzle will interfere aerodynamically, resulting in a 3 to 9 percent lowering of C_p. It has been demonstrated that about 3/4 inch free space between the pitot tube and nozzle will essentially eliminate this effect.[2]

(2) Effect of Thermocouple - When a thermocouple wire is attached to a Type-S pitot tube and placed in such a way that the tip of the wire is in line with the centerline of the pitot tube impact openings, aerodynamic interference occurs, causing a sharp reduction in the value of C_p (up to 9 percent).[3]

(3) Effect of Probe Sheath, (I) - In small ducts (~ 12 to 36 inches in diameter), a reduction in C_p (up to 4 percent) can occur, resulting from reduction of the effective cross-sectional area of the duct by the probe sheath.[5]

(4) Effect of Probe Sheath, (II) - If a pitobe assembly is constructed in such a way that the distance from the center of the pitot

* Emission Measurement Branch, ESED, OAQPS, EPA, RTP, NC. Presented at 1st Annual Meeting, Source Evaluation Society, Dayton, Ohio, September 18, 1975 Published in Source Evaluation Society Newsletter 1(1), January 1976

tube impact openings to the leading edge of the probe sheath is less than 3 inches, a slight reduction (up to 3 percent) in C_p can occur.[5]

It is therefore evident that if comprehensive Type-S pitot tube calibration guidelines are to be written, each of the above effects must be taken into consideration.

GENERAL GUIDELINES FOR THE DETERMINATION OF TYPE-S PITOT TUBE COEFFICIENTS

I. Apparatus and Experimental Set-Up

A. Flow System - Calibration shall be done in a flow system (see Figure 1) having the following essential design features:

(1) The flowing gas stream must be confined to a definite cross-sectional area, either circular or rectangular. For circular cross-sections, the minimum duct diameter shall be 30.5 cm (12 inches); for rectangular cross-sections, the width (shorter side) shall be at least 25.4 cm (10 inches).

(2) The cross-sectional area of the flow system must be constant over a distance of 10 or more duct diameters. For rectangular cross-sections, use an equivalent diameter, calculated as follows, to determine the number of duct diameters:

$$D_e = \frac{2\ LW}{(L + W)} \qquad \text{(Equation 1)}$$

Where:

D_e = Equivalent diameter

L = Length

W = Width

To ensure the presence of stable, well-developed flow patterns at the calibration site ("test section"), the site shall be located at least 8 duct diameters downstream and 2 diameters upstream from the nearest disturbances.

(3) The flow system shall have the capacity to generate a test-section velocity around 3000 ft/min, which is the approximate midpoint of the "normal working range" ($\sim$ 1000 to 5000 ft/min). This velocity must be constant with time, to guarantee steady flow during calibration.

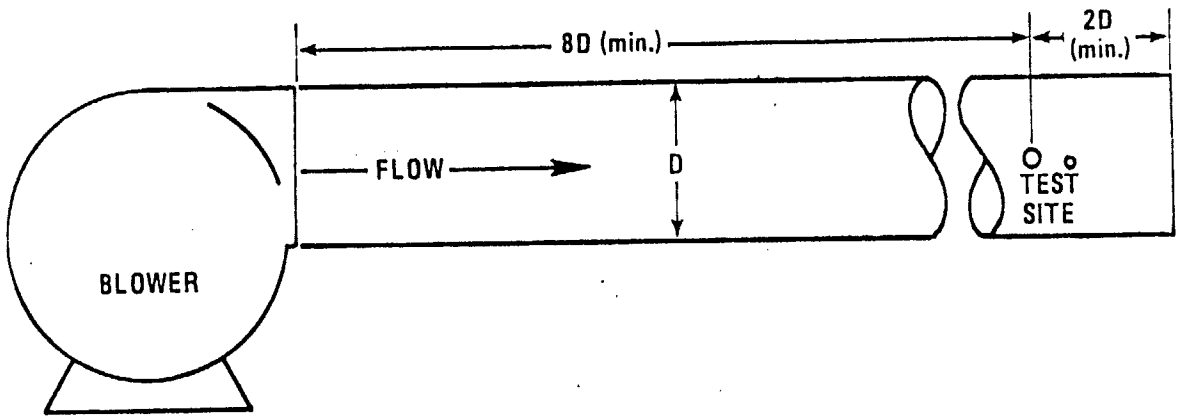

Figure 1. Pitot tube calibration system.

Note that Type-S pitot tube coefficients obtained by single-velocity calibration at the midpoint of the normal working range will generally be valid to within ± 2 percent over the entire range.[7] If a more precise correlation between C_p and velocity is desired, the flow system shall have the capacity to generate a number of distinct, time-invariant test-section velocities, covering the normal working range, and calibration data shall be taken at regular velocity intervals between 1000 and 5000 ft/min (see Section II).

(4) Two entry ports, one each for the standard and Type-S pitot tubes, shall be cut in the system test section. The standard pitot tube entry port shall be located slightly downstream of the Type-S port, so that the standard and Type-S impact openings will lie in the same plane during calibration. To facilitate alignment of the pitot tubes during calibration, it is advisable that the test section be constructed of plexiglas or some other transparent material.

B. Calibration Standard - A standard pitot tube shall be used to calibrate the Type-S pitot tube. The standard pitot tube shall have a known coefficient, obtained either directly from the National Bureau of Standards in Gaithersburg, Maryland, or by calibration against another pitot tube with a known (NBS traceable) coefficient. Alternatively, a modified ellipsoidal nose pitot-static tube, designed according to the criteria illustrated in Figure 2, can be used. This is the only type of standard pitot tube recommended by the British Standards Institute (B.S.I.) for use without individual calibration.[6] Note that the coefficient of the ellipsoidal nose tube is a function of the stem/static hole distance; therefore, Figure 3 should be used as a guide in determining its precise coefficient value.*

C. Differential Pressure Gauge - An inclined manometer, or equivalent device, shall be used to measure velocity head (ΔP). The gauge shall be capable of measuring ΔP to within ± 0.13 mm H_2O (0.005 in. H_2O).

D. Pitot Lines - Flexible lines, made of Tygon or similar tubing, and equipped with appropriate fittings (preferably quick-disconnect type) shall serve to connect the pitot tubes to the differential pressure gauge.

---

*See "Addendum"

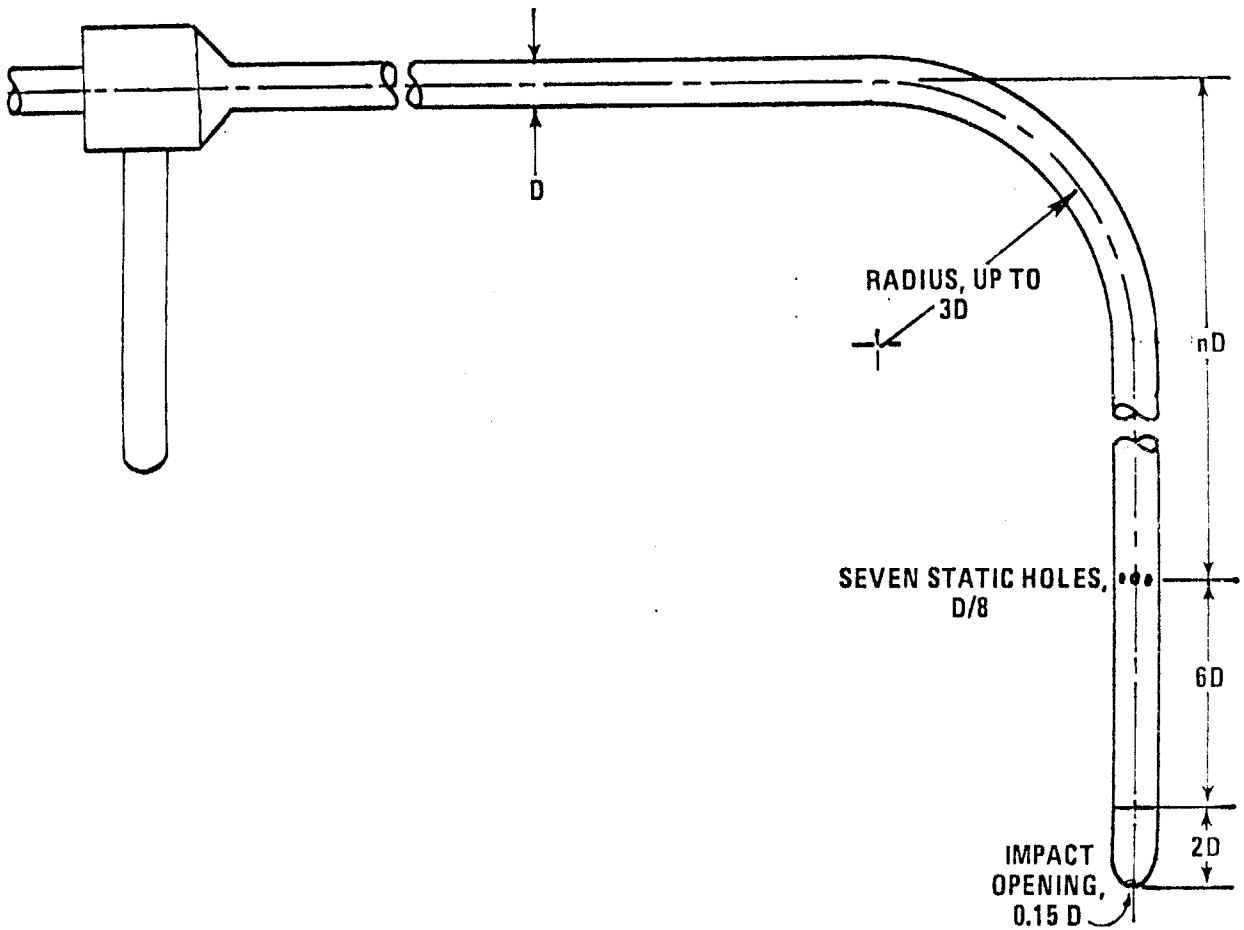

Figure 2. Ellipsoidal-nose pitot-static tube.

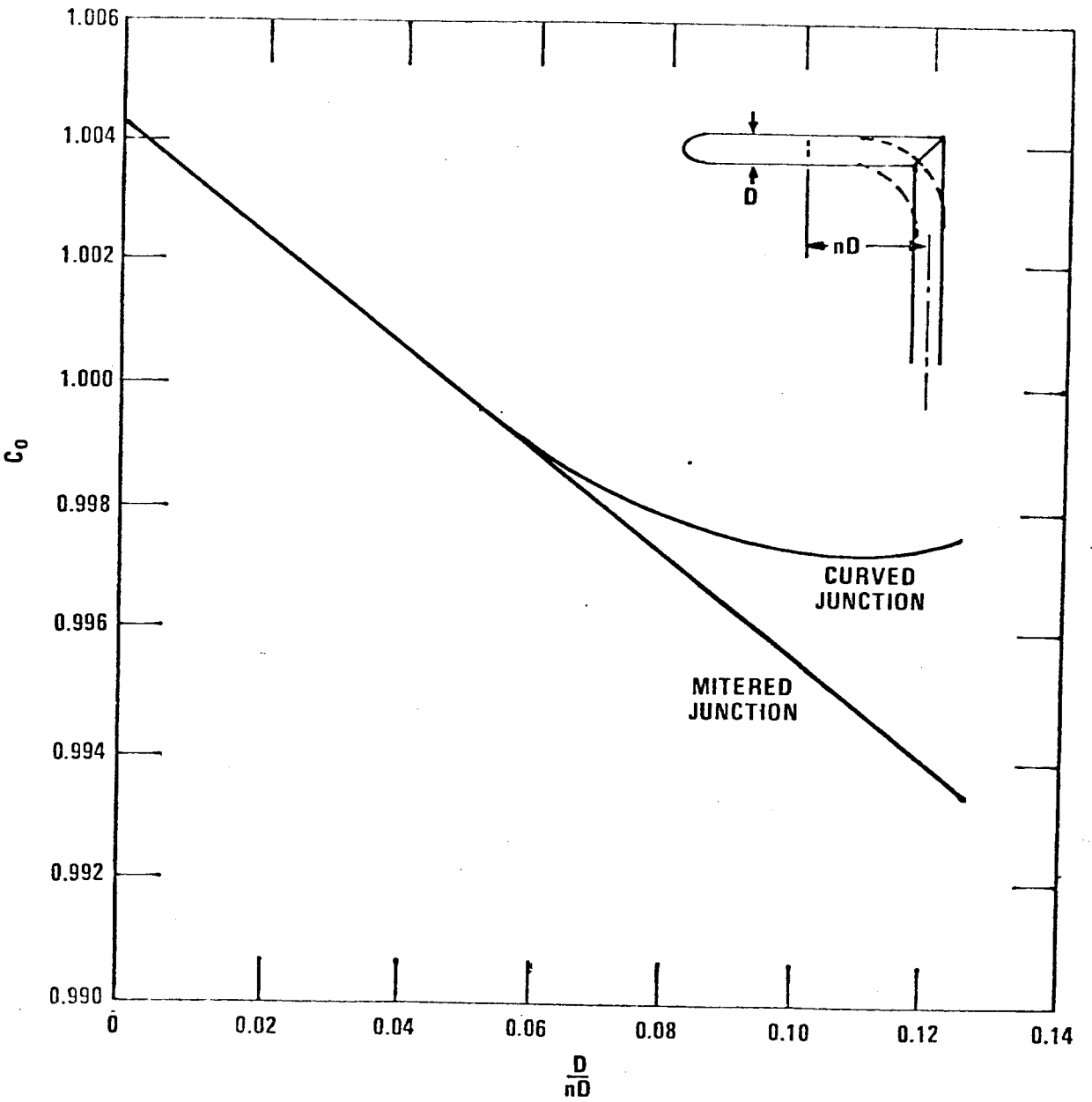

Figure 3. Effect of stem/static hole distance on basic coefficient, C_0, of standard pitot-static tubes with ellipsoidal nose.

II. Calibration Procedure* - The Type-S pitot tube shall be assigned a permanent identification number. This number shall be permanently marked or engraved on the body of the tube. Also, one leg of the tube shall be marked "A," and the other, "B." To obtain calibration data for the A and B sides of the tube, proceed as follows:

A. Make sure that the manometer** is properly filled and that the oil is free from contamination. Inspect and leak-check all pitot lines; repair or replace if necessary.

B. Level and zero the manometer. Turn on the fan and allow the flow to stabilize; if single-velocity technique is used, the test section velocity should be about 3000 ft/min. If multi-velocity calibration technique is used, begin with a test-section velocity of about 1000 ft/min. Seal the Type-S entry port.

C. Position the standard pitot tube at the calibration point (determined as outlined in sections IV and V), and align it so that its tip is pointed directly into the flow. Particular care should be taken in aligning the tube, to avoid yaw and pitch angles. Make sure that the entry port surrounding the tube is properly sealed.

D. Read ΔP_{std} and record its value in a data table, similar either to the one shown in Figure 4a (single-velocity calibration), or the one shown in Figure 4b (multi-velocity calibration). Remove the standard pitot tube from the duct and disconnect it from the manometer. Seal the standard entry port.

E. Connect the Type-S pitot tube to the manometer. Open the Type-S entry port. Insert and align the Type-S pitot tube so that its "A" side impact opening is at the same point as was the standard pitot tube, and is pointed directly into the flow. Make sure that the entry port surrounding the tube is properly sealed.

F. Read ΔP_s and enter its value in the data table. Remove the Type-S pitot tube from the duct and disconnect it from the manometer.

G. Repeat steps C through F above, until three sets of velocity head readings have been obtained.

* Note that this procedure is a general one, and must not be used without first referring to the specific considerations presented in sections IV, V, VI, and VII.

** If used; otherwise, check differential pressure gauge to be sure that it is operating properly.

PITOT TUBE IDENTIFICATION NUMBER:_____DATE:_____

CALIBRATED BY:_____

	"A" SIDE CALIBRATION			
RUN NO.	Δp_{std} (in. H_2O)	$\Delta p_{(s)}$ (in. H_2O)	$C_{p(s)}$	DEVIATION $C_{p(s)} - \bar{C}_p$
1				
2				
3				
		$\bar{C}_p$ (SIDE A)		

	"B" SIDE CALIBRATION			
RUN NO.	Δp_{std} (in. H_2O)	$\Delta p_{(s)}$ (in. H_2O)	$C_{p(s)}$	DEVIATION $C_{p(s)} - \bar{C}_p$
1				
2				
3				
		$\bar{C}_p$ (SIDE B)		

$$\text{AVERAGE DEVIATION} = \sigma\,(\text{A OR B}) = \frac{\sum_{1}^{3} \left| C_{p(s)} - \bar{C}_p(\text{A OR B}) \right|}{3} \leftarrow \text{MUST BE} \leqslant 0.01$$

$$\left| \bar{C}_p\,(\text{SIDE A}) - \bar{C}_p\,(\text{SIDE B}) \right| \leftarrow \text{MUST BE} \leqslant 0.01$$

Figure 4a. Calibration data table, single-velocity calibration.

PITOT TUBE IDENTIFICATION NUMBER: _____ DATE: _____

CALIBRATED BY: _____

A- OR B-SIDE CALIBRATION						
FAN SETTING	RUN NO.	ΔP_{std} (in. H_2O)	ΔP_s (in. H_2O)	$C_p(s)$	DEVIATION $C_p(s) - \bar{C}_p$	$\bar{V}$ (ft/min.)
A	1					
	2					
	3					
B	1					
	2					
	3					
C	1					
	2					
	3					
D	1					
	2					
	3					

AVERAGE DEVIATION AT EACH FAN SETTING $= \sigma = \dfrac{\sum_{1}^{3} |C_p(s) - \bar{C}_p|}{3}$ _____ MUST BE $\leqslant 0.01$

Figure 4b. Calibration data table, multi-velocity calibration.

H. If single-velocity calibration technique is being used, repeat steps C through G above for the B-side of the Type-S pitot tube. If multi-velocity technique is employed, repeat steps C through G for each of the remaining A-side velocity settings, and then calibrate the B-side of the pitot tube in same manner as side "A."

III. Calculations

A. For single-velocity calibrations, perform the following calculations:

1. For each of the 6 pairs of velocity head readings (i.e. 3 from side A and 3 from side B) obtained in section II above, calculate the value of the Type-S pitot tube coefficient, as follows:

$$C_p(s) = C_p(std)\sqrt{\frac{\Delta P_{std}}{\Delta P_s}} \qquad \text{(Equation 2)}$$

Where:

$C_p(s)$ = Type-S pitot tube coefficient

$C_p(std)$ = Standard pitot tube coefficient

ΔP_{std} = Velocity head, measured by standard pitot tube, cm H_2O (in. H_2O)

ΔP_s = Velocity head, measured by Type-S pitot tube, cm H_2O (in. H_2O).

2. Calculate $\overline{C}_p$ (side A), the mean A-side coefficient, and $\overline{C}_p$ (side B), the mean B-side coefficient; calculate the difference between these two average values.

3. Calculate the deviation of each of the three A-side values of $C_p(s)$ from $\overline{C}_p$ (side A), and the deviation of each B-side value of $C_p(s)$ from $\overline{C}_p$ (side B). Use the following equation:

$$\text{Deviation} = C_p(s) - \overline{C}_p \quad \text{(A or B)} \qquad \text{(Equation 3)}$$

4. Calculate σ, the average deviation from the mean, for both the A and B sides of the pitot tube. Use the following equation:

$$\sigma \text{ (side A or B)} = \frac{\sum_{1}^{3} \left| C_p(s) - \overline{C}_p \text{ (A or B)} \right|}{3} \qquad \text{(Equation 4)}$$

5. Use the pitot tube if and only if the difference between $\overline{C}_p$ (side A) and $\overline{C}_p$ (side B) is $\leq$ 0.01, and if the A and B side average deviations, calculated using Equation 4, are 0.01 or less. When a Type-S pitot tube fails to meet either of these criteria, it generally indicates that the tube has been improperly constructed.

B. For multi-velocity calibrations, perform the following calculations:

1. At each A-side velocity setting, use equation 2 to calculate the three values of $C_p(s)$ corresponding to runs #1, 2, and 3(see Figure 4b). Calculate $\overline{C}_p$, the average (mean) of these three $C_p(s)$ values.

2. For each $\overline{C}_p$ calculated in step 1 above, use equation 4 to determine σ, the average deviation from the mean.

3. Repeat steps 1 and 2 above for the B-side of the pitot tube.

4. Calculate the average test-section velocity, in feet per minute, corresponding to each A and B-side fan setting. Use the following equation:

$$\overline{v} = KC_p \sqrt{\frac{T\ \Delta\overline{P}_{std}}{PM}} \qquad \text{(Equation 5)}$$

Where:

$\overline{v}$ = Average test-section velocity at the particular fan setting, ft/min.

K = 5130 (constant)

C_p = Coefficient of standard pitot tube.

T = Temperature of flowing gas stream during calibration (ambient), °R.

P = Barometric pressure during calibration, in. Hg.

M = Molecular weight of air = 29.0.

$\overline{\Delta P}_{std}$ = Average of the three standard pitot tube readings at the particular fan setting, in. H_2O.

5. Using the $\overline{C}_p$ values and their corresponding $\overline{v}$ values as ordered data pairs, construct a plot of $\overline{C}_p$ versus $\overline{v}$; plot both the A-side and B-side data on a single set of co-ordinate axes (see Figure 5).

6. Use the pitot tube if and only if: (a) all of the A and B-side average deviations, calculated using Equation 4, are $\leq$ 0.01, and (b) the difference between the A and B-side curves (see Figure 5) is $\leq$ 0.01 for any given value of $\overline{v}$ between 1000 and 5000 ft/min.

IV. Specific Considerations Pertaining to Calibration of Isolated Type-S Pitot Tubes

When an isolated Type-S pitot tube is to be calibrated, select a calibration point at or near the center of the duct, and follow the procedures outlined in sections II and III above. The coefficients so obtained, i.e., $\overline{C}_p$ (side A) and $\overline{C}_p$ (side B), will be valid for the measurement of stack gas velocities between 1000 and 5000 ft/min, so long as the isolated pitot tube is used.[7] If, however, the pitot tube is used as a component of a pitobe assembly, the isolated coefficient values may or may not apply; this is discussed more fully in section V.

V. Pitobe Assemblies

Generally speaking, when a Type-S pitot tube is used as a component of a pitobe assembly, its A and B-side coefficients will differ appreciably from their respective isolated values, due to aerodynamic interactions among the assembly components. In fact, the isolated and assembly coefficient values will only be the same if the assembly is constructed according to the following specifications:

A. To minimize aerodynamic interactions between the pitot tube and sampling nozzle there must be a separation distance (free-space) of at least 3/4 inch between the nozzle and pitot tube, with the largest size nozzle (usually 1/2 inch, i.d.) in place (see Figure 6a).

B. To minimize aerodynamic interactions between the thermocouple

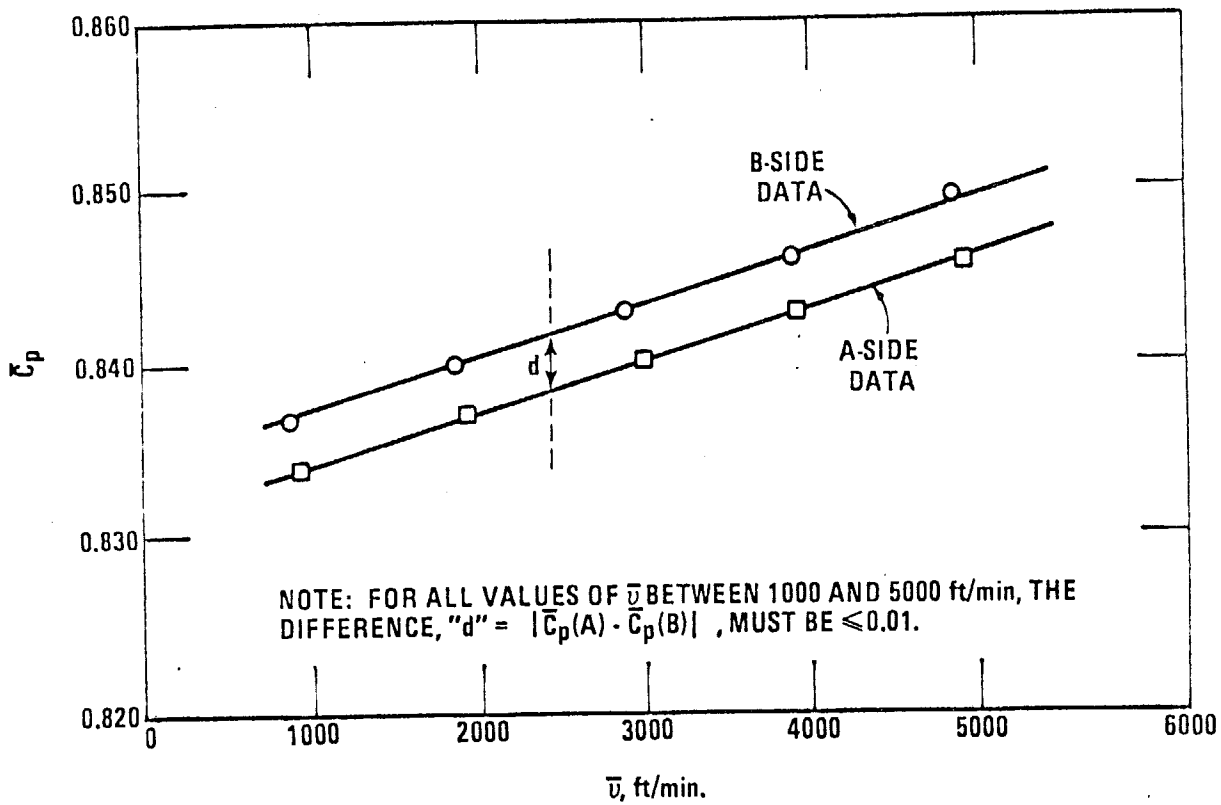

Figure 5. Typical calibration curve, multi-velocity calibration.

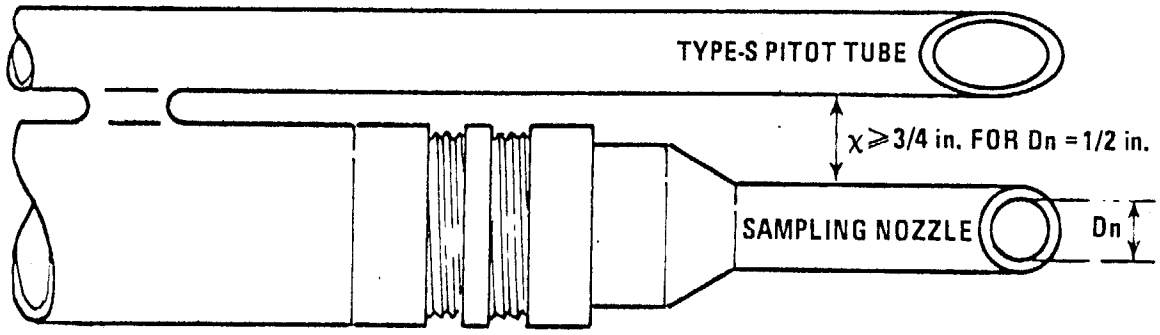

Figure 6a. Minimum pitot-nozzle separation needed to prevent interference.

and pitot tube, the thermocouple wire must be mounted on the pitot tube in such a way that the tip of the wire is in line with, but at least 3/4 inch from, the center of the pitot tube impact openings (see Figure 6b).

C. To eliminate pitot tube-probe sheath interference, there must be at least 3 inches between the leading edge of the probe and the center of the pitot tube impact openings (see Figure 6c).

For those assemblies which either (1) meet requirements A through C above but have unknown isolated coefficients, or (2) fail to meet requirements A through C, use the procedures outlined in sections II and III, in conjunction with the following special considerations, to determine the A and B-side coefficients of the Type-S pitot tube:

1. Although it is preferable that the calibration point be located at or near the center of the duct, insertion of a probe sheath into a small duct may cause significant cross-sectional area blockage, and yield incorrect coefficient values. Therefore, to minimize the blockage effect, the calibration point may be a few inches off-center if necessary. To keep the actual reduction in C_p due to blockage below 1 percent, it is necessary that the theoretical blockage, as determined by a projected-area model of the probe sheath, be 2 percent or less of the duct cross-sectional area for assemblies without external sheaths (see Figure 7a) and 3 percent or less for assemblies with external sheaths (Figure 7b).[5]

2. For pitobe assemblies in which pitot tube-nozzle interference is a factor (i.e., those in which the pitot-nozzle separation distance is less than 3/4 inch* with a 1/2 inch nozzle in place), the value of C_p will depend somewhat on the amount of free-space between the tube and nozzle[2,3]; in these instances, separate calibrations should be performed with each of the commonly-used nozzle sizes in place. Note that single-velocity calibration technique will be acceptable for this purpose, even though the larger nozzle sizes (> 1/4 inch) are not ordinarily used for isokinetic sampling at velocities around 3000 ft/min (the calibration velocity); data from a recent study have shown that for pitobe assemblies with 3/8 inch and 1/2 inch nozzles in place, C_p does not change appreciably with velocity over the normal working range.[3] If multi-velocity calibration technique is used, it is recommended, for the sake of simplicity that each nozzle size be studied only in

* Note carefully that a thermocouple wire attached to a Type-S pitot tube can cause a reduction in the effective amount of free-space between the pitot tube and nozzle, if the wire is situated between the tube and nozzle.

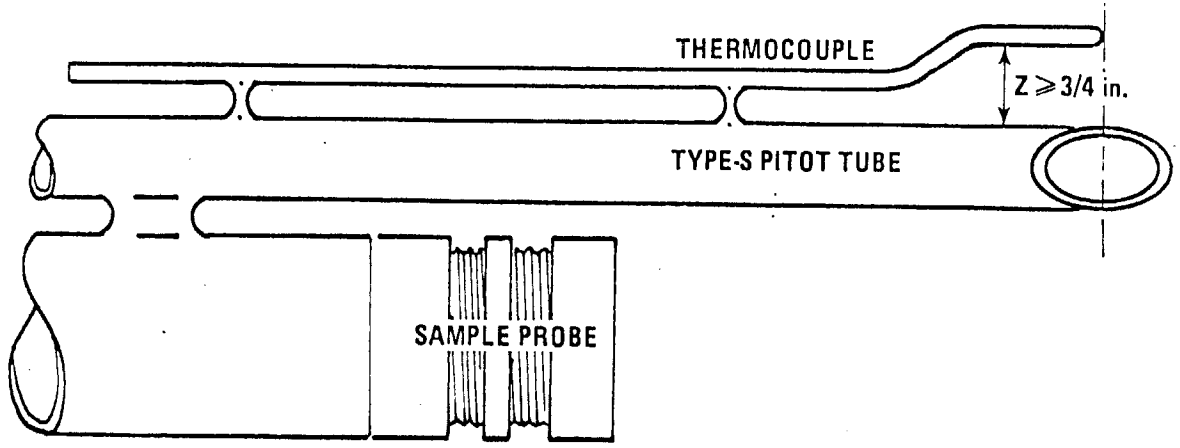

Figure 6b. Proper thermocouple placement to prevent interference.

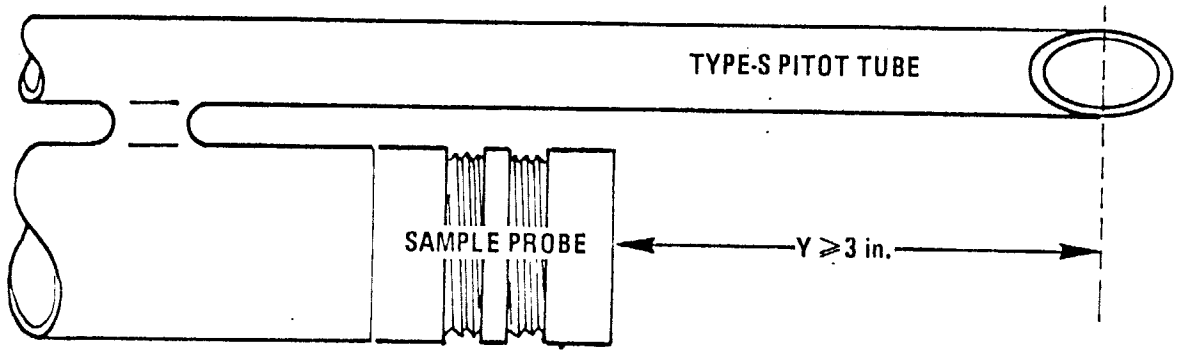

Figure 6c. Minimum pitot-sample probe separation needed to prevent interference.

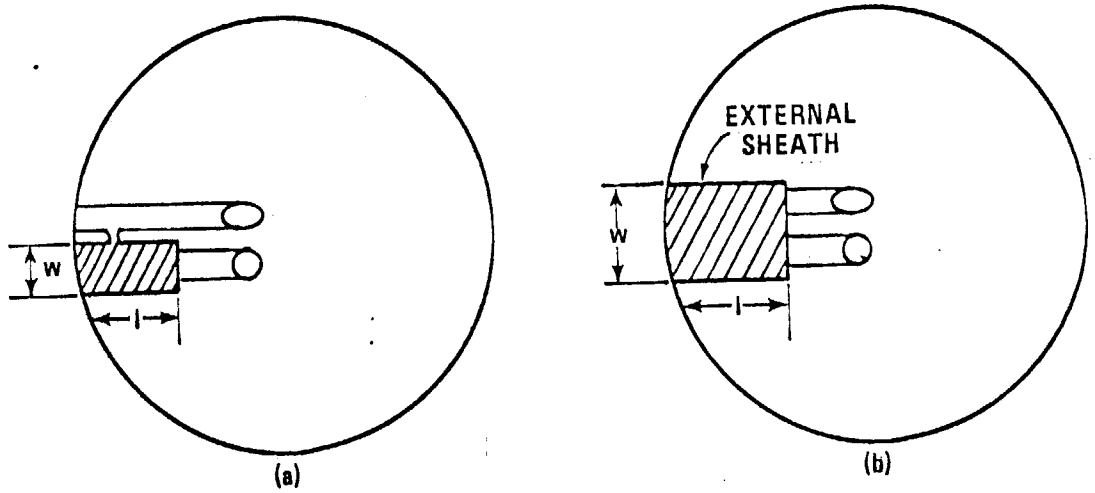

$$\text{PERCENT THEORETICAL BLOCKAGE} = \left[\frac{l \times w}{\text{DUCT AREA}}\right] \times 100$$

Figure 7. Projected-area models for typical pitobe assemblies.

that part of the normal working range in which it is ordinarily used for isokinetic sampling (see Figure 8); however, calibration data covering the entire range may be taken for each nozzle size, if desired.

VI. Recalibration and Field Use

A. The Type-S pitot tube shall be calibrated before its initial use. Thereafter, if the tube has been significantly damaged by field use (for example, if the impact openings are bent out of shape, cut, nicked, or noticeably misaligned), it shall be repaired if possible, recalibrated, and replaced if necessary.

B. When the Type-S pitot tube is used in the field, the appropriate A or B-side coefficient shall be used to perform velocity calculations, depending upon which side of the pitot tube is pointed toward the flow. For tubes calibrated by single-velocity technique, this coefficient will ordinarily be either $\bar{C}_p$ (side A) or $\bar{C}_p$ (side B), and for tubes calibrated by multi-velocity technique, it will be the appropriate value of $\bar{C}_p$, taken from the calibration curve (note, however, the important exception in section VII).

VII. The Use of Pitobe Assemblies to Sample Small Ducts

When sampling a small duct (~12 to 36 inches in diameter)* with a pitobe assembly, the probe sheath can block a significant part of the duct cross-section, causing a reduction in the value of C_p. Therefore, in certain instances it may be necessary, prior to sampling, to make adjustments in the coefficient values obtained by calibration. To determine whether or not these adjustments are necessary, proceed as follows:

A. Make a projected-area model of the pitobe assembly, with the Type-S pitot tube impact openings positioned at the center of the duct (see Figure 9a). This model represents the approximate "average blockage" of the duct cross-section which will occur during a sample traverse. Although the actual blockage will be less than this for sample points close to the near stack wall and more than this for points close to the far wall, the model approximates the average condition.

B. Calculate the theoretical average blockage by taking the ratio of the projected area of the probe sheath (in.^{2}) to the cross sectional area of the duct (in.^{2}), and multiplying by 100. If the theoretical blockage is either 2 percent or less for an assembly without an external sheath, or 3 percent or less for an assembly with an external sheath, the decrease in C_p will be less than 1 percent[5] and no adjustment in the pitot tube coefficients will be necessary. If the theoretical blockage

---

* See "Addendum"

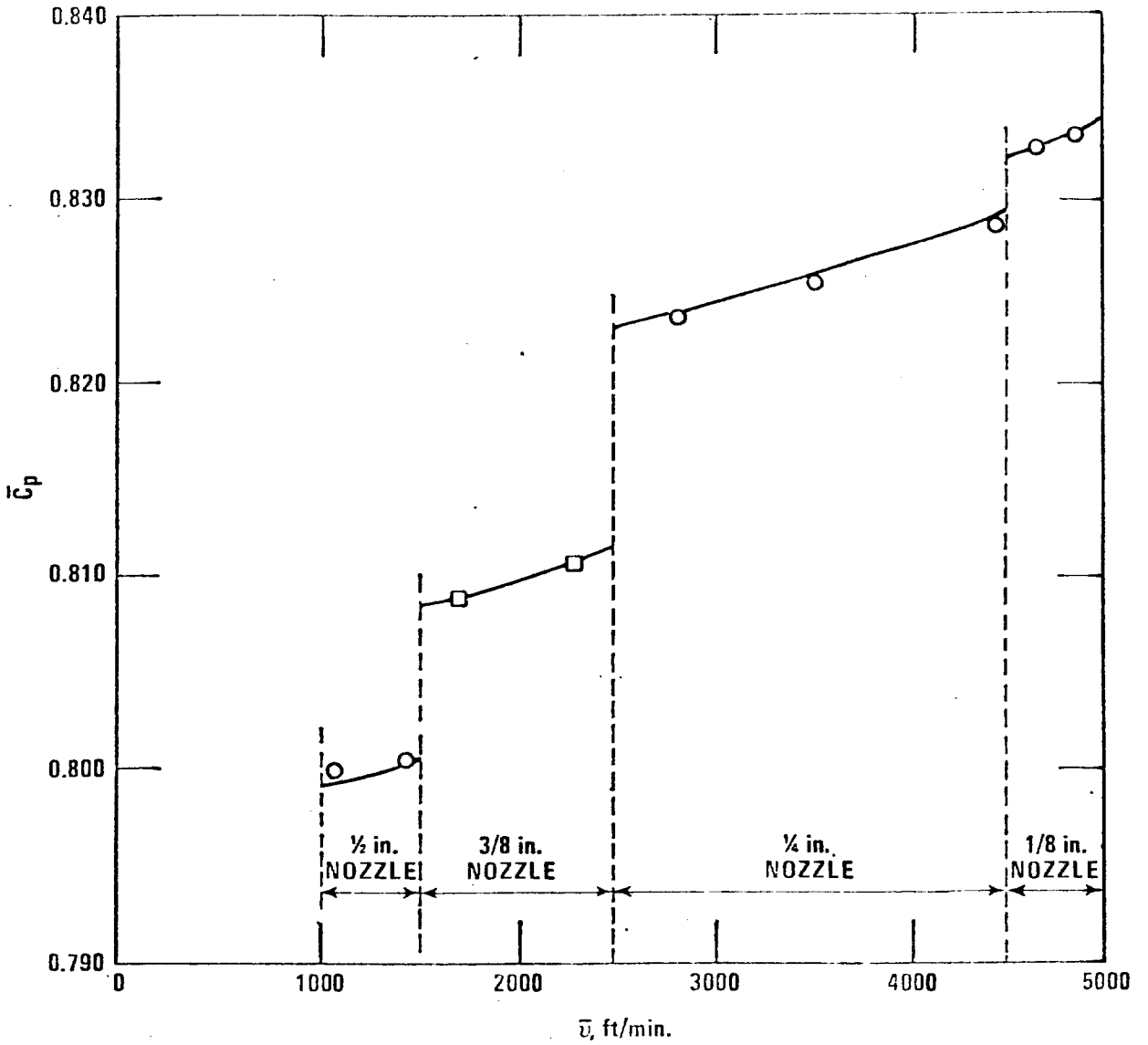

Figure 8. Typical multi-velocity calibration curve for pitobe assemblies.

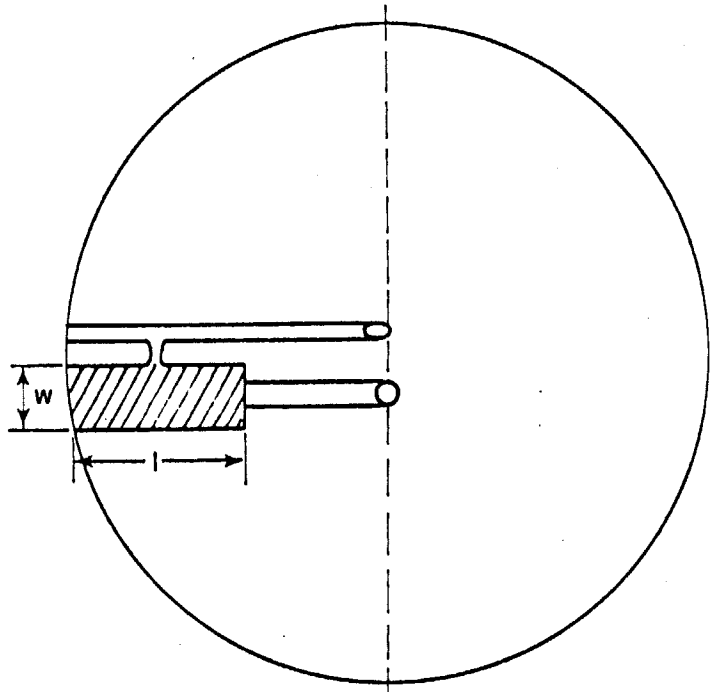

$$\text{PERCENT THEORETICAL BLOCKAGE} = \left[\frac{l \times w}{\text{DUCT AREA}}\right] \times 100$$

Figure 9a. Typical projected-area model for sampling of small ducts with pitobe assemblies.

exceeds these limits, apply corrections to the pitot tube coefficients as shown in Figure 9b; extrapolate if necessary.

REFERENCES

1. Standards of Performance for New Stationary Sources. Federal Register. 36 (247). December 23, 1971.

2. Vollaro, R. F. The Effect of Aerodynamic Interference Between a Type-S Pitot Tube and Sampling Nozzle on the Value of the Pitot Tube Coefficient. Environmental Protection Agency. Durham, N. C. February, 1975.

3. Gnyp, A. W., C. C. St. Pierre, D. S. Smith, D. Mozzon, and J. Steiner. An Experimental Investigation of the Effect of Pitot Tube - Sampling Probe Configurations on the Magnitude of the S-Type Pitot Tube Coefficient for Commercially Available Source Sampling Probes. Prepared for the Ministry of the Environment. Toronto, Canada. University of Windsor. February, 1975.

4. Vollaro, R. F. The Effects of the Presence of a Sampling Nozzle, Thermocouple, and Probe Sheath on Type-S Pitot Tube Accuracy. Environmental Protection Agency. Durham, N. C. June, 1975.

5. Vollaro, R. F. The Effects of The Presence of a Probe Sheath on Type-S Pitot Tube Accuracy. Environmental Protection Agency. Durham, N. C. August, 1975.

6. The Measurement of Fluid Flow in Pipes. British Standards Institute. London, England. BS 1042 (1971).

7. Vollaro, R. F. An Evaluation of Single-Velocity Calibration Technique as a Means of Determining Type-S Pitot Tube Coefficients. Environmental Protection Agency. Durham, N. C. August, 1975.

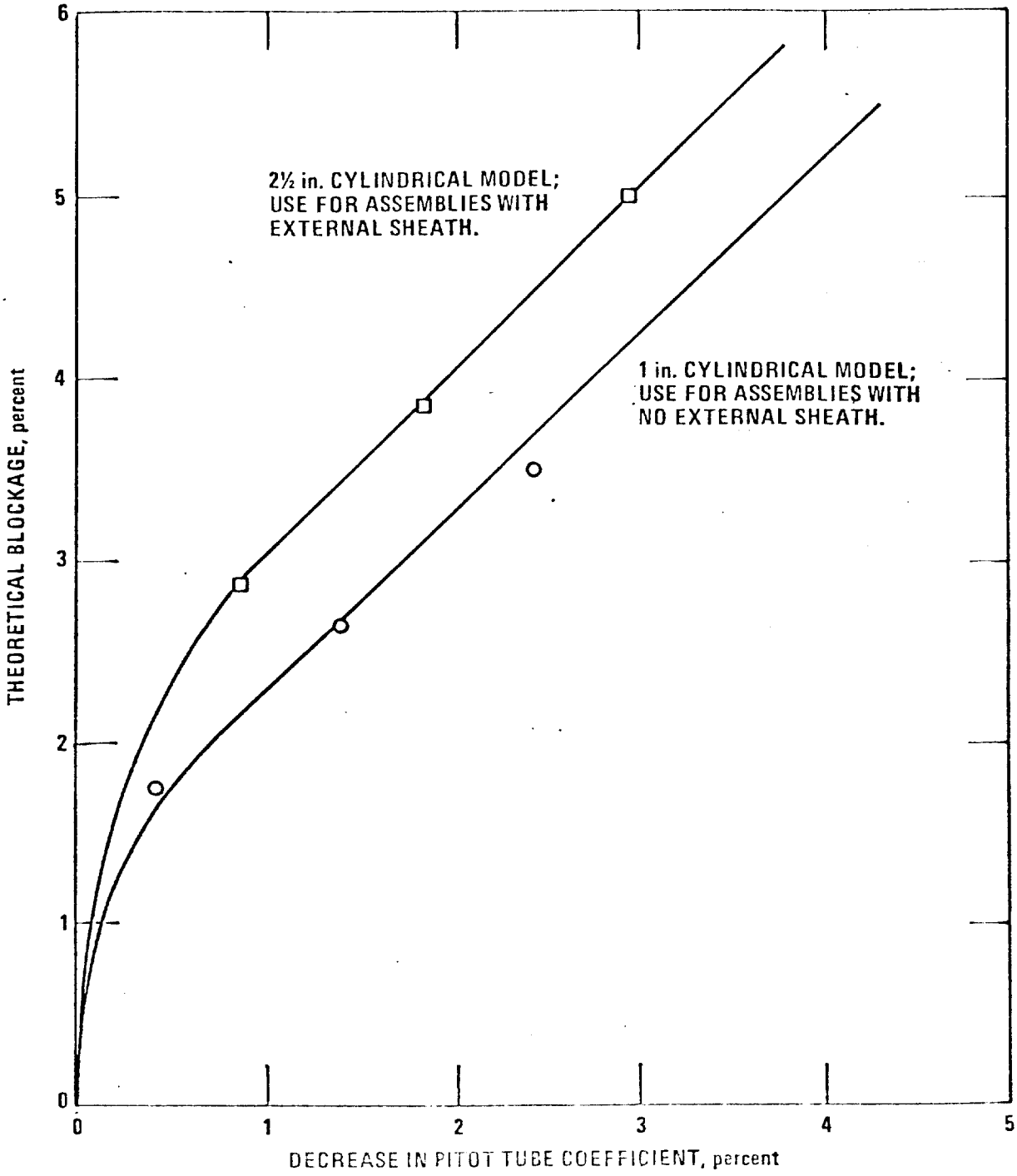

Figure 9b. Adjustment of type-S pitot tube coefficients to account for blockage effects (small ducts).

ADDENDUM TO "GUIDELINES FOR TYPE-S PITOT TUBE CALIBRATION"

I. ALTERNATIVE CALIBRATION STANDARD

According to Section I of these guidelines, it is preferable for the pitot tube which is used as the calibration standard to have a known coefficient, obtained either directly from the National Bureau of Standards, or by calibration against another pitot tube having a known (NBS traceable) coefficient. Alternatively, an ellipsoidal-nosed pitot static tube, designed according to the criteria illustrated in Figure 2, can be used as the calibration standard. The ellipsoidal-nosed pitot static tube is the only type of standard pitot tube recommended by the British Standards Institute for use without individual calibration. Despite the excellence of its design, however, the ellipsoidal-nosed tube is not always carried as a stock item by pitot manufacturers; thus, in practice, it may be difficult or expensive to obtain one.

One of the most readily-available types of standard pitot tube is the Prandtl hemispherical-nosed tube (see Figure A-1). The coefficient of a Prandtl hemispherical-nosed tube, when designed according to the criteria illustrated in Figure A-1, will be 0.99 ± 0.01; its precise coefficient value cannot be determined without individual calibration, however. From a technical standpoint, this means that calibrations done using a hemispherical-nosed pitot tube as the standard will generally not be as accurate as those done using an ellipsoidal-nosed pitot tube as the standard. Nevertheless, the Prandtl hemispherical-nosed pitot tube (designed according to Figure A-1) will, because of its availability and low cost, be considered to be an acceptable alternative to the ellipsoidal-nosed pitot static tube for use as a calibration standard.

II. ADDENDUM TO SECTION VII (SAMPLING IN SMALL DUCTS)

The usefulness of the projected-area model described in Section VII and illustrated in Figure 9a is somewhat limited, in that it applies only to: (a) circular or rectangular cross-sections, having diameters (or equivalent diameters) between 12 and 36 inches; (b) pitobe assemblies having "normal" pitot tube-probe sheath separation distances (dimension "y", Figure 6c) i.e., $2" \leq y \leq 4"$. The model may or may not be representative of the actual blockage, when duct diameters less than 12 inches are encountered, or when the pitot tube-probe sheath separation distances are outside the normal range. When these situations occur, it is recommended that the following be done:

(a) Abnormal pitot tube - probe sheath spacings

For abnormal pitot tube-probe sheath separation distances, it will be necessary to make a separate projected-area model at each traverse point, either along one of the diameters or along one of the rows, depending upon whether the cross-section is circular or rectangular; in each model, the sampling nozzle opening should be centered

around the traverse point in question. The average theoretical blockage should then be calculated, based on these models, as follows:

$$\text{Average theoretical blockage (\%)} = \left[\frac{\sum_{1}^{n} \ell_n W_n}{n A_d} \right] \times 100 \qquad \text{(Equation 1-A)}$$

Where: n = Number of traverse points on a row or diameter.

ℓ_n = Length of sheath segment inside duct, at the particular traverse point, (inches).

W_n = Width of sheath segment at the particular traverse point (inches).

A_d = Cross-sectional area of duct, (in^2).

Figure 9b should then be used to determine whether or not an adjustment in the value of C_p is necessary.

(b) <u>Ducts smaller than 12 inches in diameter</u>

At the present time, comprehensive guidelines are being prepared, by which representative sample traverses can be done in very small ($D < 12$ inches) ducts.

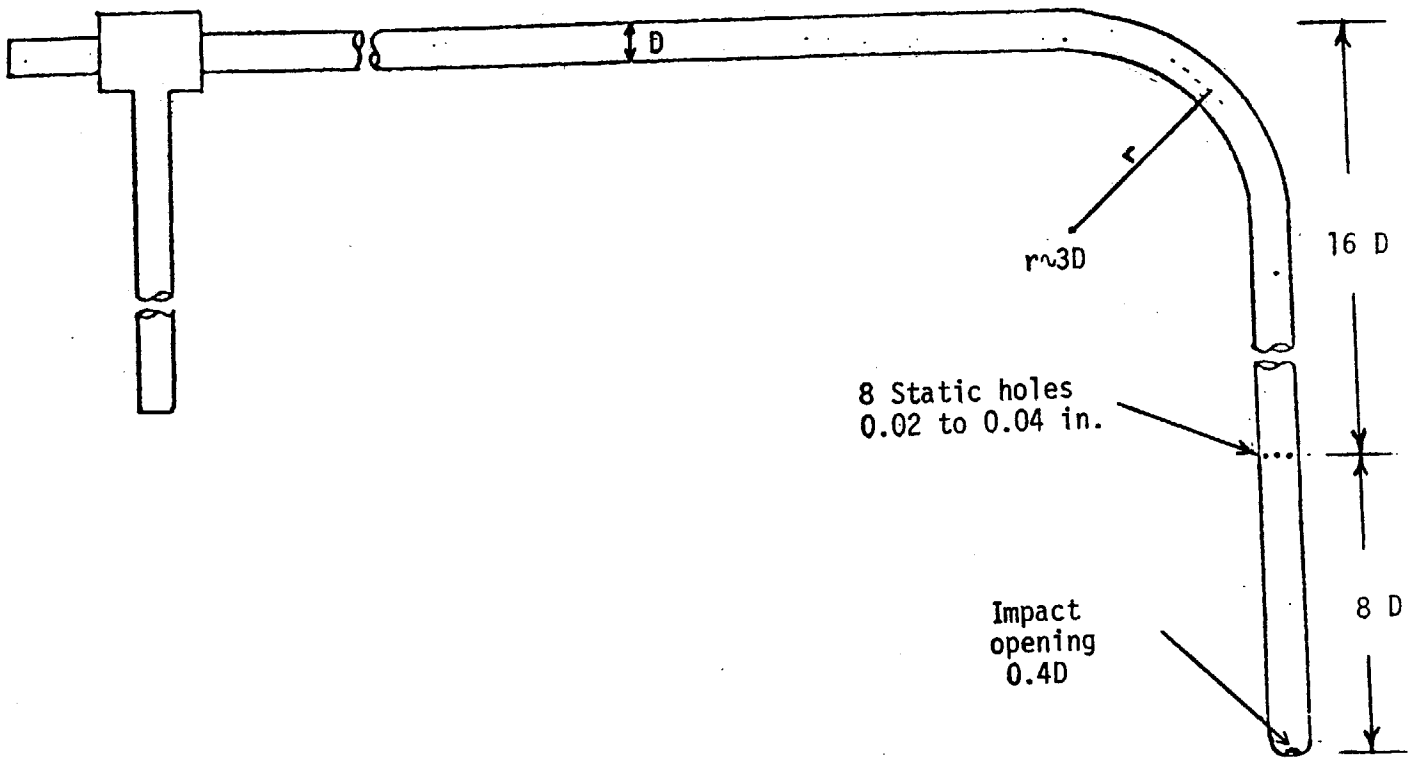

Figure A-1. Prandtl Hemispherical-Nosed Standard Pitot Tube

THE EFFECTS OF IMPACT OPENING MISALIGNMENT ON THE VALUE OF THE TYPE-S PITOT TUBE COEFFICIENT

Robert F. Vollaro
United States Environmental Protection Agency

INTRODUCTION

In source-sampling, stack gas velocity is usually measured with a Type-S pitot tube. Before a Type-S pitot tube is used in the field, its coefficient (C_p) should be determined by calibration against a standard pitot tube (1). When a Type-S pitot tube is used in the field, it is subject to considerable abuse; it is often exposed to hot, corrosive gas streams, and can incur damage when it is transported to and from field test sites. As a result of this abuse, the impact openings of the pitot tube can become misaligned, which, in turn, can cause a change in the value of C_p. Consequently, the pitot tube may need to be recalibrated after it has been used in the field. Experiments were recently done to determine quantitatively the effects of impact opening misalignment on the value of C_p. This paper presents the results of these experiments and discusses their significance.

EXPERIMENTAL METHOD

At the outset of the study, a Type-S pitot tube having properly aligned impact openings (as a new pitot tube would have, prior to field use) was constructed and calibrated against a standard pitot tube, thus providing a "reference" coefficient, C_p (ref). Subsequently, a number of special Type-S pitot tubes, having misaligned impact openings, were constructed and calibrated; the effects of each type of impact opening misalignment on the value of C_p were carefully noted. In all, six different types of misalignment were studied; these six types are considered representative of misalignment problems which can result from field-use, because they were selected based upon observations made in a previous study (2), in which 51 Type-S pitot tubes (many of which had been used extensively in the field) were carefully examined in top, side, and end-views prior to calibration. A description of each of the six types of misalignment is given below:

Type 1: Transverse axis misalignment (one opening only).
When the pitot tube is examined in end-view, one impact opening is observed to be offset by an angle, α, from its properly aligned position with respect to the transverse tube axis (Figure 1A). Three test cases were considered: $\alpha = 3°$, $\alpha = 7°$, and $\alpha = 12°$. In each case, data were taken first with the misaligned opening pointed into the flow, and then pointed away from the flow.

Type 2: Transverse axis misalignment (both openings).
In end-view, both impact openings are offset, at angles α_1 and α_2, from their properly aligned positions with respect to the transverse axis (Figure 1B). Three test cases were considered: $\alpha_1 = \alpha_2 = 2°$; $\alpha_1 = \alpha_2 = 4°$; and $\alpha_1 = \alpha_2 = 6°$.

Type 3: Longitudinal axis misalignment (one opening only).
In top-view, one impact opening of the pitot tube is offset by an angle, β, from its properly aligned position with respect to the longitudinal tube axis

(Figures 1C, 1D). Note that the angle β is arbitrarily defined as negative (-) when the impact opening is tilted upward as shown in Figure 1C, and positive (+) when the opening is tilted downward, as in Figure 1D. A total of ten test cases were considered, five with the misaligned opening pointed toward the flow (β = -2°, -5°, -8°, +5° and +8°), and five with the misaligned opening opposite the flow (β = +2°, +5°, +8°, -5° and -8°).

Type 4: Longitudinal axis misalignment (both openings).
In top-view, both openings are offset, at angles β_1 and β_2, from their properly aligned positions with respect to the longitudinal axis (Figure 1E). Four test cases were considered: (β_1 = -5°, β_2 = +5°); (β_1 = -8°, β_2 = +8°); (β_1 = +5°, β_2 = -5°); and (β_1 = +8°, β_2 = -8°).

Type 5: Length misalignment.
When the pitot tube is examined in side-view, one leg is observed to be longer than the other, by an amount, "z" (Figure 1F). Three test cases were considered: z = 1/16 in; z = 1/8 in; and z = 5/32 in.

Type 6: Planar misalignment.
When the pitot tube is examined in side-view, the centerlines of the two legs are observed to be non-coincident, by an amount, "w" (Figure 1G). Three test cases were considered: w = 1/32 in; w = 1/16 in; and w = 1/8 in.

EXPERIMENTAL RESULTS

The results of the experiments are presented in Table I. These results will now be discussed on a case-by-case basis:

Reference coefficients: The A and B sides of the geometrically perfect Type-S pitot tube had identical reference coefficient values of 0.846.

Type 1: No significant change (i.e., greater than 1 percent) from C_p (ref) was observed for any of the test cases, either with the misaligned opening facing the flow or opposite the flow.

Type 2: Again no significant change from C_p (ref) was observed for any of the test cases.

Type 3: With the misaligned impact opening facing the flow, the following results were obtained: (a) for β = -2°, C_p remained essentially equal to C_p (ref); (b) for β = -5°, C_p increased to 0.860; (c) for β = -8°, C_p increased to 0.867; (d) for β = +5°, C_p decreased to 0.834; (e) for β = +8°, C_p decreased to 0.828. With the misaligned opening opposite the flow, no change from C_p (ref) was observed for any of the five test cases. Thus, it appears that for β values up to 8°, longitudinal axis misalignment effects are "one-sided," occurring only when the misaligned opening faces the flow; the effects are also directional, in that C_p increases for negative values of β and decreases for positive β values.

Type 4: For the test case (β_1 = -5°, β_2 = +5°), a C_p value of 0.857 was obtained; for (β_1 = -8°, β_2 = +8°), C_p increased to 0.863; for (β_1 = +5°, β_2 = -5°), C_p decreased to 0.831; for (β_1 = +8°, β_2 = -8°), C_p decreased to 0.828. These results are consistent, both in magnitude and direction, with those observed for

Type 3 misalignment, indicating once again that the flow only "sees" the longitudinal axis misalignment of the impact opening which faces the flow.

Type 5: With the shorter leg of the pitot tube facing the flow, the following results were obtained: for z = 1/16 in, there was no change from C_p (ref); for z = 1/8 in, C_p decreased to 0.837; for z = 5/32 in, C_p decreased to 0.828. With the longer leg facing the flow, C_p remained essentially equal to C_p (ref), for all three values of z. Therefore, it is apparent that for values of z up to 1/8 in, length misalignment effects are one-sided, occurring only when the shorter tube faces the flow.

Type 6: For w = 1/32 in, C_p decreased to 0.838; for w = 1/16 in, C_p decreased to 0.820; for w = 1/8 in, a C_p value of 0.779 was obtained. These results show that C_p is very sensitive to planar misalignment; for w values as small as 1/8 inch, C_p can decrease by up to 8 percent.

CONCLUSIONS

A recent study of the effects of impact opening misalignment on the value of the Type-S pitot tube coefficient has demonstrated the following:

(1) The value of C_p is unaffected by transverse axis misalignment, for values of α up to about 10°.

(2) Longitudinal axis misalignment effects first begin to cause a significant (> 1%) change in C_p when β is about 5°; for β = 8°, C_p can change by 2 to 3 percent. Longitudinal axis effects are one-sided, in that they affect C_p only when a misaligned opening faces the flow. The effects are also directional; negative β values increase C_p, and positive β values decrease C_p.

(3) Length misalignment first causes a significant change (decrease) in the value of C_p when z is about 1/8 inch; the effect is one-sided, occurring only when the shorter leg of the pitot tube faces the flow.

(4) Planar misalignment first causes a significant change (decrease) in the value of C_p when w is about 1/32 inch; for w = 1/8 inch, C_p can be lowered by as much as 8 percent.

In view of the above, it can be concluded that if the impact opening misalignment of a given Type-S pitot tube is severe enough to cause a significant change in C_p (i.e., if $\alpha > 10°$, $\beta > 5°$, $z > 1/8$ in, or $w > 1/32$ in), this should be easily detectable by examining the tube in top, side, and end-views. Therefore, a Type-S pitot tube need not be recalibrated after field use, provided that it passes a careful visual inspection.

REFERENCES

1. Standards of Performance for New Stationary Sources. Federal Register, 36(247). December 23, 1971.

2. Vollaro, R. F. A Type-S Pitot Tube Calibration Study. U. S. Environmental

Protection Agency, Emission Measurement Branch. Research Triangle Park, N. C. July 1974.

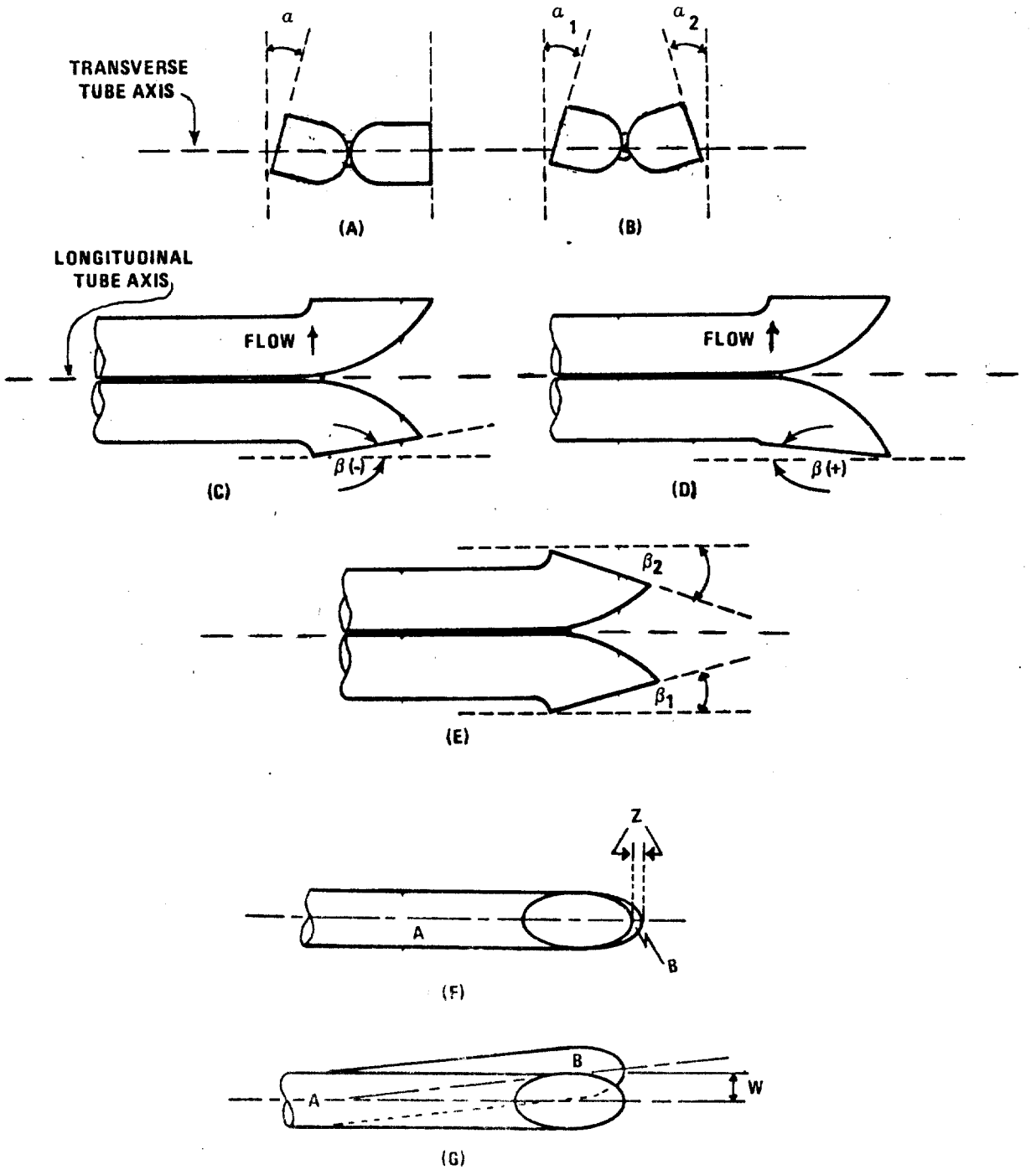

Figure 1. Types of misalignment studied.

TABLE I: SUMMARY OF RESULTS

Type of Misalignment	Test Case	C_p	C_p(ref)	Percentage Change* from C_p(ref)
1 (Figure 1A)	$\alpha = 3°$, facing flow	0.844	0.846	0.2
	$\alpha = 3°$, opposite flow	0.844		0.2
	$\alpha = 7°$, facing flow	0.846		0.0
	$\alpha = 7°$, opposite flow	0.846		0.0
	$\alpha = 12°$, facing flow	0.846		0.0
	$\alpha = 12°$, opposite flow	0.844		0.2
2 (Figure 1B)	$\alpha_1 = \alpha_2 = 2°$	0.850	0.846	0.5
	$\alpha_1 = \alpha_2 = 4°$	0.850		0.5
	$\alpha_1 = \alpha_2 = 6°$	0.844		0.2
3 (Figures 1C, 1D)	$\beta = -2°$, facing flow	0.853	0.846	0.8
	$\beta = -5°$, facing flow	0.860		1.7
	$\beta = -8°$, facing flow	0.867		2.5
	$\beta = +5°$, facing flow	0.834		1.4
	$\beta = +8°$, facing flow	0.828		2.1
	$\beta = -5°$, opposite flow	0.845		0.2
	$\beta = -8°$, opposite flow	0.846		0.0
	$\beta = +2°$, opposite flow	0.848		0.2
	$\beta = +5°$, opposite flow	0.848		0.2
	$\beta = +8°$, opposite flow	0.845		0.2
4 (Figure 1E)	$\beta_1 = -5°$, $\beta_2 = +5°$	0.857	0.846	1.3
	$\beta_1 = -8°$, $\beta_2 = +8°$	0.863		2.0
	$\beta_1 = +5°$, $\beta_2 = -5°$	0.831		1.8
	$\beta_1 = +8°$, $\beta_2 = -8°$	0.828		2.1
5 (Figure 1F)	z = 1/16", short facing flow	0.844	0.846	0.2
	z = 1/16", long facing flow	0.849		0.4
	z = 1/8", short facing flow	0.837		1.1
	z = 1/8", long facing flow	0.850		0.5
	z = 5/32", short facing flow	0.828		2.1
	z = 5/32", long facing flow	0.848		0.2
6 (Figure 1G)	w = 1/32"	0.838	0.846	1.0
	w = 1/16"	0.820		3.1
	w = 1/8"	0.779		7.9

$$* \text{ Percentage Change from } C_p(\text{ref}) = \left[\frac{|C_p - C_p(\text{ref})|}{C_p(\text{ref})}\right] \times 100$$

ESTABLISHMENT OF A BASELINE COEFFICIENT VALUE FOR PROPERLY CONSTRUCTED TYPE-S PITOT TUBES

Robert F. Vollaro

INTRODUCTION

Experiments were recently done in which 14 isolated* Type-S pitot tubes (Figure 1) were calibrated against a standard pitot tube. During construction of the 14 Type-S pitot tubes, special care was taken to ensure that the face openings of each tube were in proper alignment (see Figure 2). The purpose of the experiments was to try to establish a baseline coefficient value for properly constructed isolated Type-S pitot tubes; if this could be done, it would then be possible, in certain instances, to forego calibration and to assign coefficient values to Type-S pitot tubes on the basis of tube geometry. This paper presents the results of the experiments and discusses their significance.

EXPERIMENTAL METHOD

Prior to calibration, the face-opening alignment of each Type-S pitot tube was carefully checked by examining the tube in top, side, and end-views; micrometer readings were taken (as described in Reference 2) to confirm the alignment of the face openings with respect to the traverse and longitudinal tube axes. Each of the 14 Type-S pitot tubes met the alignment specifications of Figure 2. The port-to-port spacing (dimension "X," Figure 1) and the external tubing diameter (dimension "d," Figure 1) of each Type-S pitot tube, were also measured and recorded.

The calibrations were performed in a 12-inch-diameter wind tunnel in

---

* An "isolated" Type-S pitot tube is any Type-S pitot tube that is not used in combination with other source-sampling components (probe, nozzle, thermocouple).

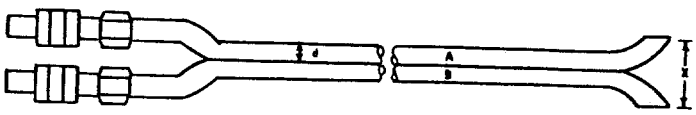

Figure 1. Isolated Type-S pitot tube.

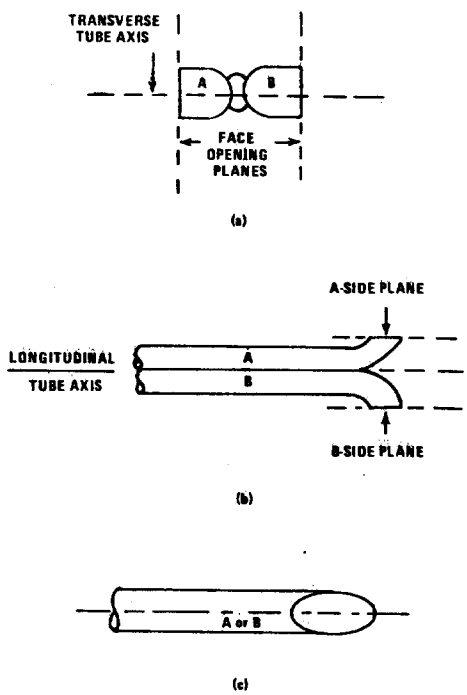

Figure 2. Properly constructed isolated Type-S pitot tube shown in: (a) end-view; face openings perpendicular to transverse axis; (b) top-view; openings parallel to longitudinal axis; (c) side-view; both legs of equal length and centerlines coincident when viewed from both sides.

which ambient ($70^{o}F$) air was flowing. During calibration, the air velocity was held constant at about 2800 ft/min. Each Type-S pitot tube was calibrated, first with the "A" side facing the flow, and then with the "B" side facing the flow. The procedures for single-velocity calibration of Type-S pitot tubes, outlined in Reference 1, were used throughout. Calibration data for each pitot tube were recorded in a data table similar to the one shown in Figure 3.

METHOD OF DATA ANALYSIS

For each Type-S pitot tube, the calibration data were analyzed as outlined in (1) through (7) below.

1. For each of the six pairs of differential pressure readings, i.e., three from side A and three from side B (see Figure 3), the value of the Type-S pitot tube coefficient was calculated as follows:

$$C_p(s) = C_p(std)\sqrt{\frac{\Delta P_{std}}{\Delta P_s}} \qquad \text{(Equation 1)}$$

where: $C_p(s)$ = individual A or B-side value of the Type-S pitot tube coefficient

$C_p(std)$ = standard pitot tube coefficient = 0.99

ΔP_{std} = differential pressure reading, made with standard pitot tube

ΔP_s = differential pressure reading, made with Type-S pitot tube

2. The mean coefficient values for the A and B sides of each Type-S pitot tube were calculated using the following equation:

PITOT TUBE IDENTIFICATION NUMBER:_____ DATE:_____

CALIBRATED BY:_____

	"A" SIDE CALIBRATION			
RUN NO.	ΔPstd (in. H_2O)	ΔP(s) (in. H_2O)	$C_p(s)$	DEVIATION $C_p(s)-\bar{C}_p$
1				
2				
3				
		$\bar{C}_p$ (SIDE A)		

	"B" SIDE CALIBRATION			
RUN NO.	ΔPstd (in. H_2O)	ΔP(s) (in. H_2O)	$C_p(s)$	DEVIATION $C_p(s)-\bar{C}_p$
1				
2				
3				
		$\bar{C}_p$ (SIDE B)		

Figure 3. Calibration data table.

$$\overline{C}_p(A \text{ or } B) = \frac{\sum_1^3 C_p(s)}{3} \qquad \text{(Equation 2)}$$

where: $\overline{C}_p(A \text{ or } B)$ = mean coefficient value for the A or B side of the Type-S pitot tube

$C_p(s)$ = individual A or B-side coefficient value

3. A histogram was constructed showing the frequency distribution of the 28 (i.e., 14 A-side and 14 B-side) values of $\overline{C}_p$.
4. The average deviation of the $C_p(s)$ values from $\overline{C}_p$ was calculated for both the A and B sides of each Type-S pitot tube as follows:

$$\sigma = \frac{\sum_1^3 |C_p(s) - \overline{C}_p(A \text{ or } B)|}{3} \qquad \text{(Equation 3)}$$

where: σ = average deviation of the $C_p(s)$ values from the mean A or B side coefficient

$C_p(s)$ = individual A or B-side coefficient value

$\overline{C}_p(A \text{ or } B)$ = mean A or B-side coefficient value

5. A histogram was constructed showing the frequency distribution of the σ values.
6. The absolute value of the difference between the mean A and B-side coefficients was calculated for each Type-S pitot tube as follows:

$$\gamma = |\overline{C}_p(A) - \overline{C}_p(B)| \qquad \text{(Equation 4)}$$

Table I. Summary of results.

Pitot tube identification number	External tubing diameter, d (in.)	Port-to-port separation,[a] in terms in tubing diameter	$\bar{C}_p$ (side A)	$\bar{C}_p$ (side B)	A-to-B side difference (γ)	Average deviation (σ)	
						Side A	Side B
A	0.375	2.2d	0.842	0.841	0.001	0.002	0.002
1	0.375	2.2d	0.846	0.844	0.002	0.001	0.001
B	0.375	2.3d	0.845	0.839	0.006	0.002	0.001
2	0.375	2.3d	0.849	0.842	0.007	0.001	0.001
C	0.375	2.5d	0.841	0.845	0.004	0.001	0.001
3	0.375	2.5d	0.845	0.847	0.002	0.001	0.001
D	0.375	2.6d	0.847	0.846	0.001	0.002	0.000
4	0.375	2.5d	0.851	0.846	0.005	0.000	0.005
E	0.375	2.6d	0.844	0.844	0.000	0.001	0.001
5	0.375	2.6d	0.843	0.836	0.007	0.001	0.001
6	0.250	2.6d	0.842	0.842	0.000	0.001	0.000
7	0.250	2.6d	0.842	0.845	0.003	0.001	0.002
8	0.188	2.8d	0.847	0.854	0.007	0.002	0.001
9	0.188	2.7d	0.850	0.846	0.004	0.001	0.002

[a]Dimension "X," Figure 1.

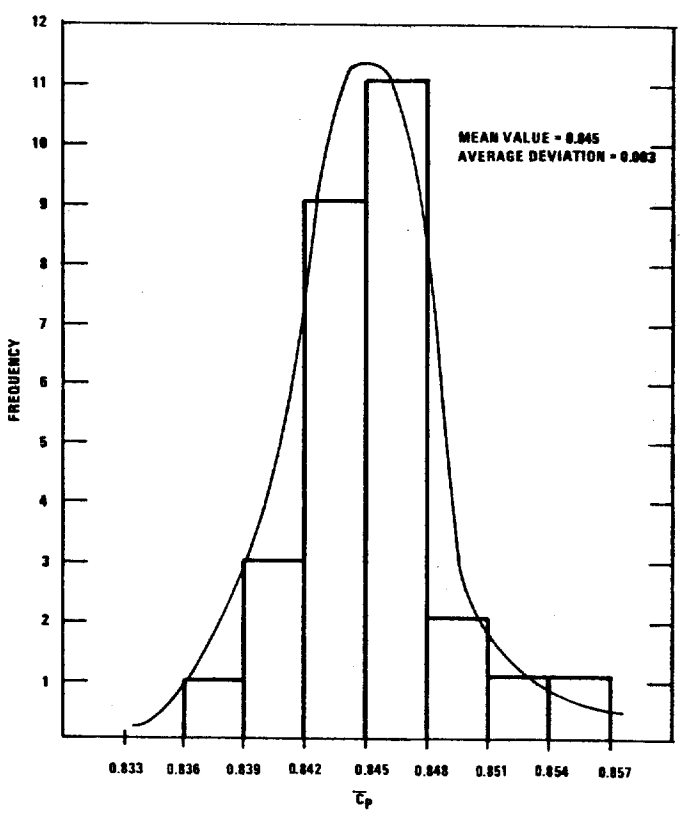

Figure 4. Frequency distribution of $\bar{C}_p$ values.

where: γ = absolute value of the difference between the mean A and B side coefficient values

$\overline{C}_p(A)$ and $\overline{C}_p(B)$ = mean A and B-side coefficient values, respectively

7. A histogram was constructed showing the frequency distribution of the γ values.

RESULTS OF DATA ANALYSIS

The results of the data analysis are presented in Table I and in Figures 4 through 6. Figure 4 shows that the average of the 28 $\overline{C}_p$ values was 0.845, with an average deviation of 0.003; all of the $\overline{C}_p$ values were between 0.836 and 0.854. Figure 5 shows that the values of average deviation (σ) for the A and B sides of the 14 Type-S pitot tubes ranged from 0.000 to 0.005, averaging 0.001; this indicates that the readings obtained during calibration with the individual Type-S pitot tubes were very consistent and reproducible. Figure 6 shows that the mean A -to -B side coefficient difference for the 14 Type-S pitot tubes was 0.004, with an average deviation of 0.002; none of the Type-S pitot tubes had an A -to -B side difference greater than 0.007.

These results compare favorably with those obtained in other recent studies.[2,3] In the studies cited, $\overline{C}_p$ values ranging from 0.841 to 0.853, and A -to -B side coefficient differences of less than 0.01 were obtained for those Type-S pitot tubes (a total of four tubes in all) having properly aligned face openings (see Table II).

CONCLUSIONS

This study has satisfactorily demonstrated that isolated Type-S pitot tubes, constructed according to the specifications of Figure 2, will consistently have

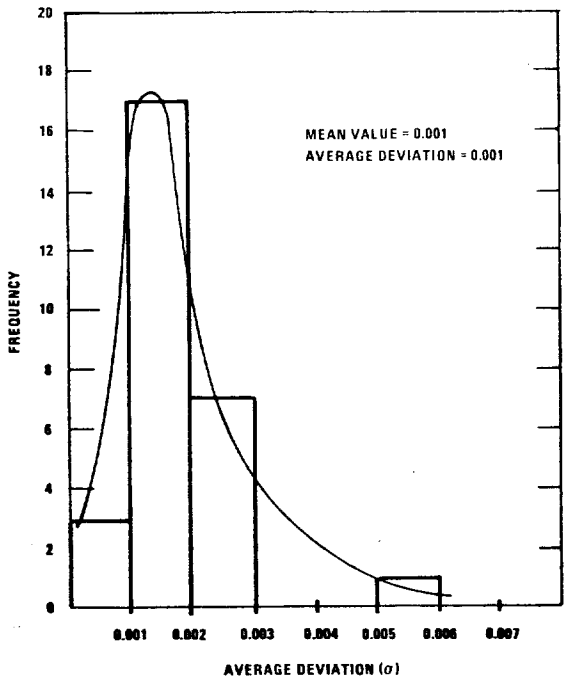

Figure 5. Frequency distribution of σ values.

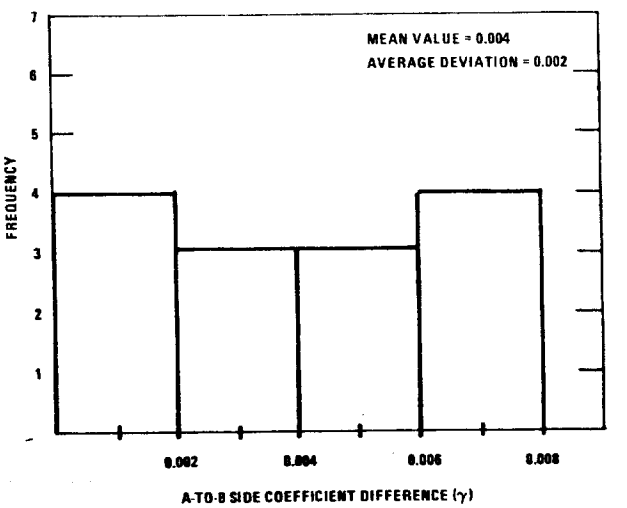

Figure 6. Frequency distribution of γ values.

Table II. Calibration coefficients of properly constructed Type-S pitot tubes (from References 2 and 3).

Study number	Pitot tube number	External tubing diameter (d) in.	Port-to-port separation in terms of tubing diameter	$\bar{C}_p$ (side A)	$\bar{C}_p$ (side B)	A-to-B side difference (γ)
2	4-15	0.375	2.9d	0.845	0.841	0.004
2	4-16	0.375	2.9d	0.843	0.850	0.007
2	4-20	0.375	2.3d	0.846	0.853	0.007
3	Ref.	0.375	2.4d	0.846	0.846	0.000

coefficient values between 0.84 and 0.85. Also, these pitot tubes will have A -to -B side coefficient differences of less than 0.01. These findings are in accord with the results of other studies. In view of this, it is justifiable to assign baseline coefficient values of 0.84 or 0.85 to properly constructed* isolated Type-S pitot tubes, without calibration. It should be carefully noted, however, that the findings and conclusions of this study are limited to those tubes having external tubing diameter ("d") values of between 3/16 and 3/8 inches, and having port-to-port spacings of between 2.2d and 2.9d.

REFERENCES

1. Vollaro, R. F. Guidelines for Type-S Pitot Tube Calibration. Presented at the First Annual Meeting of The Source Evaluation Society, Dayton, Ohio, September 18, 1975.

2. Vollaro, R. F. A Type-S Pitot Tube Calibration Study. U. S. Environmental Protection Agency, Emission Measurement Branch. Research Triangle Park, N. C. July, 1974.

3. Vollaro, R. F. The Effects of Impact Opening Misalignment on the Value of the Type-S Pitot Tube Coefficient. Presented at The Fourth Annual Conference on Energy and the Environment, Cincinnati, Ohio. October 7, 1976.

---

* Note: A recent study has shown that slight misalignments of the face openings of a Type-S pitot tube will not affect the baseline coefficient value of the pitot tube. Thus, a Type-S pitot tube need not conform exactly to the specifications of Figure 2 in order to be considered "properly constructed"; consult Reference 3 for details.

A SURVEY OF COMMERCIALLY AVAILABLE INSTRUMENTATION FOR THE MEASUREMENT OF LOW-RANGE GAS VELOCITIES

Robert F. Vollaro

INTRODUCTION

Gas velocities in industrial smokestacks and ducts typically range from about 1000 to 5000 ft/min; velocities in this range can be measured satisfactorily with a Type-S pitot tube and gauge-oil manometer. Stacks are occasionally encountered, however, in which the velocities are consistently below 1000 ft/min. Measurement of gas velocity is less straightforward below 1000 ft/min than in the 1000 to 5000 ft/min range, because most gauge-oil manometers are not sensitive enough to give accurate low-range readings. The purpose of this paper is to evaluate several commercially available instruments which are capable of measuring gas velocities below 1000 ft/min.

SURVEY OF LOW-RANGE VELOCITY INSTRUMENTATION

The following paragraphs provide a brief description and evaluation of 11 commercially available instruments, along with cost data. A summary of the descriptive information is presented in Table 1.

1. Instrument and Manufacturer: Inclined manometer, Model 125-AV (Figure 1) manufactured by Dwyer Instruments, Inc., Michigan City, Indiana.

a. Operating principle - A differential pressure signal from a primary sensing element (e.g., a Type-S pitot tube) causes a positive displacement of gauge fluid along a calibrated, inclined scale.

b. Velocity range - The full-scale range of the manometer is 0 to 1 in. water column; the scale divisions are 0.005 in. H_2O. The manometer is readable to the nearest 0.003 in. H_2O.

Table 1. LOW-RANGE VELOCITY INSTRUMENTATION

Instrument and manufacturer	Lower velocity limit, ft/min	Temperature range	Resistance to particulate	Applications
Inclined Manometer * Model 125-AV Dwyer Instruments, Inc.	700	Same as primary sensor	Same as primary sensor	Industrial stacks, ducts, vents; also lab applications; air or non-air streams
Micromanometer * Model 10133 Thermo-systems, Inc.	700 in field 400 in lab	Same as primary sensor	Same as primary sensor	Lab applications; limited use in industrial stacks, ducts, vents; air or non-air streams
Microtector * Hook Gauge Dwyer Instruments, Inc.	700 in field 100 in lab	Same as primary sensor	Same as primary sensor	Lab applications; limited use in industrial stacks, ducts, vents; air or non-air streams
Electronic Manometer * Model 1023 Datametrics, Inc.	700 in field 100 in lab	Same as primary sensor	Same as primary sensor	Lab applications; limited use in industrial stacks, ducts, vents; air or non-air streams
Mechanical Vane Anemometer Davis Instrument Co.	70	To 250°F (est.)	Fair	Industrial vents and grilles; special calibration needed for non-air streams
Extended Range Propeller Anemometer R.M. Young Co.	75	To 180°F for continuous duty	Fair	Roof monitors and vents; special calibration needed for non-air streams
Hot-wire Anemometer Model VT-1610 Thermo-Systems, Inc.	30	To 212°F	Fair to good	Industrial stacks, vents, ducts; lab applications; special calibration needed for non-air streams
Hot-film Wedge Sensor Model 1234-H Thermo-Systems, Inc.	60	To 570°F	Good	Industrial stacks, vents, ducts, lab applications; special calibration needed for non-air streams
Fluidic Velocity Sensor Model 308 R Fluidynamic Devices, Ltd.	200	To 450°F	Fair to good	Industrial stacks, vents, ducts; air or non-air streams
Stack Velocity Sampler * Model GSM-1D5K Teledyne Hastings-Raydist	100	Same as primary sensor	Excellent	Industrial stacks, vents, ducts; air or non-air streams
Differential Pressure * Transmitter Brandt Industries, Inc.	150	Same as primary sensor	Excellent	Industrial stacks, vents, ducts; air or non-air streams

*Must be used in conjunction with a Type - S pitot tube or other appropriate primary sensing element.

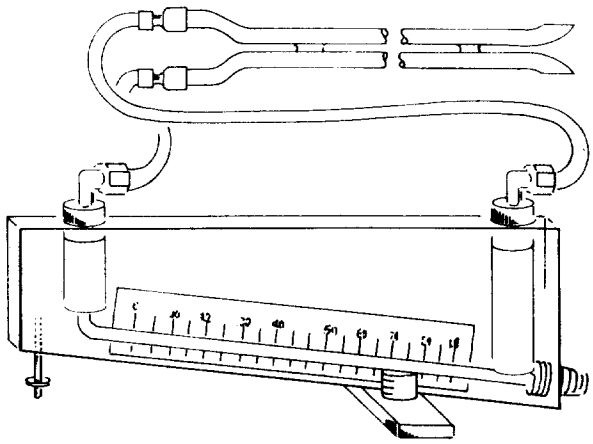

Figure 1. Dwyer inclined manometer, model 125-AV, connected to a Type-S pitot tube.

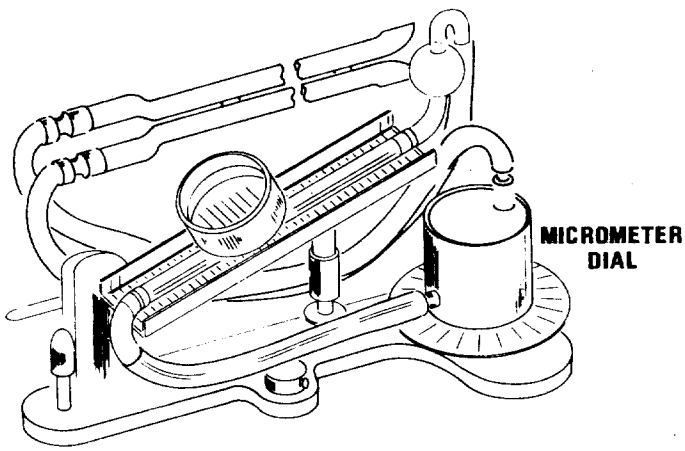

Figure 2. Thermo-Systems micromanometer, model 10133, connected to a Type-S pitot tube.

c. Temperature range - The operating temperature range of the manometer is the same as that of the primary sensing element.

d. Resistance to particulate matter - Governed by particulate resistance of primary sensor.

e. Evaluation - As previously noted, the manometer has scale divisions of 0.005 in. H_2O, and is readable to the nearest 0.003 in. H_2O. Thus, it has greater sensitivity than most inclined manometers, which have 0.01 in. H_2O divisions and are readable to 0.005 in. H_2O. Therefore, with the 125-AV, accuracy of better than 10 percent in velocity head (ΔP) readings can be ensured, provided that the manometer is not used to measure values of ΔP lower than about 0.03 in. H_2O (which corresponds to a velocity of about 700 ft/min for air flowing at $70^{o}F$).

f. Cost - Approximately $125.

2. Instrument and Manufacturer: Micromanometer, Model 10133 (Figure 2), manufactured by Thermo-Systems, Inc., St. Paul, Minnesota.

a. Operating principle - A differential pressure signal from a primary sensing element causes a displacement of gauge fluid along a calibrated, inclined scale.

b. Velocity range - The full-scale range of the micromanometer is 0 to 1.2 in. water column. The scale divisions are 0.01 in H_2O, but the instrument has a micrometer dial, making it possible to read velocity head to the nearest 0.001 in. H_2O.

c. Temperature range - Governed by the primary sensing element.

d. Resistance to particulate matter - Same as primary sensor.

e. Evaluation - The Model 10133 micro-manometer is better suited for laboratory work than for source-sampling applications, particularly at

velocities below 700 ft/min. The reason is that the performance of the manometer is adversely affected by flow pulsations, vibrations, etc. Even when it is in a vibration-free environment, the instrument cannot be used to read ΔP values below 0.01 in. H_2O, if ΔP readings within $\pm$ 10 percent of true are desired.

f. Cost - $200 or less (estimated).

3. Instrument and Manufacturer: Micro-tector Hook Gauge (Figure 3), manufactured by Dwyer Instruments, Inc., Michigan City, Indiana.

a. Operating principle - A differential pressure signal from a primary sensing element causes a slight displacement of gauge fluid. A metal "hook" mounted in a micrometer barrel is carefully lowered until its point "just" contacts the gauge fluid. The instant of contact with the fluid is detected by completion of a low-power AC circuit. On indication of contact, the operator stops lowering the hook, and reads the micrometer to determine ΔP.

b. Velocity range - The full-scale range of the gauge is 0 to 2 in. water column. The micrometer scale is readable to the nearest 0.00025 in. H_2O.

c. Temperature range - Governed by primary sensing element.

d. Resistance to particulate matter - Same as primary sensor.

e. Evaluation - The manufacturer's estimated readability (to the nearest 0.00025 in. H_2O) implies that one should be able to read ΔP values as low as 0.0025 in. H_2O with $\pm$ 10 percent confidence. In practice, however, this readability is only possible if the instrument is perfectly leveled and used in an absolutely vibration-free environment. Generally, the hook gauge will not be a useful field instrument for measuring velocities lower than about 700 ft/min.

f. Cost - About $200.

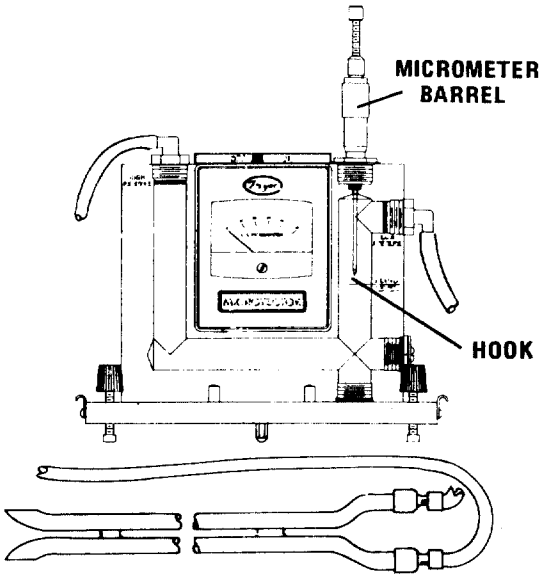

Figure 3. Dwyer microtector hook gauge, connected to a Type-S pitot tube.

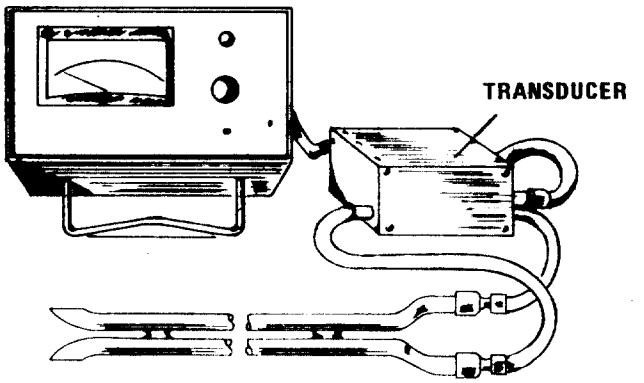

Figure 4. Datametrics electronic manometer, model 1023, connected to a Type-S pitot tube.

4. Instrument and Manufacturer: Electronic Manometer, Type 1023 (Figure 4), manufactured by Datametrics, Inc., Wilmington, Massachusetts.

a. Operating principle - A differential pressure signal from a primary sensing element is converted to an electrical signal by transducers. The output signal can, if desired, be read on a digital voltmeter or recording chart.

b. Velocity range - The manometer is useful over a wide range of velocities because of its multi-scale readout system. The least sensitive scale is 0 to 100 in. water column, and the most sensitive is 0 to 0.01 in. H_2O, full-scale. The rated accuracy of the manometer is 2 percent of full-scale for all operating ranges.

c. Temperature range - Governed by the primary sensing element.

d. Resistance to particulate matter - Same as primary sensor.

e. Evaluation - The 1023 manometer is a high-precision instrument; if zeroed with a digital voltmeter, it is capable of measuring velocity heads as low as 0.001 in. H_2O with acceptable accuracy. Note, however, that readings made on the most sensitive (0 to 0.01 in. H_2O) scale are adversely affected by connecting-line vibrations; thus, the lines from the primary sensor to the transducer must be perfectly still during use in this range. The manometer is, therefore, better suited for laboratory, rather than field, applications for measuring ΔP values below 0.01 in. H_2O.

f. Cost - About $1000.

5. Instrument and Manufacturer: Mechanical Vane Anemometer (Figure 5), manufactured by Davis Instrument Co., Baltimore, Maryland.

a. Operating principle - A gas stream flowing through the anemometer (see Figure 5), causes the propeller blades to rotate. The propeller rpm is proportional to the velocity of the flowing gas. The readout is in linear feet; dividing this readout by the total measurement time gives the gas velocity in ft/min.

b. Velocity range - The anemometer can measure velocities between 70 and 5000 ft/min with acceptable accuracy.

c. Temperature range - (The author does not have a reliable estimate of the instrument's temperature capabilities; however, there seems to be no reason why the anemometer could not be used in gas streams as hot as 200 or 250°F.)

d. Resistance to particulate matter - The propeller blades provide fairly good resistance to particulate matter, especially when the instrument is used for brief periods of time.

e. Evaluation - A mechanical vane anemometer is best suited for making a "quick check" of the exit velocities from a vent or grille. The anemometer is calibrated for use in air streams; special calibration is needed for use in non-air streams. Although the anemometer can accurately measure velocities in the 70 to 700 ft/min range (out of range of most primary sensor-manometer combinations), the instrument can only be used for a short time before it must be stopped, reset, and restarted manually. Thus, the anemometer is not easily adaptable for use in source-sampling applications.

f. Cost - Estimated at $100 or less.

6. Instrument and Manufacturer: Extended Range Propeller Vane Anemometer (Figure 6), manufactured by R. M. Young Co., Traverse City, Michigan.

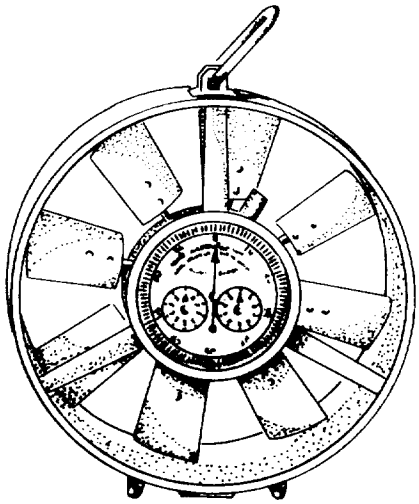

Figure 5. Mechanical vane anemometer, manufactured by Davis Instruments, Inc.

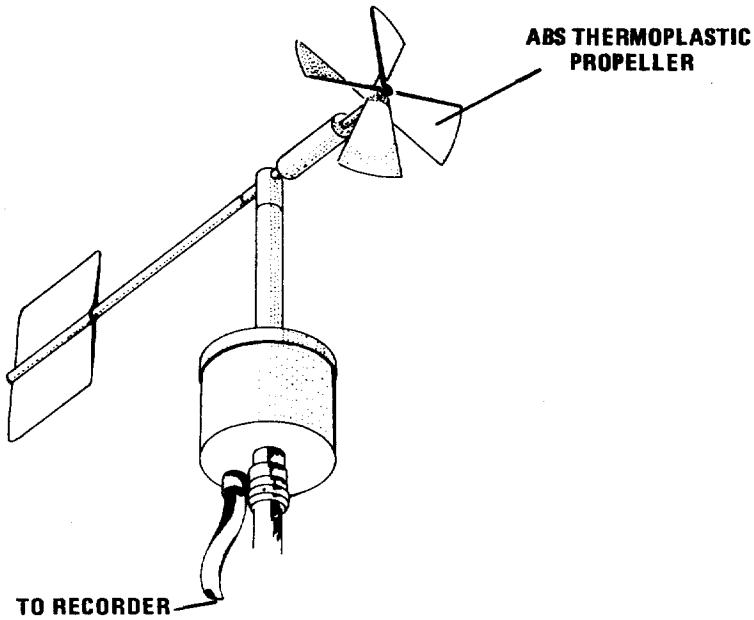

Figure 6. Extended-range propeller vane anemometer, manufactured by R.M. Young Company.

a. Operating principle - Flowing gas causes the propeller (see Figure 6) to turn at a rate proportional to the gas velocity. The propeller shaft is coupled to a d.c. generator. The generator output is an analog voltage, proportional to shaft rpm. The output signal is monitored continuously by means of a recording chart.

b. Velocity range - The velocity range for the anemometer is 75 to 6000 ft/min; 75 ft/min is the threshold velocity at which the propeller begins to turn.

c. Temperature range - With an ABS thermoplastic propeller, the anemometer can be used continuously in gas streams as hot as 180°F and, intermittently, in streams as hot as 300°F.

d. Resistance to particulate matter - The propeller blades provide fairly good resistance to particulate matter.

e. Evaluation - Because it cannot be used for extended periods of time at temperatures above 180°F, the anemometer is of limited value for source-sampling applications. It would probably be useful for continuous velocity measurement in roof monitors. The anemometer is calibrated for use in air streams; special calibration is required for use in non-air streams.

f. Cost - About $700 with recording chart.

7. Instrument and Manufacturer: Velocity Transducer, Model 1610, manufactured by Thermo-Systems, Inc., Minneapolis, Minnesota.

a. Operating principle - The VT-1610 measures the velocity of a flowing gas stream by sensing the cooling effect of the stream as it moves over the heated surface of the sensor, the "hot-wire" principle. The output signals from the sensor are electrical and non-linear. A signal conditioner

is available to linearize the output. The output signals are temperature compensated so that the readings will be in ft/min, corrected to $70^{o}F$.

b. Velocity range - The instrument can measure velocities as low as 30 ft/min (on the low scale) and as high as 12,000 ft/min (on the high scale), with acceptable accuracy ($\pm$ 2 percent).

c. Temperature range - The instrument can be used in gas streams as hot as $212^{o}F$.

d. Resistance to particulate matter - Unlike many hot-wire devices, the VT-1610 sensor is ruggedized and has fairly good resistance to particulate matter.

e. Evaluation - It appears that the VT-1610 would be most suitable for short-term use in low-temperature air streams, particularly when velocities are too low (under 700 ft/min) to be measured with most primary sensor-manometer combinations. If used continuously in a dusty environment, the instrument will tend to foul after several hours. The sensor is calibrated for use in air streams; special calibration is required if it is to be used in non-air streams.

f. Cost - About $1000 for sensor and signal conditioner.

8. Instrument and Manufacturer: Wedge Hot-Film Sensor, Model 1234-H (Figure 8), manufactured by Thermo-Systems, Inc., Minneapolis, Minnesota.

a. Operating principle - The 1234-H measures the velocity of a flowing gas stream by sensing the cooling effect of the stream as it moves over the heated sensor surface, the "hot-film" principle. The output signal is electrical and can be read continuously on a recording chart, if desired. When used with a temperature compensator, the readout will be in ft/min, corrected to $70^{o}F$.

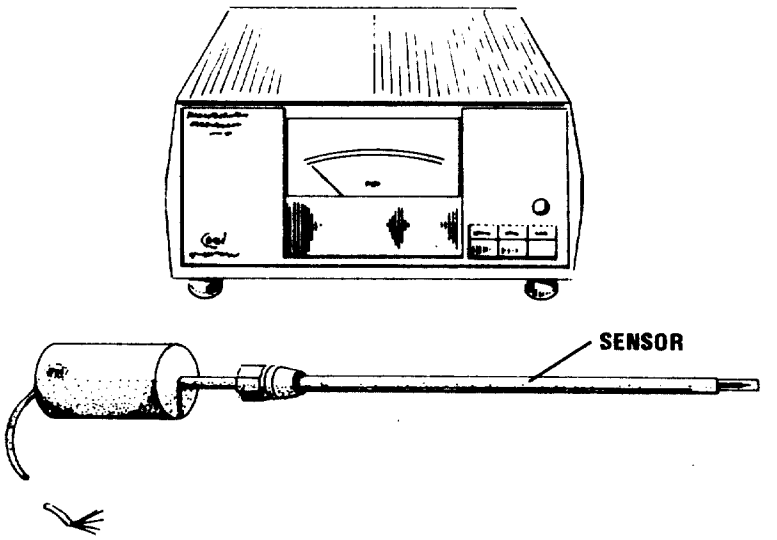

Figure 7. Thermo-Systems hot-wire anemometer, model VT-1610.

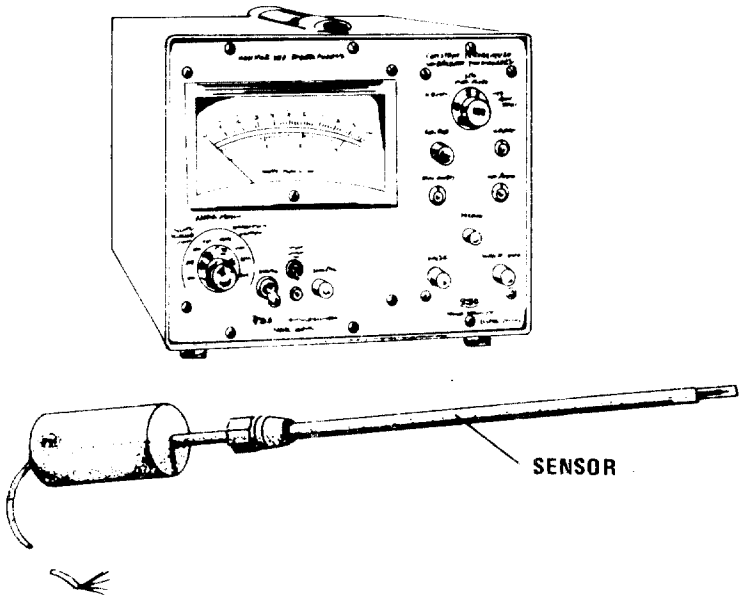

Figure 8. Thermo-Systems hot-film wedge sensor, model 1234-H.

b. Velocity range - The sensor can measure velocities as low as 60 ft/min (on the low-scale) or as high as 12,000 ft/min (on high-scale), with acceptable accuracy ($\pm$ 2 percent).

c. Temperature range - The sensor can be used in gas streams as hot as 570°F.

d. Resistance to particulate matter - The sensor is ruggedized and offers good resistance to particulate matter.

e. Evaluation - The 1234-H is best suited for short-term use in air streams, particularly when velocities are too low to be measured with primary sensor-manometer combinations. It may prove to be useful for measuring total flow rate from roof monitors, because several sensors, positioned at different points along a roof vent, can be connected to a multi-channel readout system. Like the VT-1610, the 1234-H requires special calibration for use in non-air streams.

f. Cost - About $1500, for one temperature-compensated sensor and readout system; about $500 for each additional sensor.

9. Instrument and Manufacturer: Fluidic Velocity Sensor, Model 308R (Figure 9), manufactured by FluiDynamics, Ltd., Ontario, Canada.

a. Operating principle - The following description refers to Figure 9: A free jet of supply fluid (air or N_2) is issued from a nozzle (point B), and impinges on two pick-up ports (point C). At zero cross-flow velocity, the differential pressure across the pick-up ports is zero. Any cross-flow causes the supply air jet to deflect, yielding a differential pressure signal proportional to the velocity. The output signal can be read with a differential pressure gauge or transducer.

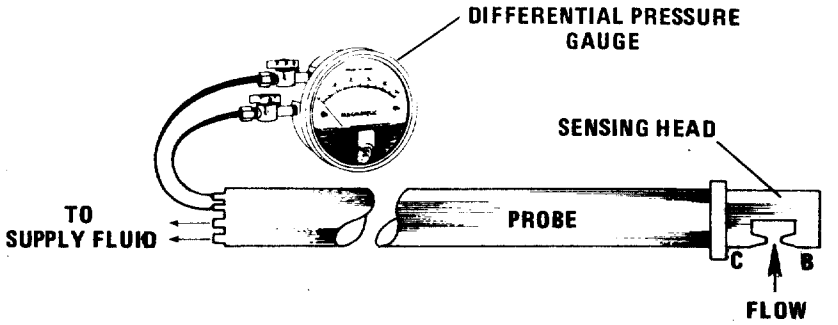

Figure 9. Fluidic velocity sensor, model 308R, manufactured by FluiDynamic Devices, Ltd.

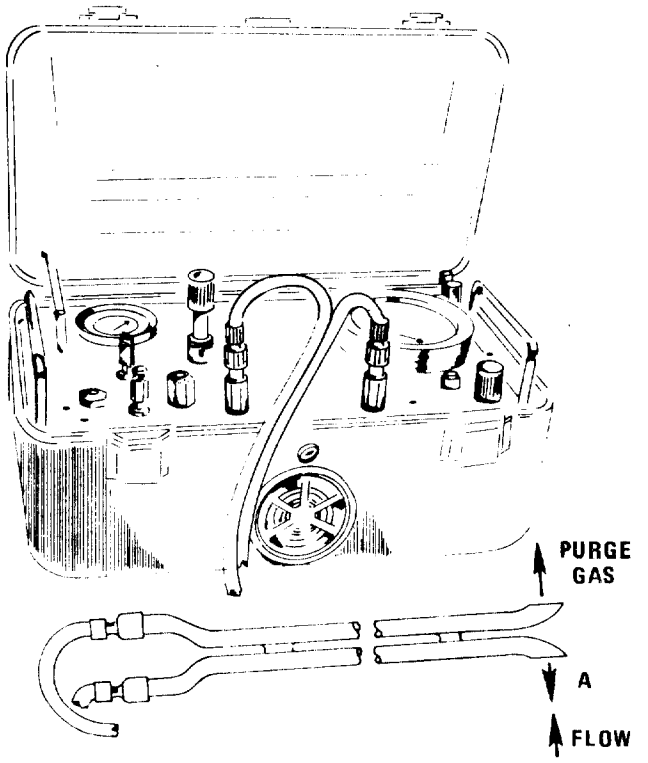

Figure 10. Stack velocity sampler, model GSM-1D5K manufactured by Teledyne Hastings-Raydist.

b. Velocity range - The sensor has a full-scale velocity range of 0 to 3600 ft/min. The accuracy of the sensor is about $\pm$ 3 percent for velocities above 600 ft/min, and $\pm$ 5 to 10 percent for velocities below 600 ft/min.

c. Temperature range - The sensor can be used in gas streams as hot as 450°F.

d. Resistance to particulate matter - The sensor has fairly good resistance to particulate matter.

e. Evaluation - One of the outstanding features of the sensor is that it has a linear, high-amplitude output signal, even at low velocities. For example, when the cross-flow velocity (v_c) is 600 ft/min, the sensor output is about 12 in. H_2O; at v_c = 200 ft/min, the output is about 4 in. H_2O. Note, however, that the sensor is difficult to zero; for this reason, its accuracy falls off appreciably for v_c < 200 ft/min. The sensing head is mounted on a cylindrical probe, making it convenient to use in source-sampling applications. The sensor can be used in non-air streams, provided that the gas density is known.

f. Cost - About $2000.

10. Instrument and Manufacturer: Stack Velocity Sampler, Model GSM-1D5K (Figure 10), manufactured by Hastings-Raydist, Hampton, Virginia.

a. Operating principle - The following description refers to Figure 10: At zero cross-flow, supply fluid (air or N_2) is continually purged at equal rates, out of both impact openings of the Type-S pitot tube. Any cross-flow velocity causes a back-pressure against the purge gas, at point A. The back-pressure signal is proportional to the fluid velocity; thermoelectric

sensors (transducers) interpret and convert this signal. The output voltage from the transducers is linear over about 90 percent of the scale; output voltage can be read with a digital voltmeter or recording chart, if desired.

b. Velocity range - The velocity range is 0 to 1500 ft/min, full scale. The lower limit of readability is about 100 ft/min.

c. Temperature range - The instrument is operable at all temperatures at which a Type-S pitot tube can be used.

d. Resistance to particulate matter - The continuous-purge principle of the sensor gives it excellent resistance to particulate matter.

e. Evaluation - The most outstanding feature of the Hastings instrument is that it works with a Type-S pitot tube; thus, it is easily adaptable for use with conventional source-sampling equipment. The voltmeter on the control panel is adequate for reading velocities between 200 and 1500 ft/min. To read accurately velocities between 100 and 200 ft/min, a digital voltmeter or sensitive chart recorder is needed. The sensor can be used in non-air streams if the density of the gas is known. Note that the instrument must be calibrated exactly as it is to be used, because different calibration curves will be obtained for different pitot tube and connecting-line lengths.

f. Cost - About $1500 to $2000.

11. Instrument and Manufacturer: Differential Pressure Transmitter (Figure 11), manufactured by Brandt Industries, Inc., Raleigh, North Carolina.

a. Operating principle - The following description refers to Figure 11: Supply fluid (air on N_2) exhausts equally out of both sides of the pitot tube at zero cross-flow velocity. Any cross-flow will cause a

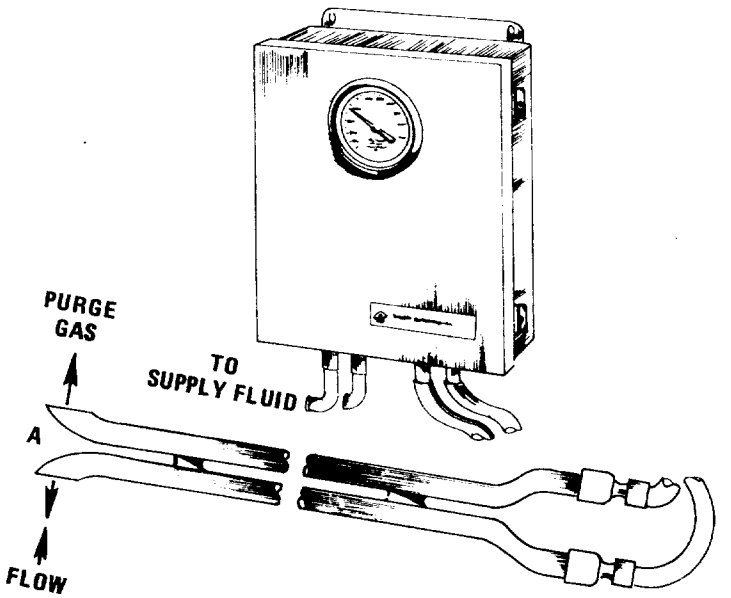

Figure 11. Differential pressure transmitter, series 200; manufactured by Brandt Industries, Inc.

back-pressure against the purge gas at point A. The magnitude of the back-pressure signal is proportional to the fluid velocity. Transducers receive and convert the back-pressure signal. The output signal from the transducers is pneumatic and linear; the output can be read continuously on a pneumatic recorder if desired.

b. Velocity range - The full-scale range of the transmitter is 0 to 0.05 in. water column. The accuracy of the transmitter is estimated at $\pm$ 2 percent of span.

c. Temperature Range - The transmitter can be used at any temperature at which the primary sensing element (pitot tube or other sensor) can be used.

d. Resistance to particulate matter - The continuous-purge action of the supply fluid gives the sensor excellent resistance to particulate matter.

e. Evaluation - The Brandt transmitter is a versatile device; it can be used as a single-point sensor, or adapted for multipoint sensing (e.g., it can be used with a pitot "rake"). The transmitter is easily adaptable for use with conventional source-sampling equipment. An especially attractive feature of the transmitter is a damping control, which allows true, time-integrated average velocity head readings to be made. Velocities as low as 150 to 200 ft/min can be read with acceptable accuracy. The instrument can be used in non-air streams if the gas density is known. One drawback of the instrument is that there is a practical upper-limit (30 ft) on the length of the connecting lines; note, also, that the connecting lines are somewhat vibration-sensitive and should be still when measurements are made.

THE USE OF TYPE-S PITOT TUBES FOR THE MEASUREMENT OF LOW VELOCITIES

Robert F. Vollaro

INTRODUCTION

In source-sampling, stack gas velocity (V_s) is usually measured with a Type-S pitot tube. Before a Type-S pitot tube is used for this purpose, its coefficient, $C_p(s)$, must be determined by calibration against a standard pitot tube. A recent study[1] has demonstrated that, in most instances, calibration at a single velocity of about 3000 ft/min is satisfactory, for both isolated Type-S pitot tubes* and pitobe assemblies;** Type-S pitot tubes calibrated by this method can be used, with acceptable accuracy, to measure velocities as low as 1000 ft/min. In most field applications, stack gas velocities will be above 1000 ft/min; however, sources having lower velocities are occasionally encountered. It is, therefore, desirable to know if calibration coefficients obtained at 3000 ft/min are sufficiently accurate for use at velocities below 1000 ft/min, or whether special calibration in the low range is necessary. Accordingly, investigators recently conducted experiments in which several isolated Type-S pitot tubes and pitobe assemblies were calibrated at velocities ranging from about 400 to 1000 ft/min. This paper reports the results of these experiments and discusses their significance.

EXPERIMENT 1

Experimental Method

In the first experiment, the coefficients of 12 isolated Type-S pitot tubes were determined by calibration against a standard pitot tube. The

---

*An isolated Type-S pitot tube is any Type-S pitot tube that is calibrated or used alone.

**A pitobe assembly is any Type-S pitot tube that is calibrated or used while attached to a sampling probe, equipped with a nozzle or thermocouple or both.

calibrations were done in a wind tunnel having a test-section diameter of 12 in. For each Type-S pitot tube, calibration data were taken at four different test-section velocities between 400 and 1000 ft/min, spaced at approximately equal intervals over this range. During calibration, velocity head (ΔP) signals from the standard and Type-S pitot tubes were continuously monitored by an electronic manometer and chart-recorder combination (Figure 1). The flow in the wind tunnel was normal, time-invariant turbulent flow;[2] therefore, it was possible to take accurate average ΔP readings from the chart recordings (see Appendix A). Figure 2 shows a segment of a typical chart recording.

Method of Data Analysis

Each of the 12 Type-S pitot tubes had been calibrated at velocities ranging from 1500 to 3500 ft/min in a previous study,[3] providing a point of reference from which to evaluate the data taken in Experiment 1. The data from Experiment 1 were analyzed as follows:

1. For each of the 12 Type-S pitot tubes, the value of the pitot coefficient was calculated, at each velocity setting; the following equation was used:

$$C_p(s) = 0.99 \sqrt{\frac{\overline{\Delta P}_{std}}{\overline{\Delta P}_s}} \qquad \text{(Equation 1)}$$

Where:

$C_p(s)$ = Type-S pitot tube coefficient

0.99 = Standard pitot tube coefficient, constant to within $\pm$ 0.5 percent for the measurement of velocities as low as 3 ft/sec (Reference 7).

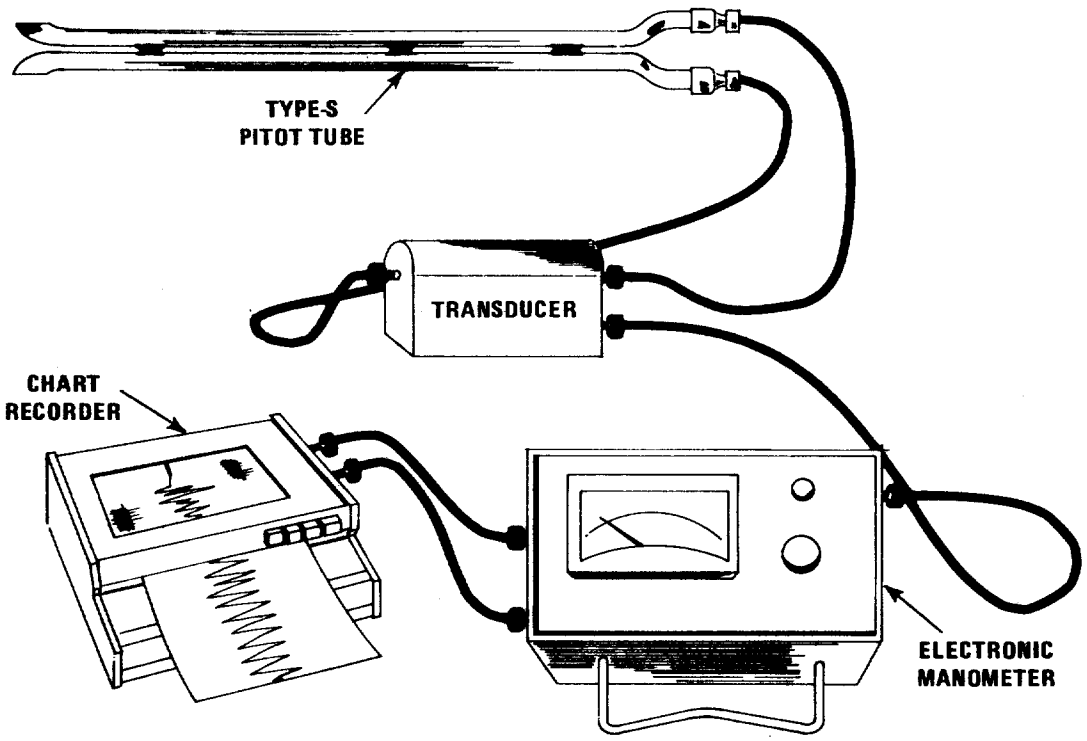

Figure 1. Electronic manometer and chart-recorder combination, connected to a Type-S pitot tube.

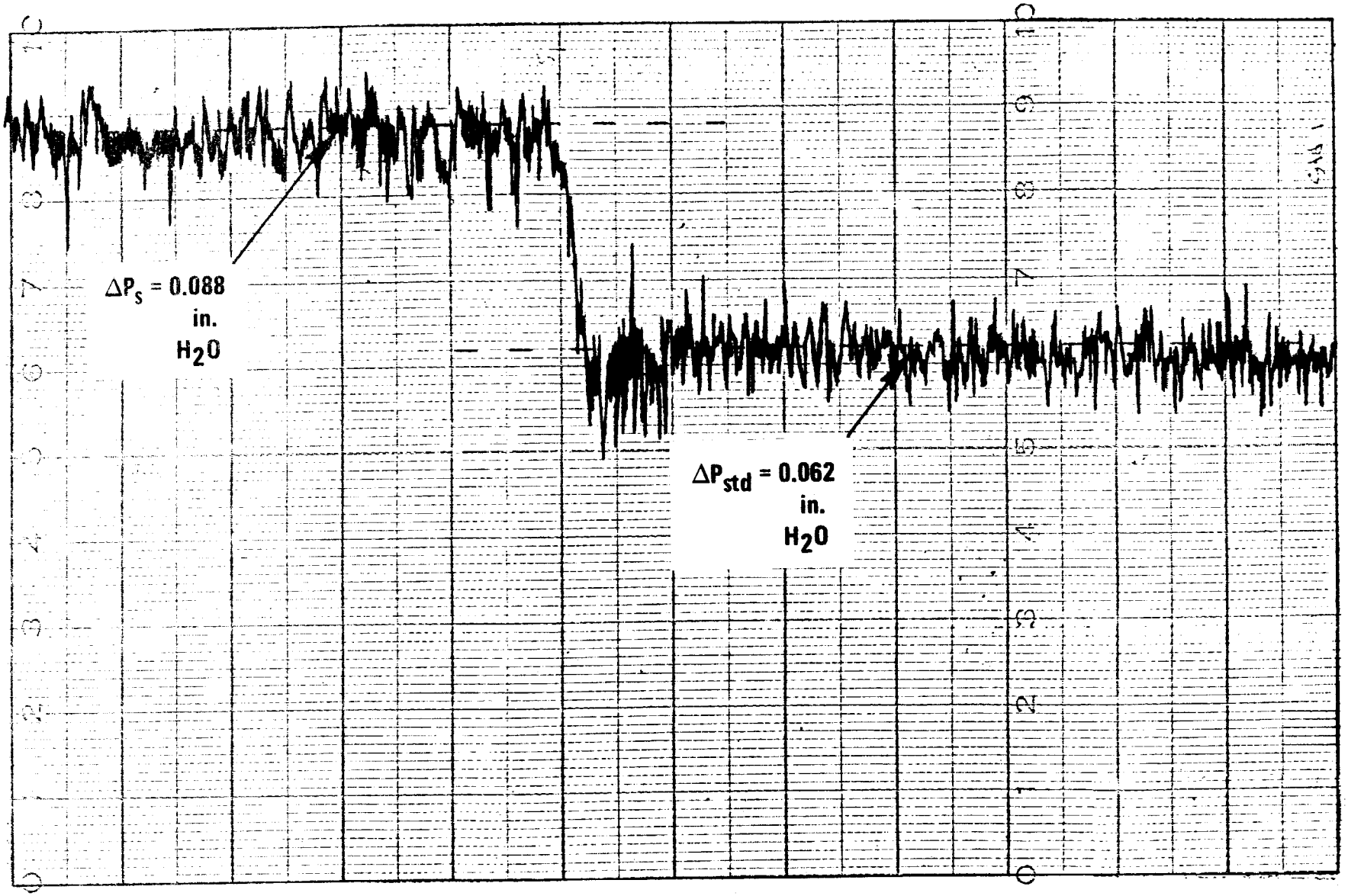

Figure 2. Segment of a typical chart recording.

$\overline{\Delta P}_{std}$ = Average velocity head signal from standard pitot tube (taken from chart recording), in. H_2O

$\overline{\Delta P}_s$ = Average velocity head signal from Type-S pitot tube (from chart recording), in. H_2O

2. The data from Experiment 1 were correlated with the "reference" data (from previous study, in the velocity range 1500 to 3500 ft/min). The percentage deviation of each $C_p(s)$ value from C_p,* its reference coefficient value at 3000 ft/min, was calculated as follows:

$$\text{Percentage deviation of } C_p(s) \text{ from } C_p^* = \phi = \left[\frac{|C_p^* - C_p(s)|}{C_p^*}\right] X\ 100 \qquad \text{(Equation 2)}$$

3. A histogram was constructed showing the frequency distribution of the ϕ values.

4. The mean and maximum values of ϕ were "adjusted," by adding 2 percent to them, to cover possible random errors in interpreting the chart recordings (see Appendix A).

5. The "adjusted" mean and maximum values of ϕ were substituted into the velocity and isokinetic error equations (see Appendix B). Note that the reason for considering the isokinetic error equation as well as the velocity error equation is that isolated Type-S pitot tubes having known C_p values are sometimes used as components of pitobe assemblies in which aerodynamic interactions among the components are minimized by proper intercomponent spacing; in such cases, the C_p values of the isolated pitot tube and pitobe assembly are equal.[8]

Results of Data Analysis

The results of the data analysis are presented in Figure 3 and Table 1. Figure 3 shows that, in general, there was little variance between the values of $C_p(s)$ and C_p^*; the mean value of ϕ was 2.1 percent, with an average deviation of 1.3 percent. The maximum value of ϕ was 6.3 percent, and 90 percent of the ϕ values were 5 percent or less. Adding 2 percent to the mean and maximum values of ϕ to cover random errors in reading the chart recordings gives an "adjusted" mean value of 4.1 percent, and an adjusted maximum value of 8.3 percent. Substituting these adjusted ϕ values into the velocity and isokinetic error equations (Equations B-5 and B-6 in Appendix B) gives the following results (see Table 1): (1) for ϕ = 4.1 percent, velocity measurements will be within $\pm$ 6.6 percent of true, and isokinetic adjustments within 7.0 percent of true, 99.6 percent of the time; (2) for ϕ = 8.3 percent, velocity measurements will be within 9.8 percent of true, and isokinetic adjustments within 10.1 percent of true, 99.6 percent of the time. Therefore, it can be concluded that when isolated Type-S pitot tubes (or interference-free pitobe assemblies constructed from them) are used to measure velocities in the range from 400 to 1000 ft/min, values of C_p^* obtained by single-velocity calibration at 3000 ft/min can be used without introducing serious error; velocity readings and isokinetic adjustments (if applicable) will be within $\pm$ 10 percent of true.

EXPERIMENT 2

Experimental Method

In the second experiment, six different pitobe assemblies (three with thermocouple and nozzle and three with sampling nozzle only) were calibrated

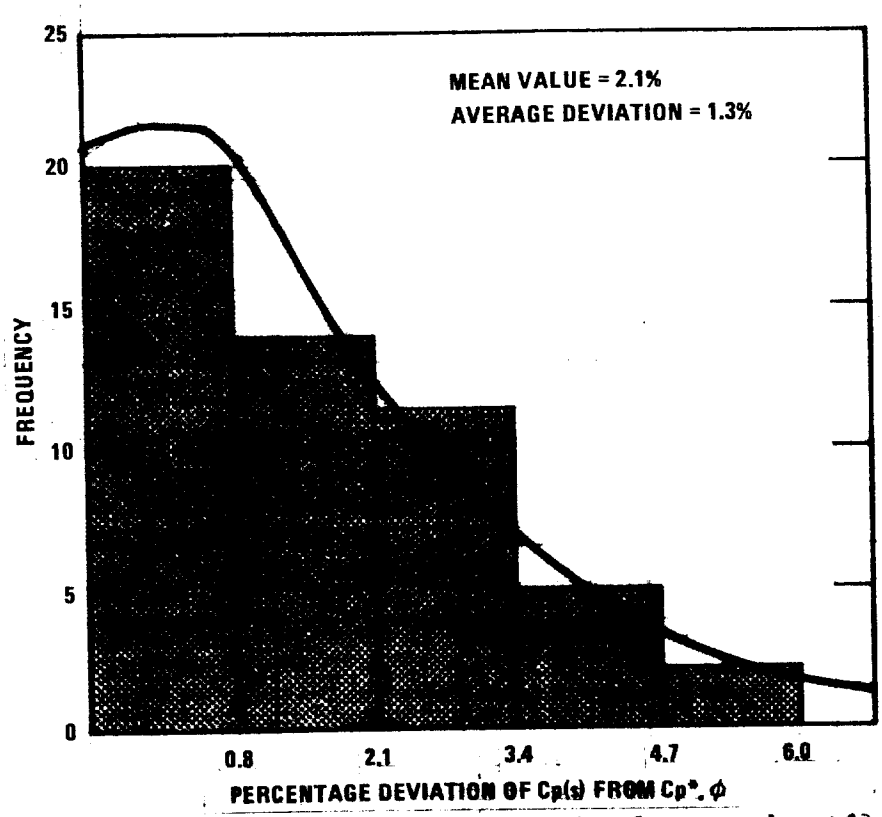

Figure 3. Frequency distribution of ϕ values from experiment 1; velocity range: 400 to 1000 ft/min.

Table 1. SUMMARY OF PROBABLE VELOCITY AND ISOKINETIC ERRORS; EXPERIMENTS 1 AND 2

Quantity, %	Experiment 1	Experiment 2
Mean value of ϕ or γ	2.1	2.4
Adjusted mean value of ϕ or γ	4.1	4.4
Maximum probable velocity error*	6.6	6.8
Maximum probable isokinetic error*	7.0	7.2
Maximum value of ϕ or γ	6.3	5.7
Adjusted maximum value of ϕ or γ	8.3	7.7
Maximum probable velocity error**	9.8	9.3
Maximum probable isokinetic error**	10.1	9.6

*using adjusted mean ϕ or γ value

**using adjusted maximum ϕ or γ value

against a standard pitot tube. The intercomponent spacings of each of the assemblies failed to meet the minimum requirements necessary to prevent aerodynamic interference. The calibrations were done in the same wind tunnel that was used in Experiment 1. Each assembly was calibrated first at a test-section velocity of 2200 ft/min (maximum for the wind tunnel) and then at four different test-section velocities, spaced at approximately equal intervals over the range from about 475 to 1150 ft/min. All ΔP signals were monitored with the electronic manometer and chart-recorder combination illustrated in Figure 1.

Method of Data Analysis

The data from Experiment 2 were analyzed as follows:

1. For each assembly, Equation 1 was used to calculate the values of $C_p(s)$, first at the "reference" velocity (2200 ft/min) and then at each of the four velocity settings between 475 and 1150 ft/min.

2. The percentage deviation of each low-range value of $C_p(s)$ from its reference coefficient, $C_p(\text{ref})$, was calculated as follows:

$$\text{Percentage deviation of } C_p(s) \text{ from } C_p(\text{ref}) = \gamma = \left[\frac{C_p(s) - C_p(\text{ref})}{C_p(\text{ref})}\right] \times 100 \qquad \text{(Equation 3)}$$

3. A histogram was constructed, showing the frequency distribution of the γ values.

4. The mean and maximum values of γ were "adjusted," by adding 2 percent to them, to cover possible random errors in interpreting the chart recordings (see Appendix A).

5. The "adjusted" mean and maximum values of γ were substituted into the velocity and isokinetic error equations (see Appendix B).

Results of Data Analysis

The results of the data analysis are presented in Figure 4 and Table 1. Figure 4 shows that, generally, there was little variance between the values of $C_p(s)$ and $C_p(ref)$; the mean value of γ was 2.4 percent, with an average deviation of 1.4 percent. The maximum value of γ was 5.7 percent, and about 90 percent of the γ values were within 5 percent. These results are nearly identical to those obtained with isolated Type-S pitot tubes in Experiment 1 (compare Figures 3 and 4). Adding 2 percent of the mean and maximum values of γ, to cover random errors in reading the chart recordings, gives an "adjusted" mean value of 4.4 percent, and an adjusted maximum value of 7.7 percent. Substituting these adjusted γ values into the velocity and isokinetic error equations gives the following results (see Table 1): (1) for γ = 4.4 percent, velocity measurements will be within 6.8 percent of true, and isokinetic adjustments within 7.2 percent of true, 99.6 percent of the time; (2) for γ = 7.7 percent, velocity measurements will be within 9.3 percent of true and isokinetic adjustments within 9.6 percent of true, 99.6 percent of the time. Therefore, when pitobe assemblies having aerodynamic interference problems are used to measure velocities in the range from 475 to 1150 ft/min, the use of coefficient values obtained by single-velocity calibration at 3000 ft/min will not introduce serious error; velocity readings and isokinetic adjustments will be within $\pm$ 10 percent of true. Note that this conclusion is justifiable, even though the reference coefficients in Experiment 2 were determined at 2200 ft/min, rather than 3000 ft/min; analysis of data from two recent studies,[4,5] in which 47 and 45 (respectively) pitobe

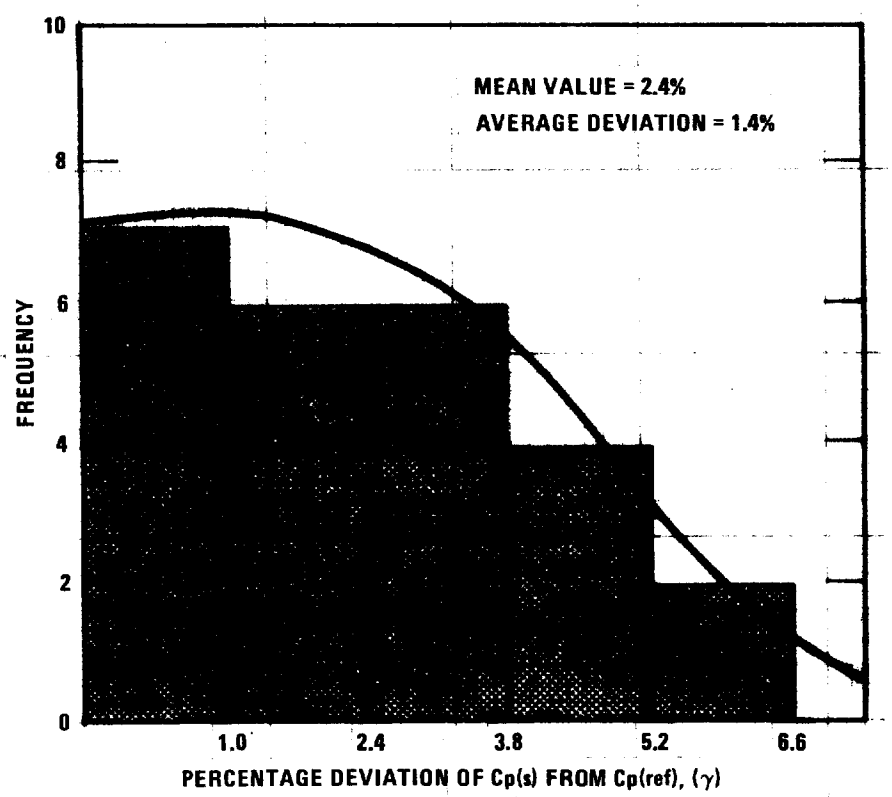

Figure 4. Frequency distribution of γ values from experiment 2; velocity range: 475 to 1150 ft/min.

assemblies were calibrated, shows the average difference (ρ) between the values of $C_p(s)$ at 2200 ft/min and 3000 ft/min to be 0.5 percent or less (see Figures 5 and 6).

CONCLUSIONS

It has been demonstrated that, in the velocity range from about 400 to 1000 ft/min, the value of the Type-S pitot tube coefficient, $C_p(s)$, will generally be within 2 to 5 percent of C_p*, the coefficient value at 3000 ft/min; occasional differences of 6 to 8 percent between $C_p(s)$ and C_p* can be expected. These points have been demonstrated for isolated Type-S pitot tubes and pitobe assemblies. It has also been shown that these deviations from C_p* are sufficiently small to warrant the use of C_p* values to measure velocities in the 400 to 1000 ft/min range.** Thus, special calibration of Type-S pitot tubes in the 400 to 1000 ft/min velocity range is unnecessary.

** It is assumed, of course, that a differential pressure gauge capable of reading ΔP to within $\pm$ 10 percent, is available. Gauge oil manometers generally cannot meet this requirement at velocity head (ΔP) values below 0.03 in. H_2O.

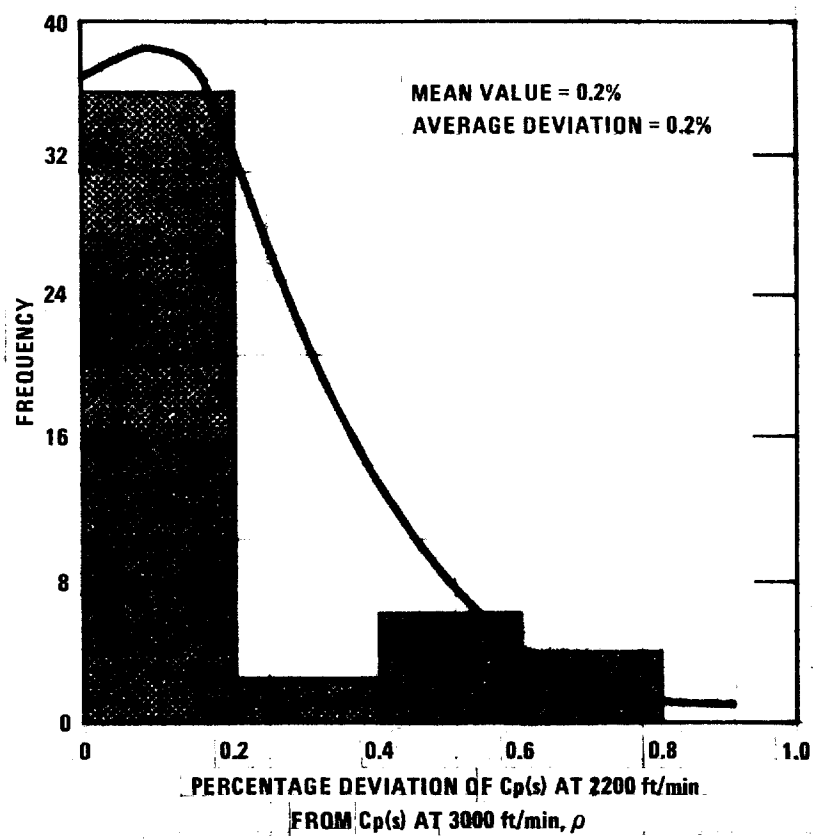

Figure 5. Frequency distribution of ρ values for 47 pitobe assembly calibration runs, based on data from recent North Carolina State University study.

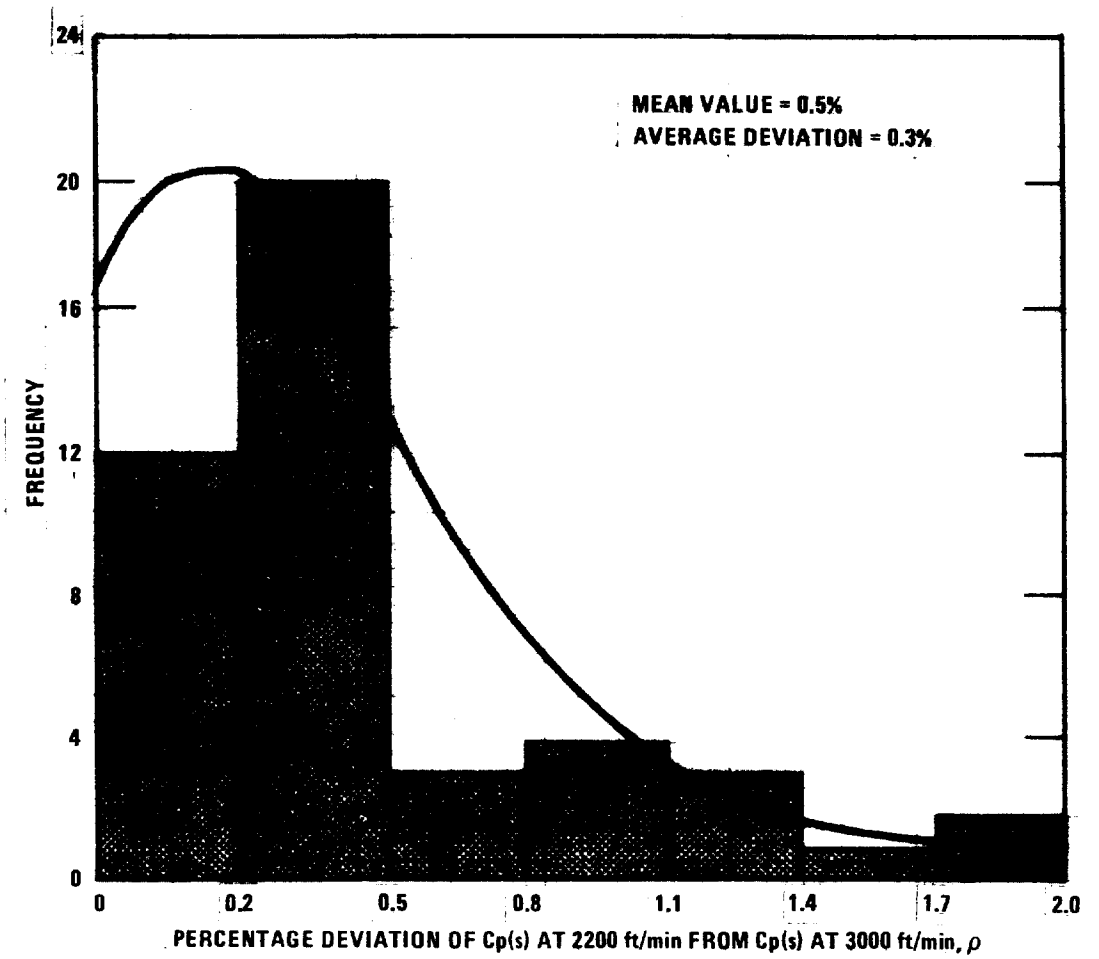

Figure 6. Frequency distribution of ρ values for 45 pitobe assembly calibration runs, based on data from recent University of Windsor study.

REFERENCES

1. Vollaro, R. F. An Evaluation of Single-Velocity Calibration Technique as a Means of Determining Type-S Pitot Tube Coefficients. U. S. Environmental Protection Agency, Emission Measurement Branch. Research Triangle Park, N. C. August, 1975.

2. McCabe, Warren L., and Julian C. Smith. Unit Operations of Chemical Engineering. New York, McGraw-Hill Book Company, Inc., 1956. p. 40-41.

3. Vollaro, R. F. A Type-S Pitot Tube Calibration Study. U. S. Environmental Protection Agency, Emission Measurement Branch. Research Triangle Park, N. C. July, 1974.

4. Terry, Ellen W., and Herbert E. Moretz. First Annual Report on the Effects of Geometry and Interference on the Accuracy of S-Type Pitot Tubes. (Submitted to U. S. Environmental Protection Agency by the Mechanical and Aerospace Engineering Department of North Carolina State University. Raleigh, N. C. August 1975.)

5. Gnyp, A. W., C. C. St. Pierre, D. S. Smith, D. Mozzon, and J. Steiner. An Experimental Investigation of the Effect of Pitot Tube-Sampling Probe Configurations on the Magnitude of the S-Type Pitot Tube Coefficient for Commercially Available Source Sampling Probes. (Prepared by the University of Windsor for the Ministry of the Environment. Toronto, Canada. February 1975.)

6. Shigehara, R. T., W. F. Todd, and W. S. Smith. Significance of Errors in Stack Sampling Measurements. Presented at Annual Meeting of Air Pollution Control Association. St. Louis, Mo. June, 1970.

7. Ower, E., and R. C. Pankhurst. The Measurement of Air Flow. London, Pergamon Press, 1966. p. 35.

8. Vollaro, R. F. Guidelines for Type-S Pitot Tube Calibration. (Presented at the First Annual Source Evaluation Society Meeting. Dayton, O. September 18, 1975.)

APPENDIX A

Experimental Error Considerations

A.1 ACCURACY OF REFERENCE COEFFICIENTS

In Experiments 1 and 2, values of Cp(s), obtained at 3000 and 2200 ft/min, were used as points of reference from which to evaluate the low-range data. It is, therefore, desirable to establish the reliability of these reference coefficients.

The reference coefficients used in Experiment 1 were taken from a previous calibration study.[3] A detailed discussion of the accuracy of these coefficients is presented in the Appendix of Reference 3; considering random errors only (i.e., errors caused by sensitivity limitations of the manometer, incorrect "sight-weighted" averaging of flow pulsations, etc.), the uncertainty in each coefficient value is estimated at $\pm$ 1 percent (0.01).

The reference coefficients used in Experiment 2 were based on data taken during Experiment 2. With the test-section velocity in the wind tunnel held constant at 2200 ft/min, ΔP signals from the standard and Type-S pitot tubes were monitored for several minutes each, in order that accurate determinations of $\overline{\Delta P}$ could be made from the chart recordings. The $\overline{\Delta P}$ values taken from the chart recordings were readable to the nearest 0.005 in. H_2O (see Figure A1). To estimate the uncertainty in each value of Cp (ref), calculated from two such $\overline{\Delta P}$ readings, consider the following example:

Suppose that the values of $\overline{\Delta P}_{std}$ and $\overline{\Delta P}_s$, taken from a chart recording, were 0.300 in. H_2O and 0.420 in. H_2O, respectively. The value of Cp (ref) corresponding to these $\overline{\Delta P}$ values would be, by Equation 1, $0.99\sqrt{0.300/0.420} = 0.837$. Referring to Figure A1, it is evident that

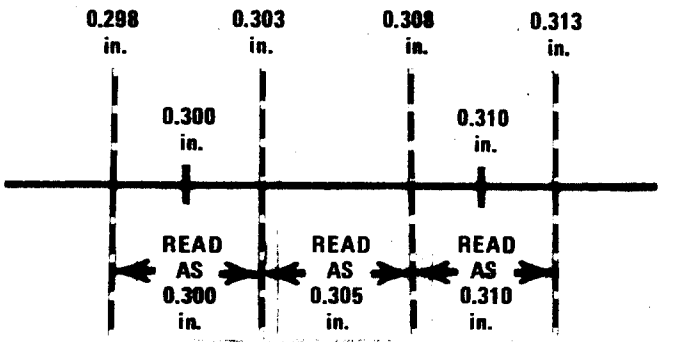

Figure A1. Reading of ΔP to the nearest 0.005 in. H_2O, from Reference 3.

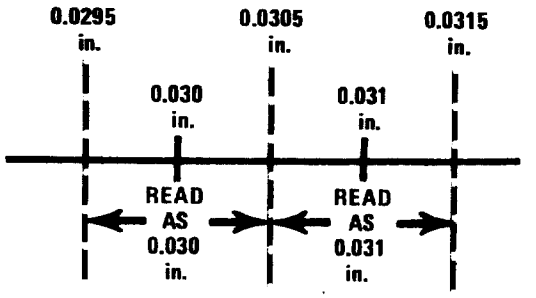

Figure A2. Reading of $\overline{\Delta P}$ to the nearest 0.001 in. H_2O; 600 fpm $\leqslant V_s \leqslant$ 1150 fpm; Experiments 1 and 2.

although $\overline{\Delta P}_{std}$ was read as 0.300 in. H_2O, it actually could have been as high as 0.303 in. H_2O, or as low as 0.298 in. H_2O. Similarly, the value of $\overline{\Delta P}_s$, read as 0.420 in. H_2O, could have been as high as 0.423 in. H_2O or as low as 0.418 in. H_2O. Considering the extreme cases only, this implies that the actual value of Cp(ref) could have been as high as $0.99\sqrt{0.303/0.418} = 0.843$, or as low as $0.99\sqrt{0.298/0.423} = 0.831$. Therefore, the uncertainty in each value of Cp(ref) is estimated at about (0.006/0.837) x 100, or 0.7 percent.

A.2 RANDOM ERRORS IN LOW-RANGE COEFFICIENTS

Figures A2 and A3 illustrate the way in which the average ΔP readings from Experiments 1 and 2 were taken from the chart recordings. Figure A2 shows that for velocities between 600 ft/min and 1150 ft/min, $\overline{\Delta P}$ could be read to the nearest 0.001 in. H_2O, whereas Figure A3 shows that for velocities between 400 and 600 ft/min, $\overline{\Delta P}$ was readable to the nearest 0.0005 in. H_2O. The reason for the difference is that for $V_s < 600$ ft/min, the flow was "quieter" (i.e., the magnitude of the pulsations was less), making $\overline{\Delta P}$ easier to read.

To estimate the uncertainty in each value of Cp(s), calculated from two $\overline{\Delta P}$ values, consider the following typical examples:

<u>Case 1</u>: 600 ft/min $\leq V_s <$ 1150 ft/min

Suppose that the values of $\overline{\Delta P}_{std}$ and $\overline{\Delta P}_s$, taken from a typical chart recording, were 0.030 in. H_2O and 0.040 in. H_2O, respectively. The value of Cp(s), corresponding to these $\overline{\Delta P}$ values would be, by equation 1, $0.99\sqrt{0.030/0.040} = 0.857$. Referring to Figure A2, it is evident that although $\overline{\Delta P}_{std}$ was read as 0.030 in. H_2O, it could have

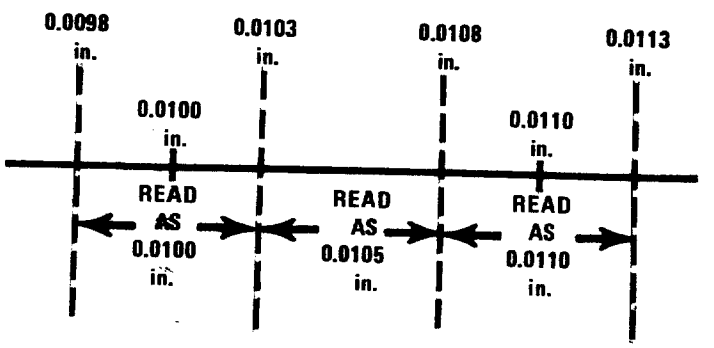

Figure A3. Reading of $\overline{\Delta P}$ to the nearest 0.0005 in. H_2O; 400 fpm $\leqslant V_s < 600$ fpm; Experiments 1 and 2.

been as high as 0.0305 or as low as 0.0295 in. H_2O. Similarly, the value of $\overline{\Delta P}_s$ could have been as high as 0.0405 in. H_2O or as low as 0.0395 in. H_2O. Considering the extreme cases only, this means that the actual value of Cp(s) could have been as high as $0.99\sqrt{0.0305/0.0395}$ = 0.870, or as low as $0.99\sqrt{0.0295/0.0405}$ = 0.845. Therefore, the uncertainty in the value of Cp(s) is estimated at 0.013/0.857 x 100, or 1.5 percent.

Case 2. 400 ft/min $\leq V_s <$ 600 ft/min

Suppose that the values of $\overline{\Delta P}_{std}$ and $\overline{\Delta P}_s$, taken from a typical chart recording, were 0.0100 in. H_2O and 0.0140 in. H_2O, respectively. The Cp(s) value corresponding to these values of $\overline{\Delta P}$ would be, by Equation 1, $0.99\sqrt{0.0100/0.0140}$ = 0.836. Referring to Figure A3, it is clear that although $\overline{\Delta P}_{std}$ was read as 0.0100 in. H_2O, it actually could have been as high as 0.0103 in. H_2O, or as low as 0.0098 in. H_2O. Similarly, $\overline{\Delta P}_s$ could have been as high as 0.0143 in. H_2O, or as low as 0.0138 in. H_2O. Considering the extreme cases only, this implies that Cp(s) could have been as high as $0.99\sqrt{0.0103/0.0137}$ = 0.858, or as low as $0.99\sqrt{0.0098/0.0143}$ = 0.820. Therefore, the uncertainty in the value of Cp(s) is estimated at 0.020/0.836 x 100, or 2.4 percent.

In the light of the above examples, it seems safe to conclude that, because of random errors in interpreting the chart recordings, an uncertainty of 2 percent in the low-range values of Cp(s) is introduced.

APPENDIX B

Velocity and Isokinetic Error Equations

The following two equations, developed by Shigehara et al.[6], are expressions for calculating the probable error (i.e., the error within 3 standard deviations (3 σ) of the mean) when (1) stack gas velocity, V_s, is measured with a Type-S pitot tube, and (2) isokinetic conditions, V_n/V_s, are set with a sampling train, utilizing a pitot tube and orifice meter:

$$\sigma(V_s) = \left[\left(\frac{dC_p}{C_p}\right)^2 + \left[(1.35)(d\,B_{ws})\right]^2 + \frac{\left(\frac{dT_s}{T_s}\right)^2 + \left(\frac{dM_d}{M_d}\right)^2 + \left(\frac{dP_{atm}}{P_s}\right)^2 + \left(\frac{dP_{gs}}{P_s}\right)^2 + \left(\frac{d\Delta P}{\Delta P}\right)^2}{4}\right]^{\frac{1}{2}}$$

(Equation B1)

$$\sigma\left(\frac{V_n}{V_s}\right) = \left[\left(\frac{dK_m}{K_m}\right)^2 + \left(\frac{dC_p}{C_p}\right)^2 + \left(\frac{2dD_n}{D_n}\right)^2 + \left(\frac{dB_{ws}}{1-B_{ws}}\right)^2 + \frac{\left(\frac{dT_s}{T_s}\right)^2 + \left(\frac{dP_{gm}}{P_m}\right)^2 + \left(\frac{dP_{gs}}{P_s}\right)^2 + \left(\frac{dT_m}{T_m}\right)^2 + \left(\frac{dM_d}{M_d}\right)^2 + \left(\frac{d\Delta m}{\Delta m}\right)^2 + \left(\frac{d\Delta P}{\Delta P}\right)^2}{4}\right]^{\frac{1}{2}}$$

(Equation B2)

where: V_s = stack gas velocity, ft/sec

C_p = Type-S pitot tube coefficient

T_s = Absolute stack gas temperature, ^oR

ΔP = velocity head of stack gas, in. H_2O

P_s = absolute stack gas pressure, in. H_2O

M_d = molecular weight of stack gas (dry basis), lb/lb mole

D_n = diameter of sampling nozzle, in.

V_n = gas velocity at the tip of the sampling nozzle, ft/sec

B_{ws} = mole fraction of moisture in the stack gas

Δm = pressure drop across orifice meter, in. H_2O

K_m = orifice meter coefficient

P_{atm} = atmospheric pressure, in. Hg

P_{gs} = gage pressure of stack gas, in. Hg

P_{gm} = meter gage pressure, in. Hg

In the above equations, the derivative, $\frac{dq}{q}$, of a particular quantity, q, represents the percentage error associated with the measurement of that quantity. Assuming maximum values of percentage error[6] for all quantities except C_p (see Table B1), equations B1 and B2 simplify to:

$$3\sigma(V_s) = \left[\left(\frac{dC_p}{C_p}\right)^2 + 27.2\right]^{1/2} \qquad \text{(Equation B3)}$$

$$3\sigma\left(\frac{V_n}{V_s}\right) = \left[\left(\frac{dC_p}{C_p}\right)^2 + 32.4\right]^{1/2} \qquad \text{(Equation B4)}$$

In order to make equations B3 and B4 relevant to the present study, the term $\frac{dC_p}{C_p}$ will be rewritten as $\frac{dC_p(s)}{C_{p(ref)}}$, where $C_p(s)$ refers to the value of the pitot coefficient at a point in the velocity range from 400 to 1000 ft/min, and $C_p(ref)$ is the coefficient value, obtained by calibration at a higher "reference" velocity. The term $\frac{dC_p(s)}{C_{p(ref)}}$ refers, therefore, to the percentage error that would be made by assuming (without proof) that the value of $C_p(ref)$ is valid in the range from 400 to 1000 ft/min. Thus, $\frac{dC_p(s)}{C_{p(ref)}}$ can be replaced by ϕ (Experiment 1) or γ (Experiment 2), and equations B3 and B4 can be rewritten as follows:

Table B1. MAXIMUM ERROR IN MEASUREMENT OF VARIOUS SOURCE - SAMPLING PARAMETERS*

Measurement	Maximum error, %
Stack temperature, T_s	1.4
Meter temperature, T_m	1.0
Stack gage pressure, P_{gs}	0.42
Meter gage pressure, P_{gm}	0.42
Atmospheric pressure, P_{atm}	0.21
Dry molecular weight, M_d	0.42
Moisture content, d B_{ws} (absolute)	1.1
d B_{ws}/1 - B_{ws}	1.0
Pressure head, Δp	10.0
Orifice pressure differential, Δm	5.0
Orifice meter coefficient, K_m	1.5
Diameter of probe nozzle, D_n	0.80

*Adapted from Reference 6.

$$3\sigma\left(V_s\right) = \left(\phi^2 + 27.2\right)^{1/2} \quad \underline{\text{or}} \quad \left(\gamma^2 + 27.2\right)^{1/2} \qquad \text{(Equation B5)}$$

$$3\sigma\left(\frac{V_n}{V_s}\right) = \left(\phi^2 + 32.4\right)^{1/2} \quad \underline{\text{or}} \quad \left(\gamma^2 + 32.4\right)^{1/2} \qquad \text{(Equation B6)}$$

By substituting the appropriate values of ϕ and γ into equations B5 and B6, the probable errors in velocity measurement and isokinetic adjustments, resulting from the assumption that C_p(ref) is valid in the velocity range from 400 to 1000 ft/min, can be determined.

United States
Environmental Protection
Agency

Office of Air Quality
Planning and Standards
Research Triangle Park NC 27711

EPA-450-2-78-042c
October 1978

Air

EPA

Stack Sampling Technical Information

GRIMLEY

A Collection of Monographs and Papers Volume III